RIGA TECHNICAL UNIVERSITY
Faculty of Civil Engineering
Institute of Heat, Gas and Water technology

Andrejs SNEGIRJOVS
Doctoral student of the Heat, Gas, and Water Technology programme

PHOTOVOLTAIC SOLAR AIR CONDITIONING

Doctoral Thesis

Scientific Supervisor:
LAS Academician, Prof., *Dr. habil. sc. ing.*
Peteris SHIPKOVS

Scientific Consultants:
Dr. Paul GANTENBEIN
Dr. Lana MIGLA

Riga 2016

Acknowledgment

Financial support by the Swiss Sciex Programme and by the LATENERGI State Research Programme is gratefully acknowledged. The author is also grateful to the Institute of Physical Energetics (Riga) for financial support.

Part of the research was performed at the Institute for Solar Technology SPF, HSR University of Applied Sciences Rapperswil. The tolerance and support of the SPF crew and officers is highly appreciated.

ABSTRACT

The theme of the Doctoral Thesis is “Photovoltaic Solar Air Conditioning” (PV-SAC).

The objective of this study is to develop, to test and to evaluate the technology of the enhanced grid-connected photovoltaic solar air conditioning.

Ever-decreasing costs of system components combined with energy-efficient concepts in the area of solar energy technologies open new opportunities for application of hot- and cold-storage systems in different building sectors. In the current market situation, photovoltaic electric-driven compression chillers are more profitable as compared with solar thermal-driven sorption cooling devices due to a smaller size of their components such as compressor and heat rejection unit.

In the research, a concept has been developed for the solar air conditioning system operating on PV electric energy, in which cooling by a compression chiller is combined with free cooling. The PV-SAC system is intended for a single-family house. The definition and analysis of the working parameters and of the system yield are presented.

The PV-SAC research has been carried out in two parts: 1. Dynamic simulation of a system model (for three different climatic zones) in the Polysun® program software. 2. A real system operation in a temperate climatic zone. The system is compared with that based on the sorption solar air conditioning technologies.

The research results have been reported at 11 international scientific conferences and are described in 28 publications. The Doctoral Thesis consists of five chapters; it has been illustrated by 63 figures and 6 tables, and its volume is 105 pages. In the Thesis, 51 literature sources have been used.

ANOTĀCIJA

Darba tēma ir „Fotoelektriska saules enerģijas gaisa kondicionēšana” (PV-SAC).

Darba mērķis ir izstrādāt, pārbaudīt un izvērtēt tīklam pievienotas uzlabotas fotoelektriskas saules enerģijas gaisa kondicionēšanas tehnoloģiju.

Komponentu izmaksu samazināšana kombinācijā ar energoefektīvu sistēmas koncepciju saules enerģijas tehnoloģiju jomā paver plašākas iespējas to izmantošanai dažādos tautsaimniecības sektoros. Pašreizējā tirgus situācijā fotoelektriski darbināma kompresijas dzesēšana ir ekonomiski izdevīgāka, salīdzinot ar termiski darbināmiem sorbcijas dzesētajiem. Tas saistīts ar to, ka šajā tehnoloģijā dažas sistēmas sastāvdaļas –kompresors un siltuma novadīšanas tornis – nepieciešamas mazāka izmēra.

Saules enerģijas gaisa kondicionēšanas koncepcija, kurā kombinējas fotoelektroenerģija, kompresijas dzesēšana un brīvā dzesēšana, tika izstrādāta un projektēta vienģimenes mājai. Darbā ir noteikti darbības parametri un saražotās elektroenerģijas apjoms un veikta siltumspējas analīze.

PV-SAC pētījums galvenokārt sastāv no divām daļām: 1. sistēmas modeļa dinamiskā simulācija (trijās dažādās klimatiskajās zonās) ar Polysun® programmu; 2. reālas sistēmas darbināšana mērenā klimatiskajā zonā. Sistēma tika salīdzināta ar divu tipu sorbcijas saules enerģijas gaisa dzesēšanas tehnoloģijām.

Promocijas darba rezultāti ir ziņoti 11 starptautiskās zinātniskās konferencēs un atspoguļoti 28 publikācijās, ir saņemts patents. Promocijas darbā ir piecas nodaļas, un tā apjoms ir 105 lappuses, kurās ietverti 63 attēli un sešas tabulas. Darbā izmantots 51 literatūras avots.

CONTENTS

SYMBOLS AND ABBREVIATIONS

A	Area, m^2,
ARR	Accounting Rate of Return, %,
AB	ABsorption,
AC	Alternating Current,
AD	ADsorption,
BS	Base System,
C	Heat capacity, W/(kg·K),
C_0	Total initial investment, €
CAC	Conventional Air Conditioning,
CAC&H	Conventional Air Conditioning and Heating,
CC	Cold Ceiling,
CM	Cooling Machine,
COP	Coefficient of Performance,
cos φ	Power factor,
CS	Cold Storage,
C_t	Net currency inflow, €,
d	Diameter, m,
DC	Direct Current,
DHW	Domestic Hot Water,
EF	Emission Factor, kg of CO_2/Wh,
EU_{mix}	Average values in Europe Union countries,
G	Irradiation of the inclined surface, Wh/m^2/a,
G_h	Global solar irradiation of a horizontal surface, Wh/m^2/a,
GHG	Greenhouse gas,
HP	Heat Pump,
HS	Hot Storage,
HVAC	Heating, Ventilation, and Air Conditioning,
I	Electric current, A,
IPCC	Intergovernmental Panel on Climate Change
IRR	Internal Rate of Return, %,
LCV	Lower Calorific Value, J/m^3 and Wh/kg,
MPP	Maximum Power Point,
MW	Molecular Weight, g/mcl,
NG	Natural Gas,

NPV	Net Present Value, €,
nT	Number of time periods,
OU	Outdoor Unit (a heat rejection tower),
P	Electrical power, W,
PEF	Primary Energy Factor, Wh,
PV	PhotoVoltaic,
PV-SAC	PhotoVoltaic Solar Air Conditioning,
Q	Energy, Wh,
$\dot{Q}$	Heat flow rate, W,
r	Discount rate, % ,
RES	Renewable Energy Sources,
R	Thermal resistance, $(m^2 \cdot K)/W$,
RT	Room Temperature, °C,
SAC	Solar Air Conditioning,
SEER	Seasonal Energy Efficiency Ratio,
T, t_i	Temperature, K and °C,
t_p	Time period, h,
U	Electric potential difference (voltage), V,
U-value	Heat loss coefficient of the building, $W/K \cdot m^2$,
vol.%	Volume percentage, (v/v)%,
wt.%	Mass percentage, (w/w)%,
α	Heat transfer coefficient, $W/(m^2 \cdot K)$,
δ	Layer thickness, m,
λ	Thermal conductivity coefficient, $W/(m \cdot K)$,
η	Efficiency,
ρ	Density, kg/m^3.

INTRODUCTION

Novelty of the research

Information on the electrical-driven solar air conditioning (SAC) is rather scanty. A considerable body of technical data mostly concerns large-scale photo-voltaic (PV) solar air conditioning (PV-SAC) systems. Reliable information about the energy output has arisen only in the last years; however, it is still not easily accessible, and sometimes its sources are closed. Despite all that, a great interest in this type SAC systems comes from solar energy researchers, observers, and designers. In this study, performance evaluation is done for the PV-SAC technology, in which low-power (up to 15 kW_p of cooling power on average) systems are used. Such a system contains a PV electric-driven compression chiller with cold and heat sensible thermal storage capacities, and a rejected energy unit used for preheating domestic hot water (DHW). In a non-cooling season it is possible to partly employ the system in the reverse mode for DHW production. In this mode the ambient air serves as a heat source. Besides, free cooling is integrated in the PV-SAC concept.

Objective and tasks

The objective of this study is to develop, to test and to evaluate technology of the enhanced grid-connected Photovoltaic Solar Air Conditioning.

The tasks set for reaching this objective:

1) To develop and test a PV-SAC pilot system by driving it in real weather conditions.
2) To evaluate the energy consumption and output of PV-SAC system using dynamic simulation of a system model in Polysun® software.
3) To evaluate the potential of a PV-SAC system implemented in common HVAC engineering field.
4) To determine the influence of PV-SAC system components on its yield and working parameters.
5) To compare the PV-SAC technology with the most common solar air conditioning technologies (ADsorption, ABsorption, Simple PV-SAC).
6) To evaluate the PV-SAC system productivity in different climatic conditions.
7) To assess its economic and ecological impact.
8) To determine the potential of enhanced grid-connected PV-SAC system.

Relevance of the thesis

Expected increase in the cooling loads for comfort needs in private and office buildings calls for alternatives to the conventional energy sources in order to reduce global greenhouse gas emissions, e.g. CO_2. Solar energy – as a renewable energy source – is available at the same time when room air conditioning is needed, and in this case a SAC system can be a reasonable alternative. Reduction in the component costs and innovative solutions in the area of solar energy technologies opens wider opportunities for their application in different building sectors. The authors of works [20, 27, 38] are reporting about the increase in the number of solar cooling and air conditioning systems in the last decade. These authors offer several ways for conversion of the solar radiation into cold using solar cooling components. Today, the most popular technologies are thermal-driven ab- and adsorption chillers in combination with solar thermal collectors. However, because of high costs of the sorption machines and collectors, the market for these technologies is growing very slowly. At the same time, the photo-voltaic (PV) market develops fast, with a continuously reduced PV module prices. This economical reason increases the attractiveness of solar-electrical air conditioning systems. Therefore, the coupling of PV modules with an electrical-driven system of the type presents the concept of PV-based air conditioning. It should be noted that all components of PV electricity driven air conditioning systems are commercially available.

Electric-driven heating and cooling equipment, such as vapour compression heat pumps (HPs), chillers or reversible HPs, in connection with hot and/or cold storages is an attractive option for the energy supply in buildings. However, except for some European regions, today only a few complete system solutions using photovoltaics for the energy supply in buildings are available on the market. Therefore, a lack of information on the overall cost and performance of such systems is identified (see e.g. [20])

The existing pilot-systems and research activities [3, 9, 17, 27, 44] show that there are options for installation and use of PV-driven cooling systems, e.g.:

- a grid-connected system with PV electric power being fed into the public grid and a standard grid-powered air-conditioner [41];
- a grid-independent system (stand-alone) with electrical energy storage to bridge the PV converted solar irradiation and the cooling needs [4]. Most of such systems are installed in Europe.

The international energy agency “Solar heating and cooling programme” set a new “Task 53” in May, 2014: “New Generation Solar Cooling & Heating Systems (PV or solar

thermally driven systems)". The main objective of this task is to assist in an active and sustainable market development of solar PV or new innovative thermal cooling systems. It is focusing on solar-driven systems for both cooling (ambient and food conservation) and heating (ambient and domestic hot water) [22]. These activities have received a high feedback, including conference organization [21]. One of the topics of the "Photovoltaic driven Solar Air Conditioning Systems" conference was exactly meant for PV-SAC technology. Open source reports as well as "Handbook on efficient new generation cooling and heating systems" [36] are included in the working plan of "Task 53" activities. Part of the thesis study described here was also presented at the mentioned conference and raised a great interest. The attention was received from potential PV-SAC manufacturers.

Approbation of the results

Results of the conducted research and scientific innovations are published in 1 patent, 1 book and in 27 periodic editions. The results are presented at 11 international conferences and 3 local scientific workshops. The studies have been partly done under research projects, with some of the results presented in scientific reports.

Experimental and mathematical studies of thermal-driven SAC technologies have been done in the work to compensate a deficiency of reliable information on their operation parameters and yields. Results of comparison of the thermal-driven technologies with the electric-driven solar air conditioning technology had been published earlier.

Results of the work are also contained in the scientific publications listed below.

Patent

1. Snegirjovs A., et al. Siltuma saules kolektora darba vadības sistēma. – Patent P-15-10. – Jan 30, 2015.

List of publications

1. Gantenbein P., Omlin L., Notter D., and Snegirjovs A. Combined PV solar compression cooling and free cooling system// 32nd European Photovoltaic Solar Energy Conference. – Munich, Germany: EU PVSEC, June 2016. – 4 p. (in press)
2. Снегирёв А. С., Шипковс П. Я, Гантенбайн П. К., Мигла Л. С., Лебедева К. В., Кашкарова Г. П., Шипковс Я. П. ФЭ – солнечное кондиционирование// XV Минский международный форум по тепломассообмену. – Минск, Республика Беларусь: МИФ, май 2016. – 10 стр.

3. Snegirjovs A., Gantenbein P., Omlin L., and Shipkovs P. Improved model of combined PV solar cooling and free cooling system// 6th Conference Solar Air-Conditioning. – Regensburg, Germany: OTTI, 2015. – pp. 162–167.

4. Inovatīvas tehnoloģijas siltuma un aukstuma ieguvei un jaunu produktu ražošanai, izmantojot vietējos atjaunojamos energoresursus. Metodiskais materials/ Šipkovs P. u.c. – Riga, Latvia: SIA Agentura radars, 2015. – 110 p.

5. Snegirjovs A., Gantenbein P., Rommel M., and Shipkovs P. Key model of PV solar cooling// The 12th International Conference of Young Scientists on Energy Issues. – Kaunas, Lithuania: CYSENI, 2015. – 9 p.

6. Shipkovs P., Shipkovs J., Snegirjovs A., Kashkarova G., Lebedeva K., Migla L., and Lekavichius V. Optimization of solar cooling system in Latvia// REHVA 2015. – Riga, Latvia: REHVA, 2015. – pp. 195–198.

7. Shipkovs P., Snegirjovs A., Shipkovs J., Kashkarova G., Lebedeva K., and Migla L. Solar thermal cooling on the Northernmost latitudes// Energy Procedia 70. – 2015. – pp. 510–517.

8. Shipkovs P., Snegirjovs A., Kashkarova G., Lebedeva K., and Migla L. Solar cooling in high latitudes conditions// EuroSun 2014. – Aix-les-Bains, France: EuroSun, 2014. – 6 p.

9. Shipkovs P., Kashkarova G., Lebedeva K., Migla L., and Snegirjovs A. Solar panels produced electricity impact on electricity network// Renewable Energy and Power Quality Journal (RE&PQJ), No.12. – 2014. – 5 p.

10. Lvovs A., Priedite I., and Snegirjovs A. Study on reliability improvement possibilities assuming probabilistic wind and solar generation// Electric Power Quality and Supply Reliability Conference (PQ). – 2014. — pp. 111–118.

11. Shipkovs P., Snegirjovs A., Kashkarova G., and Shipkovs J. Potential of solar cooling in Latvian conditions// Energy Procedia 57. – 2014. – pp. 2629–2635.

12. Shipkovs P., Kashkarova G., Lebedeva K., Migla L., Snegirjovs A., and Shipkovs J. Potential and analysis of grid integrated renewables in Latvia// Energy Procedia 57. – 2014. – pp. 735–744.

13. Snegirjovs A., Shipkovs P., Vanags M., and Mila L. Photovoltaic batteries with modified glazing// The 10th International Conference of Young Scientists on Energy Issues. – Kaunas, Lithuania: CYSENI II, 2013. – pp. 87–93.

14. Shipkovs P., Vanags M., Snegirjovs A., and Migla L. Modified glazing for PV batteries// ISES Solar World Congress 2013. – Trondheim, Norway: ISES SWC, 2013. – 5 p.

15. Shipkovs P., Kashkarova G., Lebedeva K., Vanags M., Snegirjovs A. and Barkans V. Cross-sectional temperature field of a solar collector's absorber in the case of annular pipe// Renewable Energy and Power Quality Journal (RE&PQJ), No. 11. – 2013. – 5 p.

16. Shipkovs P., Snegirjovs A., and Migla L. Heat losses influence on solar thermal systems// The 9th International Conference of Young Scientists on Energy Issues. – Kaunas, Lithuania: CYSENI II, 2012. – pp. 61–70.

17. Shipkovs P., Snegirjovs A., Vanags M., and Migla L. Cost-effective pipelines insulation of solar thermal system// World Renewable Energy Forum. – Denver, Colorado: WREF, 2012. – 6 p.

18. Shipkovs P., Vanags M., Snegirjovs A., et al., Optimization of solar thermal system's pipelines insulation// EuroSun2012. – Rijeka, Croatia: EuroSun, 2012. – 7 pp.

19. Снегирёвс А.С., Шипковс П.Я., Кашкарова Г.П., Мигла Л.С. Теплопотери в системе солнечного теплоснабжения. XIV Минский международный форум по тепломассообмену. - Минск, Республика Беларусь: МИФ, 2012. – 10 стр.

20. Shipkovs P., Snegirjovs A., Vanags M., and Migla L. Determination of cost–effective pipelines insulation of solar thermal system// The 8th International Conference of Young Scientists on Energy Issues. – Kaunas, Lithuania: CYSENI II, 2011. – pp. 84–87.

21. Shipkovs P., Kashkarova G., Snegirjovs A., Vanags M., Lebedeva K., Shipkovs J., and Migla L. Investigation of solar collector's in Latvian conditions// Renewable Energy and Power Quality Journal. – Las Palmas, Spain: RE&PQJ, 2011. – pp. 1–4.

22. Shipkovs P., Kashkarova G., Lebedeva K., Vasilevska L., Pankars M., Shipkovs J., and Snegirjovs A. Solar collectors' operation methods effect on system efficiency// ISESCO Science and Technology Vision 7 (11). – 2011. – pp. 38–42.

23. Shipkovs P., Migla L., Lebedeva K., Pankars M., and Snegirjovs A. Modeling of solar heating systems in Latvia// 10th REHVA World Congress on Sustainable Energy Use in Buildings. CLIMA 2010. – Antalya, Turkey: REHVA, 2010. – 8 p.

24. Shipkovs P., Kaspars G., Snegirjovs A., and Vasilevska L. Combination of the solar energy systems for household use and apartment buildings// 10th REHVA World Congress on Sustainable Energy Use in Buildings. CLIMA 2010. – Antalya, Turkey: REHVA, 2010. – 6 p.

25. Shipkovs P., Snegirjovs A., Vanags M., Lebedeva K., Shipkovs J., Migla L., and Pankars M. Comparison of solar collectors operation methods// The 7th International Conference of Young Scientists on Energy Issues. – Kaunas, Lithuania: CYSENI II, 2010. – pp. 67–74.

26. Shipkovs P., Snegirjovs A., Vanags M., and Vasilevska L. Utilization of solar combisystems in Latvian conditions// International Conference on Solar Heating, Cooling and Buildings. EuroSun 2010. – Graz, Austria: EuroSun, 2010. – pp. 1–8.

27. Shipkovs P., Kashkarova G., Lebedeva K., Vanags M., Snegirjovs A., and Vasilevska L. Testing solar equipment in Latvian conditions// International Conference on Solar Heating, Cooling and Building. EuroSun 2010. – Graz, Austria: EuroSun, 2010. – pp. 1–8.

28. Shipkovs P., Kashkarova G., Lebedeva K., Vanags M., Snegirjovs A., and Migla L. Solar energy use for sustainable development// ISES Solar World Congress 2009. – Johannesburg, Republic of South Africa: ISES SWC, 2009. – pp. 1881–1888.

List of presentations

1. Фотоэлектрическое солнечное кондиционирование// XV Минский международный форум по тепломассообмену. - Минск, Республика Беларусь. - 23–26 мая 2016.
2. Photovoltaic electric driven solar air cooling// Riga Technical University 56th International Scientific Conference. - Riga, Latvia. - October 14–16, 2015.
3. Improved model of combined PV solar cooling and free cooling system// The 6th Conference Solar Air-Conditioning. - Rome, Italy. - September 24–25, 2015.
4. Key model of PV solar cooling// The 12th International Conference of Young Scientists on Energy Issues. - Kaunas, Lithuania. - May 27–28, 2015.
5. CoCoSol - Cooling Concept with Solar PV-Electricity. Swiss-Latvian workshop// STV meeting. - Riga, Latvia. - April 30, 2015.
6. The modified glazing influence on the efficiency of photovoltaic panels// Riga Technical University 54th International Scientific Conference. - Riga, Latvia. - October 14–16, 2013.
7. Photovoltaic batteries with modified glazing// The 10th International Conference of Young Scientists on Energy Issues. - Kaunas, Lithuania. - May 28–30, 2013.
8. Influence of thermal insulation on solar thermal systems efficiency// Riga Technical University 53rd International Scientific Conference. - Riga, Latvia. - October 11–12, 2012.
9. Теплопотери в системе солнечного теплоснабжения// XIV Минский международный форум по тепломассообмену. - Минск, Республика Беларусь. - 10–13 сентября 2012.
10. Heat losses influence on solar thermal systems// The 9th International Conference of Young Scientists on Energy Issues. - Kaunas, Lithuania. - May 24–25, 2012.
11. Determination of cost-effective pipelines insulation of solar thermal system// The 8th International Conference of Young Scientists on Energy Issues. - Kaunas, Lithuania. - May 26–25, 2011.
12. Saules enerģijas izmantošanas iespējas// FEI seminars: - Riga, Latvia. - August 25, 2011.
13. Comparison of Solar Collectors Operation Methods// The 7th International Conference of Young Scientists on Energy Issues. - Kaunas, Lithuania. – May 27–28, 2010.
14. Saules pētišanas poligons// FEI seminar: Saules Enerģijas izmantošana Latvijā. - Riga, Latvia. - June 16, 2009.

List of scientific projects

1. National research program “Energy efficient and low-carbon solutions for a secure, sustainable and climate variability reducing energy supply (LATENERGI)”. Complexes research on renewable energy production and utilization for innovative technologies use and investigation of biogas production potential in the waste recycling sector, 2014–2017.
2. Swiss Sciex Programme: “CoCoSol - Cooling Concept with Solar PV-Electricity”, 2014–2015.
3. ESF project “Development of innovative technologies for heat and cold save and production”, 2014–2015.
4. KPFI project "Energy effective solar panel glass design”, 2011.
5. National research programme LATENERGI “Technologies for Innovative Production and Use of Energy Resources and Provision of Low Carbon Emissions by means of Renewable Energy Resources, Support Measures for the Mitigation of Environmental and Climate Degradation”, 2010–2014.
6. National Energy Research Programme „Development of modern methods and technologies for utilization of renewable energy resources, rational use of energy and improvement of energy supply”, 2006–2009.

1 EVALUATION OF PV-SAC POTENTIAL

1.1 Classification

Active and passive cooling implies the heat rejection from the operation field i.e. a heat source, to a heat sink. Therefore, the notion “air conditioning” in this work mainly relates to cooling, while it might include heating in some cases.

Solar cooling can be passive and active. Passive solar cooling implies the absence of external energy inflow; systems of the type are not observed in this thesis. In turn, active solar cooling as a driving source uses electricity or heat energy. The heat energy for thermal-driven chillers is produced mostly by solar collectors. Electricity for electric-driven chillers is obtained from photo-voltaic panel arrays, or from large solar stations via steam turbines. A solar cooling technology is usually chosen according to the energy source, the area of applications, and the weather conditions.

The solar cooling technology tree shown in fig. 1.1 was obtained by summarizing the latest information from different sources. [20, 27]

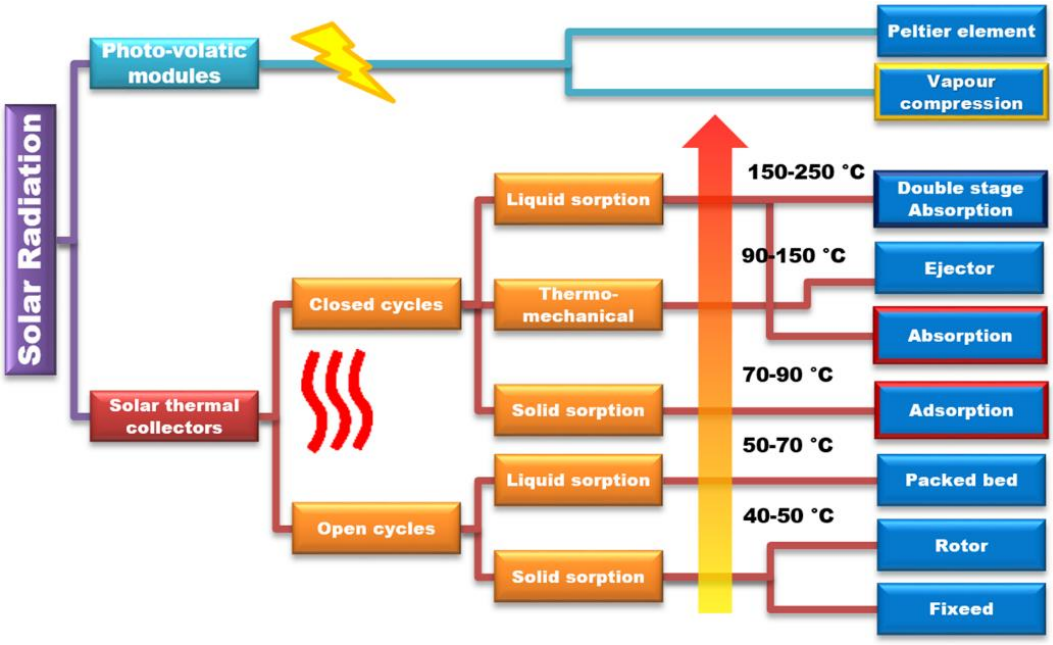

Fig. 1.1. Solar cooling technology tree

The PV-SAC technology was compared with two most widespread solar air conditioning technologies. Most commonly used nowadays is a single-stage ABsorption thermal-driven chiller. Closest followers of the market leader are ADsorption and double-stage ABsorption technologies.

Thermo-electric solar cooling technologies – e.g. using Peltier elements – are unable to participate in this market because of low efficiency and high costs of the heat rejection power. They are about four times less efficient in cooling applications than conventional compression cycle technologies. Therefore, thermo-electric technologies do not have a high potential for applications.

Desiccant evaporative cooling technologies use solid- or liquid-based open systems where combination of evaporative cooling with air dehumidification is applied. In a solid-based system, desiccant wheels with hydroscopic material are used for absorbing moisture from the inlet air in dehumidification process. The dry inlet air is cooled by wet heat exchangers. When a desiccant wheel rotates, the hydroscopic material alternately contacts the inlet and the outlet air. This material regenerates by heated outlet air. The heat for this purpose is produced by a solar thermal system.

In the liquid-based desiccant cooling, the moisture is absorbed into the desiccant liquid. The diluted wet desiccant solution flows to a heat exchanger where the heat from a solar thermal system removes the moisture, thus concentrating the solution. The regenerated desiccant solution then flows back to the medium for reuse. Direct contact with cooling air in desiccant evaporative cooling technologies may not meet some of the hygienic criteria.

Most of installed SAC systems are of the thermal-driven type, while PV electric-driven SAC is relatively less spread. Official reports on SAC systems in 2014 show that only few of these systems have photovoltaics in combination. The SAC systems might be medium-large and large, with the cooling power over 200 kW_p. All these systems are grid-connected.

A single-stage and a double-stage ABsorption thermal-driven systems are the most used types of installed SAC systems, fig. 1.2. Those of adsorption type are more suitable for colder regions where cooling systems are widespread. In turn, adsorption thermal-driven machines are mostly of small-to-medium size, with the cooling power up to 130 kW_p. The adsorption thermal-driven SAC systems are less applied.

The main technologies for solar cooling systems with a low cooling capacity (< 50 kW_p) are of absorption and adsorption type. They are mostly used as central air conditioning systems with decentralized fan coils or cooled ceilings. During the last few years – especially in Europe – various new sorption chillers of small-scale and medium-scale cooling capacity have been developed. Many of these sorption chillers have passed over from a prototype stage into a batch production. [39]

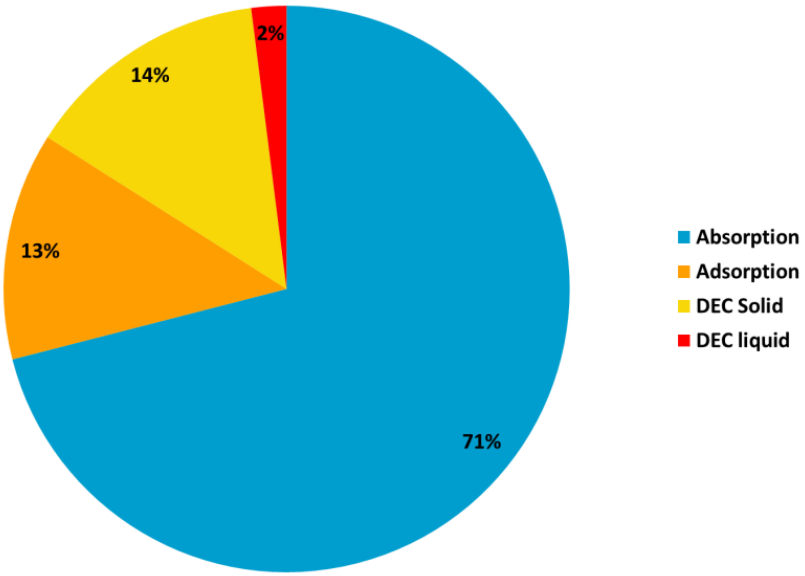

Fig. 1.2. Market share of solar-driven sorption chillers (2009) [28]

The adsorption chiller with a cooling capacity of 7.5 kW_p is meant for residential buildings, while the 12 kW_p ammonia/water absorption chiller – for office buildings or cooling processes, e.g. milk cooling; the 15 kW_p water/silica gel absorber as well as the 17.5 kW_p water/lithium bromide absorber are intended for air conditioning in office buildings, hotels, banks, bakeries, public and administration buildings [24]

The solar cooling systems basically contain solar thermal collectors with hot water storage, pump-sets, a chiller, a re-cooler, a partly cold water storage, and a control unit. The existing cooling kits are developed for the European market, whereas other re-coolers can be offered according to the country (e.g. in Spain these are dry re-coolers). As a reference value for thermal-driven absorption and adsorption chillers a 3.5-4.5 m^2/kW_p cooling capacity of specific collector surface can be considered. Such values are only rough references, and cannot replace those obtained at detailed design and simulation of a system. The specific total costs of installed solar cooling systems in Europe in 2007 were between 5.000 and 8.000 Euro/ kW_p. In the future, the costs of 3.000 Euro/ kW_p are expected [46].

1.2 Brief outline of solar cooling history

Variations in fossil fuel prices have given impetus to an active search for alternative energy sources. First mention about the use of solar energy for cold production was made in 1869 by a French inventor of the earliest solar energy apply technology – Augustin Mouchot [35]. The first solar cooling system was publicly demonstrated by the same author at the Universal Exhibition in Paris, 1878 [34]. Ice cubs were produced by the system with an

ammonia-water absorption chiller and a parabolic reflector. The next solar cooling demonstrations were resumed as late as the 1980s. That time, the public attention was captured only for several years. The newest restart of wide thermal solar cooling research was made at the beginning of 21th century, when the ideas as to combining PV and electric-driven chillers were spread among researchers.

1.3 Solar cooling development

Nowadays, many research institutes are engaged in development of direct and indirect solar air conditioning technologies.

At the Institute of Physical Energetics (Latvia) a northernmost thermal solar air conditioning (SAC) system was designed, built, and launched. This is a pilot and demonstration ADsorption type SAC system that works in real climatic conditions and has a real cooling demand for office rooms. Apart from that, a basic PV-SAC system is installed at the solar energy testing polygon. First results evidence that improvement and optimization of the SAC and PV-SAC systems are made nowadays. Below, these systems are described in detail and compared with reference PV-SAC systems.

The closest to Latvia SAC investigations are underway at the Vilnius Gediminas Technical University (Lithuania). Also their ADsorption SAS system is driving in real weather conditions but it has manually controlled cooling demand.

In Europe and worldwide, SAC investigations become more and more extensive. Leading research groups from Algeria, Australia, Austria, Belorussia, Brasilia, France, Germany, India, Israel, Italy, Korea, Netherlands, China, Russia, Spain, Sweden, Switzerland, and United States of America are working in this area many years.

1.4 Topicality of cooling

Ever rising comfort requirements in buildings and transportation makes the cooling demand and thus the cooling market growing.

These comfort requirements are leading to the air conditioning as a necessity in commercial buildings, and is not anymore seen as a luxury. With these premises and the aim of CO_2 reduction, a fast growing market of solar air conditioning systems can be expected. This has remained relatively unnoticed by policy makers, partly because cooling needs are traditionally being met by electrical air conditioners, hiding the cooling element within the building's overall electricity consumption [36].

In Europe, a rise in the share of commercial buildings equipped with cooling systems is expected to reach at least 60 % by the year 2020. The maximum potential cooling demand in Europe – if 100 % of all useful space would be air-conditioned – is estimated to be annually 1400 TWh cooling [40].

Solar cooling communities [36, 50] expect an impetuous solar cooling development in nowadays growing use of renewable energy sources (RES). This rise in RES implementation in energy sector gets support from EU directive [10] and regularities of energy use. The recent building directive [11] has a subtask of decreased cooling load development. Not less impact has had a directive 2020 concerning "nearly zero energy buildings", which means that direct fossil fuel and electricity consumptions should predictably decrease. Indeed, it is possible to reduce the energy consumption instead of reducing the comfort level by using energy saving technology as well in solar air conditions. But this also means that significant changes are coming and big work has to be done in the nearest future.

1.5 Market of solar air conditioning systems

The European SAC market has grown rapidly during the last decade (fig. 1.3). The number of installed SAC systems had risen more than 17 times in the time from 2004 to 2013.

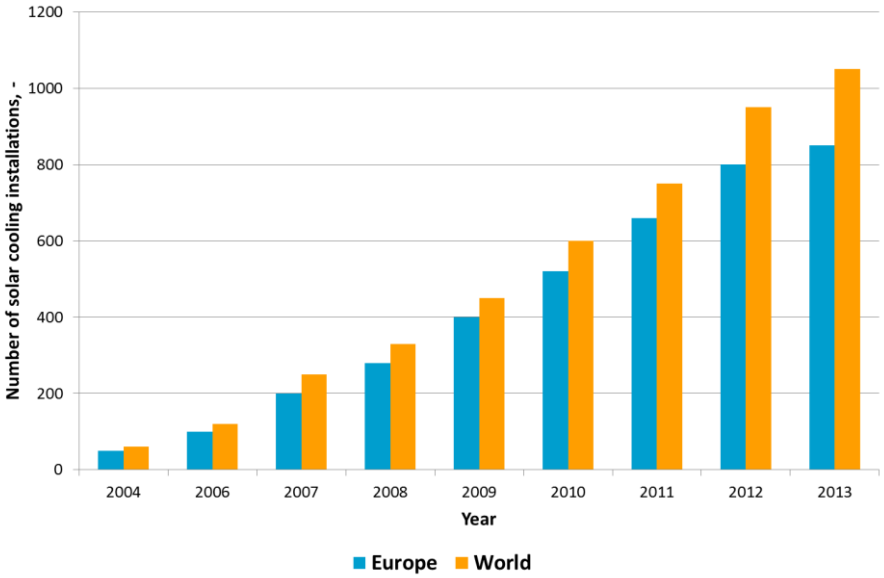

Fig. 1.3. Market development in 2004–2013 of small- to large-scale solar air conditioning and cooling systems [33]

Approximately 80 % of the solar cooling systems worldwide are installed in Europe, most notably in Spain, Germany and Italy. The majority of these systems are equipped with flat plate or evacuated tube collectors. By contrast, some examples for thermal cooling machines

driven by concentrated solar thermal energy (with concentrating solar thermal collectors such as parabolic troughs or Fresnel's collectors) were reported from India, Australia and Turkey. The overall number of systems installed to date indicates that solar cooling is still a niche market, but one which is developing. Since 2007, a cost reduction of about 50 % had been realized as a result of the further standardization of the solar cooling kits. [33]

Air conditioning market distribution follows the growth of living conditions. Small-scale air conditioning systems have a short lifetime (usually from 2 to 5 years), which implies continuous replacement of the elements of such a system. Despite all this, the market growth is observed almost every year in the last decade, fig. 1.4.

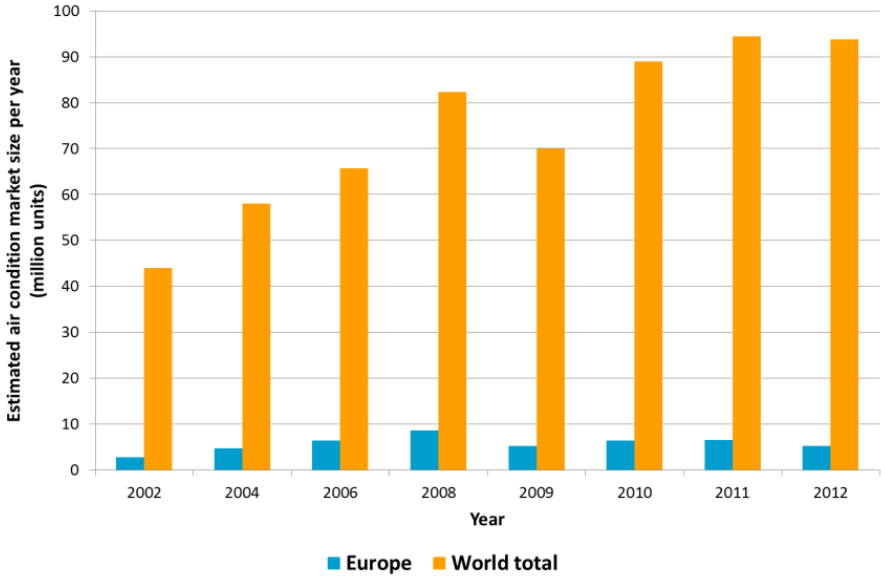

Fig. 1.4. Market situation of conventional air-condition units up to 5 kW_p [23]

Small-scale air conditioning market size in Europe is tripled in the time from 2002 to 2008; then in 2009 a market reduction occurred. In the market development, the influence of changeable economic situation could be seen worldwide and especially in Europe.

Distribution of air condition units in the 21th century is redirected from developed countries to dashingly developing counties; new distribution trends are now seemingly targeted for the Asia region.

Regarding mass manufacturing, acceleration of air condition production becomes simultaneously the main focus of the major Asian manufacturers in the last 20 years. [23, 48]

1.6 Photo-voltaic market

The main energy source for PV-SAC is the electricity produced by a PV array. The dynamics of PV installation is inversely proportional to initial investments in terms of Euro/kW_p. The price reduction for PV products in the last decade is in proximity to 10 % a year, and every year the lowest cost records per installed PV nominal power are set for systems of all scales.

In late 2009, the world's cumulative installed PV capacity was more than 23 GW. A year later it was 40.3 GW, having risen to 70.5 GW by the end of 2011. In 2012, the 100 GW mark was reached, and by 2013 almost 138.9 GW of PV had been installed globally – an amount capable of producing at least 160 terawatt hours (TWh) of electricity every year. This energy volume is sufficient to cover the annual power supply needs of over 45 million European households. This is also the equivalent of the electricity produced by 32 large coal power plants. The global cumulative installed capacity could have even reached 140 GW in 2013 if the additional 1.1 GW in China were taken into account. [32]

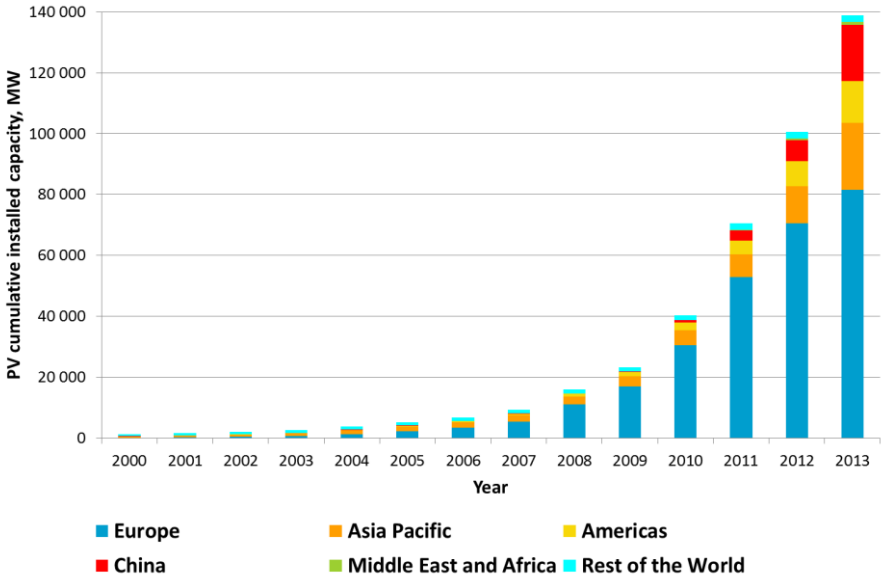

Fig. 1.5. Evolution of global PV cumulative installed capacity 2000-2013 [32]

Europe remains the world's leading region in terms of cumulative installed capacity, with 81.5 GW as of 2013. This represents about 59 % of the world's cumulative PV capacity, down from 70 % in 2012 and about 75 % of the world's capacity in 2011. As illustrated in figure 1.5, Asia Pacific countries are growing fast, with 40.6 GW now installed. Next in the rankings are both the Americas (13.7 GW). [32]

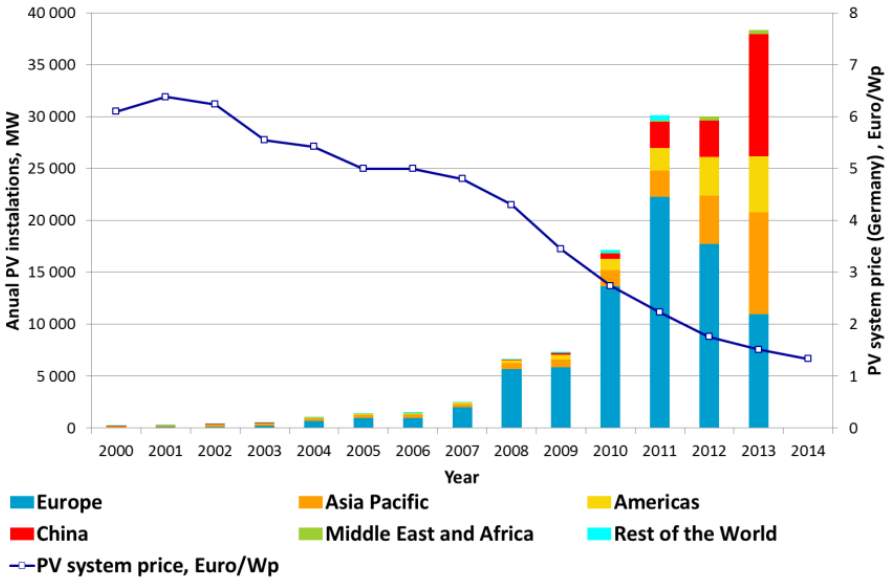

Fig. 1.6. Evolution of global annual installations 2000-2013 [32]

*PV price sources: 2006-2014 [1]; 2009-2014 [37], installation power up to 100 kW_p.

With at least 37GW [13] of newly-added capacity globally, 2013 was a record year as that for photovoltaic installations. These figures show that the internationalization trend of PV markets already observed in 2012 was then accentuated in 2013, with Asia taking the lead over Europe as number 1 region for new PV installations.

These globally positive figures result from a much qualified situation at regional level, with Europe losing its leading role in the PV market in 2013. While it concentrated more than 70 % of the world's new PV installations in 2011 and still around 59 % a year later, with more than 10 GW of new capacity installed in 2013, Europe accounted only for 28 % [13, 16] of the world's market.

2 EXPERIMENTAL PHOTO-VOLTAIC SOLAR AIR CONDITIONING SYSTEM

At the Institute for Solar Technology SPF (Rapperswil, Switzerland) a pilot small-scale PV-SAC system has been developed and built up.

This system (fig. 2.1) is intended for covering the cooling demand in a laboratory room by using solar energy.

In the following sections, a description of the system and its components is given.

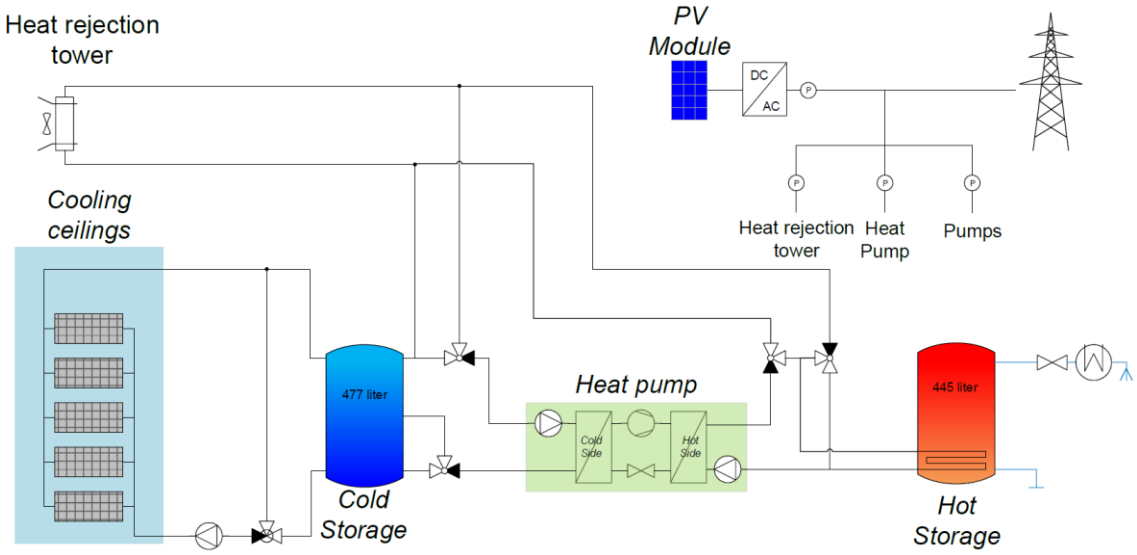

Fig. 2.1. Schematic of the photovoltaic solar air conditioning system

2.1 The photovoltaic panel array

The main components of the PV-SAC (fig. 2.2) forming a reference system are photovoltaic modules combined with a DC/AC inverter, an electric-driven chiller, indoor cold distribution elements (cold ceilings), and an outdoor heat rejection unit. The pilot system under consideration contains also a hot storage, a cold storage, and a heat rejection tower (outdoor unit) for preheating the domestic hot water (DHW).

The monocrystalline silicon PV cells provided by Mayer Burger absorb solar energy and transform it to electricity. The size of each module is 1.65 m^2, and efficiency of the cells is 17.4 %. The frameless PV modules are covered by a 5 mm solar glass with antireflection coating, their total thickness thus being 9 mm. The total area of nine installed PV modules is 14.77 m^2. The nominal power of each PV module at maximum irradiation (G=1000 W/m^2) is P_{PV}=285 kW_p, with an error of ±3 %. The nominal peak power of the whole PV array is $P_{PVarray}$=2.565 kW_p at the maximum irradiation. It correspond to the maximum electrical power of cooling machine $P_{hp.max}$ = 2.5 kW described below. The voltage at the maximum power point

(U_{MPP}) of the PV module is U_{MPP}=31.2 V, and the open circuit voltage is U_{OC} = 38.3 V. The current at MPP of the PV module is I_{MPP} =8.7 A, and the short-circuit current is I_{SC} = 9.2 A.

Fig. 2.2. The photovoltaic panel array (left);
The DC/AC inverter (red) adjacent to the cold storage (right)

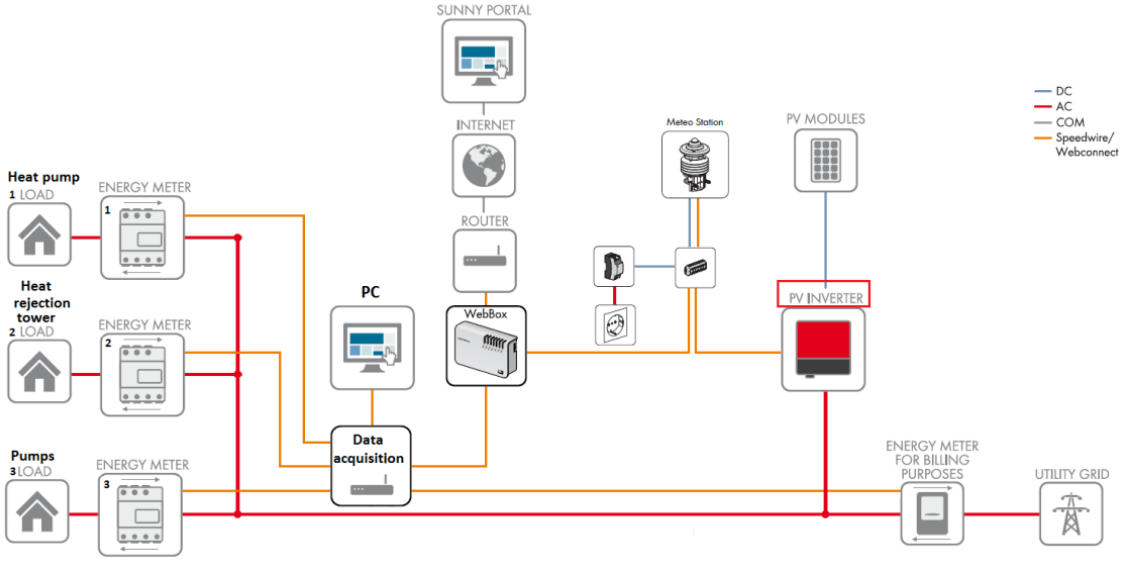

Fig. 2.3. Schematic of the electrical network of integrated PV modules,
the electricity distribution and the data acquisition unit

The over-current protection is set to I=18A, therefore all PV modules are electrically connected in parallel. The total U_{MPP} voltage is then 280.8 V and is in the range of maximum

system voltage up to U=1000 V. The manufacturers' recommendation for the connection of PV modules is their maximum number of 60 at serial connection. The manufacturer guarantees for these type of PV modules a minimum performance of 90 % after 10 years of use and of 80 % after 25 years. Therefore, decrease in the PV nominal power with time is to be taken into account in the calculations. The annual decrease in the efficiency is ~ 0.9 % of the previous year's value.

At mounting, the unframed PV modules are fixed on the laboratory roof. The modules are mounted at 15° inclination to horizon. The roof has a 5° slope, respectively a module's profile slope is 10°. This angle suffices for electric connection under the modules. For profiling unframed modules, aluminium is used. The PV mounting is designed in view of protection against flexion and possible shifts due to thermal expansion. Protection against flexion from top is designed regarding snow masses, and that from bottom – regarding winds. To allow thermal expansion shifts, rubber gaskets between PV the modules and the mounting are used.

2.2 DC/AC inverter

The PV array produces direct current (DC), while most of PV-SAC components – a heat pump, a heat rejection tower, and pumps are designed to use alternating current (AC).

The PV inverter converts the direct current from PV array to grid-compliant alternating current and feeds it into the SAC system and into the electricity grid. The inverter is chosen according to the parameters of PV array. The inverter's maximum DC power, voltage and current should be higher than the nominal values of PV array. In turn, the minimal starting operation parameters should be high enough for efficient PV use (see Table 2.1).

Table 2.1

DC Input of the PV inverter [2]

Maximum DC power at cos φ = 1*	2'650 W
Maximum input voltage	750 V
MPP voltage range	180 V to 500 V
Rated input voltage	400 V
Minimum input voltage	125 V
Initial input voltage	150 V
Maximum input current	15 A
Maximum input current per string	15 A
Number of independent MPP inputs	1
Strings per MPP input	2

*cos φ – power factor.

The DC cable length from a PV array to the inverter is ~ 40 m. The required cable cross-sections are from 2.5 to 6 mm^2. Two 1.5 mm^2 three-wire cables are used for both strings. The cables are connected to the wall and are placed in a metallic chamber in compliance with the fire safety rules.

For the PV-SAC experimental setup the inverter with a high protection level is chosen. Electricity grounding is used for all electric parts of the PV-SAC system. The inverter suitable for the indoor and outdoor use has also a high environment protection level, and placed indoors to ensure easy connection to the data acquisition unit. The inverter is supplied with electronic solar switch, which prevents electric arcs from forming at removal of the DC connector. The overvoltage protection is provided by two varistors. The inverter is also equipped with an integrated all-pole-sensitive residual-current monitoring unit. This system's component can automatically differentiate between residual currents and normal capacitive leakage currents, and is equipped with a protective conductor monitoring device, which detects the absence of a protective conductor's connection, in this case disconnecting the inverter from the grid. In the system, a self-test was run, during which the inverter consecutively checks the response time for the overvoltage, undervoltage, the maximum frequency and the minimum frequency. [2]

As concerns the compatibility between the PV-electricity production and the cooling processes it is so far an unsolved problem. Therefore, for the pilot PV-SAC system a flexible and controllable PV inverter is required.

Various operating parameters serve to control the functionality of the inverter. The inverter is equipped with grid control functions, making it possible to activate and configure the functions depending on the requirements of the network operator or SAC control strategy via operating parameters (such as reactive power or active power limitation, etc.)

The inverter has an info display, which shows the current operating data of the inverter as well as faults and disturbances. It is possible to observe there the state, power, input voltage and current, the daily and the total amounts of energy fed in, etc.; the display alternately shows the output voltage and the output current of inverter. As well it is possible to observe the diagram of changes of power in the last 16 feed-in hours, or the energy yields in the last 16 days. Optionally, monitoring and collection of the inverter operating parameters is provided using Bluetooth, RS485, or Speedwire/Webconnect. In our case, the inverter is upgraded with RS485 slot for the communication interface. This is also fitted with a slot for multi-function interfaces. This slot is designed for connecting a simple multi-function relay, a power control module, or a fan retrofit kit to be used in future.

Table 2.2

AC output of the PV inverter [2]

Rated power at 230 V, 50 Hz	2'500 W
Maximum apparent AC power cos φ = 1	2,500 VA
Rated grid voltage	230 V
AC nominal voltage	220 V / 230 V / 240 V
AC voltage range	180 V to 280 V
Nominal AC current at 230 V	230 V 10.9 A
Maximum output current	12.4 A
Maximum output current in the case of faults	12.4 A
Total harmonic factor of output current at AC total harmonic factor < 2 %, AC power > 0.5 nominal AC power	≤ 4 %
Rated grid frequency	50 Hz
Operating range at AC grid frequency 50 Hz	45 Hz to 55 Hz
Feed-in phases	1

2.3 Heat pump – Cooling machine

Qualitative and quantitative room air heat rejection (also called room cooling) is the purpose of a SAC system. According to the second law of thermodynamics, heat cannot spontaneously flow from a colder location to a hotter area. The heat pump uses AC electricity to transfer the heat energy from the low-temperature loop (cold side) to the hot energy loop (hot side). The vapour-compression cycle is mostly used in heat pump machines, and in our case – in the pilot PV-SAC system. The vapour-compression cycle is based on the principle of reversed Carnot cycle.

The HP loop is divided into two parts with a vapour compressor and an expansion valve. The low-pressure loop part is called HP cold side, and the high pressure loop part – HP hot side. The vapour compressor consumes electricity for pumping up refrigerant from the cold side of HP to its hot side. In the vapour-compression cycle two heat exchangers are used (evaporator on the cold side and condenser on the hot side, (see fig. 2.4). Both heat exchangers are of water-water type due to using liquid brine in cold and hot loops of PV-SAC.

In the heat pump evaporator, the brine releases its energy to the refrigerant, which is then vaporized and compressed in the compressor. The refrigerant, the temperature of which has now been raised, passes to the condenser where it gives off its energy to the heating medium circuit and, if necessary, to any docked water heater. If there is a greater need for heating or hot water than the compressor can provide, there is an integrated immersion heater [7]. It should be noted that heater is not used in our PV-SAC experiments.

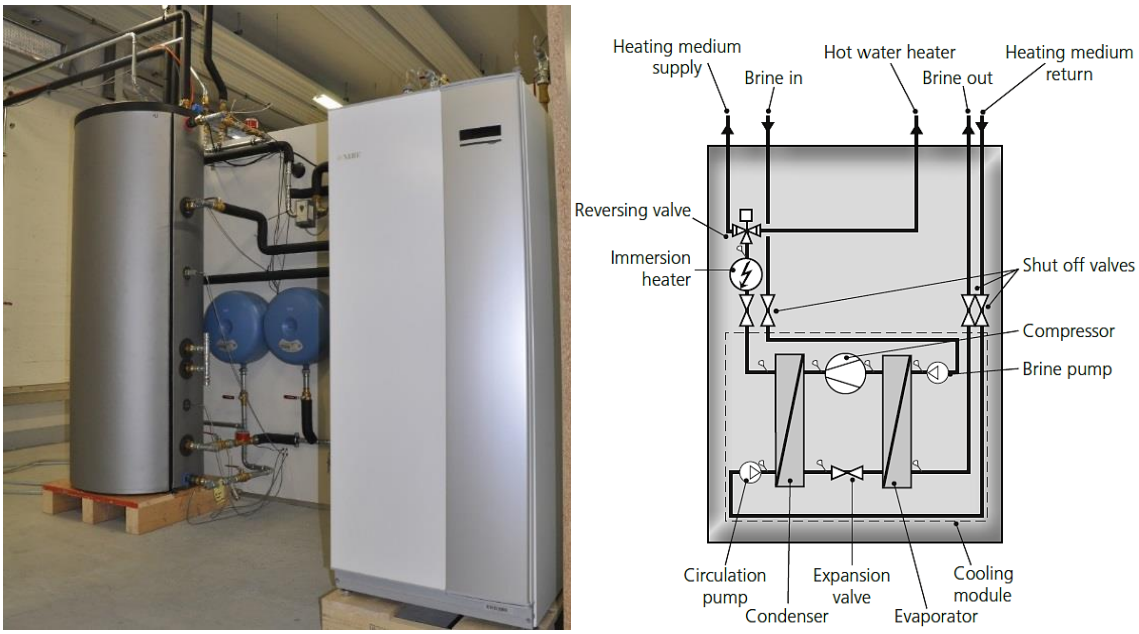

Fig. 2.4. (left) Hot Storage unit and cooling machine;
(right) Schematic of the heat pump design [7]

In the PV-SAC pilot system, small-scale and highly efficient industrial heat pumps are used. The nominal cooling power of heat pump is 5 kW_{cold} [7].

Decreasing the energy consumption in a long-term operation is reached by using a speed-variable compressor, which functions according to the prevailing heating demand. Speed variation of compressor is done with inverter. Low-energy circulation pumps and flexible hoses are integrated in HP. The liquid brine circuits can be connected on either side. Controllable expansion valve is used for dosed refrigerant expansion to the low-pressure loop.

A HP can be driven using AC 1x230V, 3x230V, or 3x400V on a standard frequency of 50 Hz.

Table 2.3

Coefficient of performance of the heat pump including two pumps of hot and cold loops

Cold circuit T / Hot circuit T	**0/35**	**0/45**	**10/35**	**10/45**
Rated output, kW	3.15	2.87	4.3	3.98
Electrical imput, kW	0.67	0.79	0.66	0.83
COP	4.72	3.61	6.49	4.79

* Output data according to EN 14511:2011 nominal (50 Hz)

The coefficient of performance (COP) of heat pump is mainly dependent on the temperature difference between the hot and the cold loops. The temperature itself also affects the efficiency of cooling, being based on the physical parameters of refrigerant, and more

specifically on its vapour-condensate temperature. A heat pump uses 1.16 kg of R407C refrigerant.

Such a heat pump has hot and cold loops with internal automatically controlled pumps. When the compressor is running, the required operational speed for the pumps is set automatically to obtain the optimal temperature difference between the supply and the return lines. This means that the operational speed correction is to be set at the beginning of cooling process.

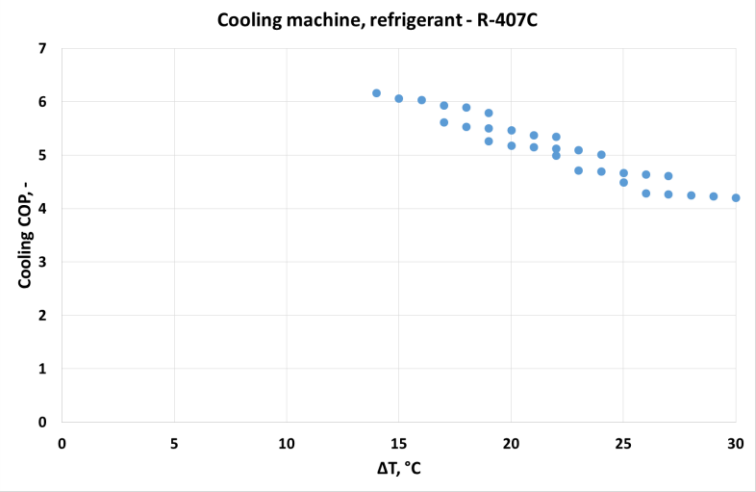

Fig. 2.5. Coefficient of performance (COP) vs. temperature difference ΔT
of the cooling machine including hot loop and cold loop circulation pumps of PV-SAC

The nominal flow of brine is 0.18 l/s on cold side, and 0.08 on hot side at 50Hz. The pumps are speed-variable, so the flow rate is from 0.03 l/s to 0.52 l/s on cold side, and from 0.03 l/s to 0.33 l/s on hot side. The values of pump flows can be decreased with hydraulic resistance of PV-SAC components. The highly efficient brine pumps are designed for the minimum energy consumption. Therefore, the requirements for pressure losses are ≤ 69 kPa on cold side and ≤ 64 kPa on hot side at the nominal flow rate. This sets the limits for the number of measuring elements. It should be noted that there is a problem as to installation of conventional system in non-research application. The hydraulic pressure losses in conventional PV-SAC systems are less than a third of the maximum set for the PV-SAC experimental system, where a range around 10 kPa is set for such losses including those from all measuring elements. The operating pressure in cold and hot loops should be in the range from 0.05 MPa to 0.45 MPa.

The weight of a complete heat pump is 150 kg, the most of which is that of cooling module (~90 kg). The cooling module consists of a vapour compressor, a condenser, an

expansion valve, an evaporator, hot- and cold-side pumps, temperature and flow sensors, and connection pipes, see fig. 2.4. The HP parts not included in a cooling module are the covering body, the control box and the armature for connection to the hydraulic and electric networks of the building. A DHW 100 l tank can optionally be included in HP (though absent in the experimental PV-SAC system). Advantage of such a heat pump is the easily removable cooling module, which reduces the time to be spent on system adjustment and repair.

The HP under consideration is made on a robust frame with durable panels and effective soundproofing for the best possible comfort. The pump cooling power is limited at 5 kW for reducing the noise level. Noise output (according to EN 12102) at 0/35 is from 36 dB to 43 dB. The sound pressure level calculated (according to EN ISO 11203) at 0/35 and a distance of 1 m is from 21 dB to 28 dB. The pump cooling power can be increased up to 6 kW, but in this case the noise output will increase up to 47 dB.

2.4 Cold distribution: cooling ceilings

The room heat rejection is done by radiant ceiling panels – a cooling ceiling.

A radiant cooling system refers to a temperature-controlled surface that cools the indoor temperatures by removing sensible heat and where more than half of heat transfer occurs through thermal radiation. [18]

Fig. 2.6. Cold distribution element: cooling ceiling, type Zip

Cooling panels are installed 0.2 m under the ceiling. The panels use no electrical energy and are totally maintenance-free. Since they do not disperse any dust, they help prevent allergic reactions and colds. Four lines of steel pipes are connected at the upper side of cooling ceiling, to which brine is flowing from the cold storage. The temperature of brine is controlled with a dew point sensor at the mixing valve before the inlet of cooling ceiling. A portion of brine recirculates in cooling ceilings, and another portion is exchanged in the cold storage unit. The

temperature of cooling ceilings is constantly kept over the dew point (including a 2 °C margin). This is done for protection from condensate appearance. Smooth surface is galvanized and also coated with a high-quality polyester paint.

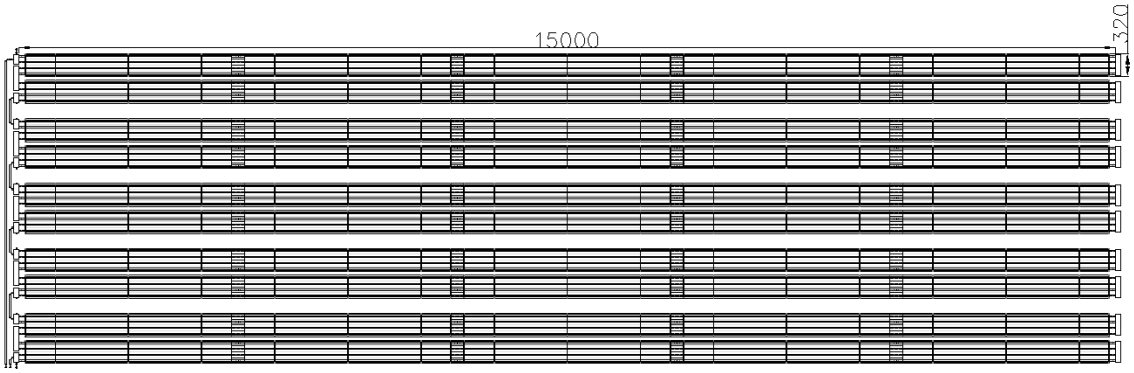

Fig. 2.7. Hydraulic connections of the cold ceiling units

Cooling ceiling consists of 50 cells, see fig. 2.7. The cells are 3 m long and 0.32 m wide, all of them being series-connected. Conventionally, there are five rows of cell connection. The rows have two lines, each line including five cells.

The top of cooling ceiling is covered with stone wool insulation. Specific cooling output with insulation is 11 W/m^2/K [6]. The total area of cooling ceilings is 48 m^2. Non-isolated pipes also participate in heat exchange. These pipe lines extend from the mixing valve to the cooling ceilings and between them. The cooling output of cooling ceiling is 535 W/K including non-insulated pipes. The maximal operation temperature is 95 °C.

Short operating time of cooling ceiling is due to its low inertial mass and low brine mass. The net weight of a cooling ceiling is 120 kg with insulation and without brine. The volume of brine is almost 0.16 m^3. The maximum operating overpressure is 0.5 MPa.

2.5 Outdoor heat rejection unit

The biggest part of hot side heat is rejected to outdoor air. For this purpose a heat rejection tower (also called Outdoor Unit (OU)) is used. The nominal OU power is 5.35 kW$_n$. The main OU component is the brine-air heat exchanger. Air from a fan is blowing over heat exchanger and enhances the heat transfer from its external surface to the outdoor air.

A proportion of rejected heat ($\dot{Q}_{ou}$) per 1 K of the difference between the inlet brine temperature and the outdoor air temperature determined from measurement results. The results show that $\dot{Q}_{ou}$ is 502 W/K.

The OU weight is 63 kg – mostly that of the aluminium heat exchanger having 34.3 m^2 external surfaces.

The 200 W fan operates on 3-phase AC 400 V, 50 Hz; its diameter is 0.5 m, and nominal revolutions per minute is 640. The nominal air flow at fan operation is 4100 m^3/h.

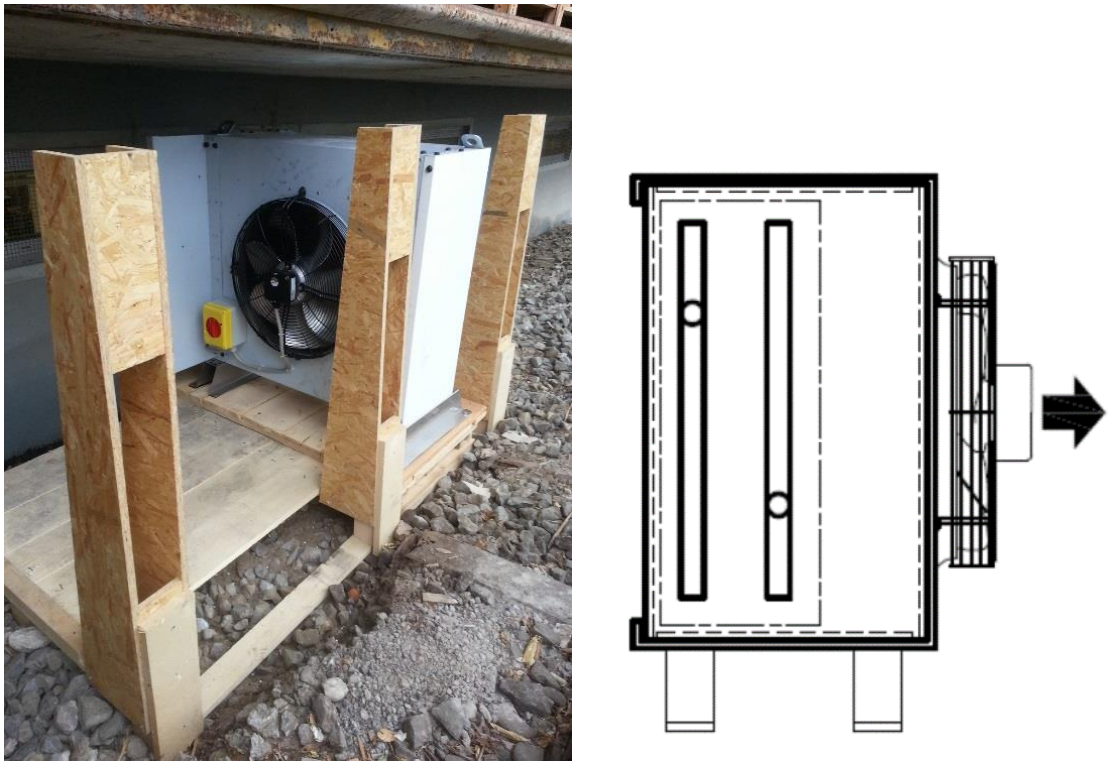

Fig. 2.8. Heat rejection unit / heat exchanger (outdoor unit, OU)

The outdoor unit shown in fig. 2.8 is mounted vertically near the wall. It is placed on the southern side of building but under a balcony in the shadow. The noise produced at fan operation in front of OU is 30 dB, and on the side – 10 dB. Between the heat rejection tower and neighbour living buildings there is an open area. Since the air conditioning system is intended for human comfort and not for producing new irritants, the noise protection wall is placed in front of the building after OU – i.e. the system should be perpendicular to this wall. In this case, noise will be considerably weaker without reducing the OU heat rejection rate.

The OU is designed for operation with brine – such as 20 % ethanol (C_2H_6O)-water mixture. The brine flow should be turbulent in order to ensure the qualitative heat transfer from this brine to the heat exchanger plates. The brine nominal flow through OU is 0.28 l/s, which is 150 % of the heat rejection pump flow. Nevertheless, a turbulent flow in the heat exchanger has been reached.

2.6 Hot storage

A portion of heat is rejected to hot storage (HS), which presents a water tank with insulation. Into the tank, a heat exchanger of the internal coil type is integrated, which separates brine and water. The exchanger consists of two parts, with the first being at the top and the second – at the bottom of tank.

The nominal volume of the tank without the coils is 500 l, and its volume with immersed coils is 445 l. The external surface is 4.3 m^2 of the upper coil and 1.8 m^2 of the bottom one. The water tank and the coil-wound heat exchanger are of stainless steel. The maximum operating temperature is 110 °C, and the maximum operating pressure is 1 MPa.

The heat storage (HS) tank is 1.86 m high and 0.6 m in diameter. It has a polyurethane foam thermal insulation with a thickness of d=50 mm on the cylinder and 97 mm on the top. The thermal conductivity of this insulation is λ=0.03 W/(m·K). The total weight of the empty tank with coil heat exchangers and insulation is 210 kg.

2.7 Domestic hot water

The preheating of domestic hot water (DHW) is done via heat rejection through the hot storage tank.

The DHW daily consumption is 200 l, which corresponds to the consumption of a single family house. The cold water inlet is at HS bottom, flowing to it from the district drinking water network. The DHW consumption meets the corresponding standards [18], being the same every day. The incoming water temperature in winter is around 5 °C, and in summer – around 15 °C. The DHW supply temperature is 50 °C. Preheating based on the PV-SAC technology is done to the greatest extent, while after-heating is done using the primary heat source. The mixing valve should be placed after HS or after the primary heat source due to the reasons of safety for DHW consumers. Cold water and HS outlet water should be mixed in the case of HS temperature increasing over the DHW supply temperature. Since this latter is mostly over 50 °C, such mixing makes the hygienic dangers minimal.

The maximum HS temperature is 57 °C, being limited due to specific brine and heat pump properties. The maximum temperature difference in HS is 52 °C, which means that up to 27 kWh of heat energy can be stored there. The daily energy consumption for DHW heating is from 8.1 kWh to 10.5 kWh, depending on the temperature of incoming cold water.

2.8 Cold storage

Cold storage (CS) is integrated as a cold brine buffer. On the one hand, it allows preparation of the necessary cold in advance. In this case, at the outdoor air or HS temperature decreasing the heat rejection potential, and, consequently, the COP of HP are increasing. On the other hand, this reduces the cooling power peaks at the maximum cooling demand. Besides, this allows reducing the number of start/stop switchings of HP and of the pump on cold side. Therefore, this increases the lifetime of this unit and of the PV-SAC system as a whole.

The cold storage presents a 477 l tank, in which up to 7 kWh of cold can be stored. The CS tank has no internal heat exchanger, is 1.92 m high and 0.7 m in diameter. Its envelope is covered with a polyurethane foam insulation. The thermal conductivity coefficient of CS insulation is λ=0.03 W/(m·k). The insulation has a thickness of d=50 mm thick on the cylinder, 50 mm on the top, and 50 mm on the bottom. Its weight with insulation is 120 kg, and the maximum operating pressure is 0.3 MPa.

The cold storage tank is connected to two loops. First of them is cold loop between the heat pump and the tank. This loop has two inputs at the CS bottom and middle levels, while the output is on the top level of CS tank. A three-way valve opens the brine input between the bottom and middle levels of the tank, thus making it possible to cool the whole tank or only its upper part.

The second loop is that of cooling ceiling between the CS and the ceiling. The 2nd loop has one input on the tank top and one output at its bottom. In total, the tank has 16 threaded holes. At the bottom, middle and top levels three temperature sensors are installed.

The cooling ceiling pump is meant for permanent brine flow in the ceiling. The mixing valve controls the brine recirculation and its exchange in CS tank. Therefore the flow rate is not constant between CS and the cooling ceiling.

This type of connection reduces the probability of water hammer and its impact.

2.9 Heat transfer fluid: thermo-physical properties of the brine

In experiments water was replaced by brine in order to ensure the system's operation at the water freezing temperature. The minimum operating temperature of heat pump is -11 °C.

As the brine, in the PV-SAC experimental system a water-ethanol mixture is used. The ethanol mass is 16.16 wt.%, and its content by volume is 20 vol.% at the standard ambient temperature and pressure. The brine is of transparent-blue colour and its alcohol smell allows sensing leakages.

The brine freezing temperature is -10.4 °C, and the boiling temperature is 86 °C. Its density (ρ_b) is 977 kg/m^3 at T_b = 20 °C, and heat capacity (C_b) is 1191 W/(kg·K) at the same temperature [29]. The viscosity of brine is 5.61 mm^2/s. Its boiling temperature is 87.5 °C [19], which is less than the experimental system's maximum operating temperature. Therefore, the high safety requirements are applied.

The heat capacity ($c_p(T)$) and the density $\rho(T)$ of the brine are depending on the temperature. Corresponding values of these parameters were taken into account in the calculations of energy flows.

In the temperature range of T= 0 °C to 60 °C the heat capacity of the brine varies in the range around 2.51 %. The c_p minimum is at T_{br} = 26.9 °C. The heat capacity dependence of the brine temperature is shown in formula (2.1):

$$C_b = 0.0000280328\ T_b^2 - 0.0015099591\ T_b + 1.20951072 \qquad (2.1)\ [51]$$

Fig. 2.9 shows a comparison of heat capacity of water and brine. Figure are based on equations 2.1 and theoretical heat capacity dependence of the pure water temperature.

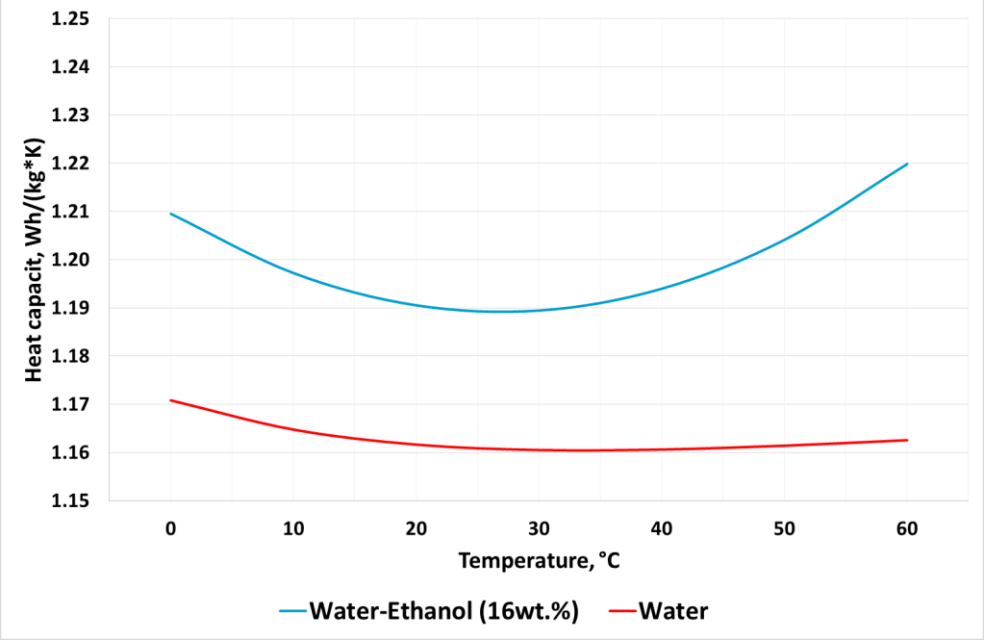

Fig. 2.9. Heat capacity of water and of 16 wt.% water-ethanol mixture (brine)

In the temperature range of T=0 °C to 60 °C the density (ρ_{br}) of the brine is decreasing by 2.69 %. The density in function of temperature is expressed in equation (2.2):

$$\rho(T) = -0.000003T^2 - 0.00025T + 0.98368 \qquad (2.2)[51]$$

A comparison of the density of water and the water-ethanol mixture (brine) is shown in figure 2.10.

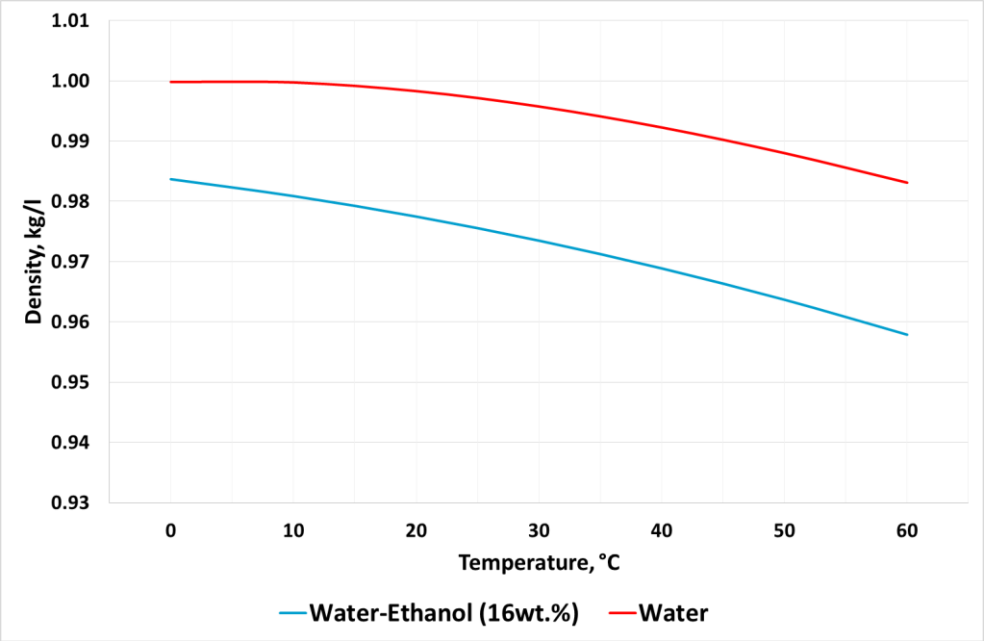

Fig. 2.10. Density of water and of 16wt.% water-ethanol mixture [51]

The hydraulic system elements are mostly made of stainless steel, while some of them are of aluminium and copper. Therefore, inhibitors are added to the brine.

2.10 Piping

In the PV-SAC experimental system, 18-28 mm stainless steel pipes are used. In the most of pipe and armature connections a “press-fit” connection technology is employed. Convenient and clamp ring-type threaded connections are used to connect HP, OU, HS, CS, CC and pumps.

The pipes and armature are thermally insulated using for this purpose polychloroprene-based synthetic rubber. Such insulation is suitable also for chilled-water and refrigeration systems. Its minimum service temperature is -50 °C, with the maximum of 150 °C. The insulation protects against thermal losses, condensation and moisture accumulation on pipes at cold side. Its heat conductivity is $\lambda_{insulation}$ (0 ºC) $\leq$ 0.033 W/(m · K). The thickness of insulation on pipe is $\geq$ 2 cm. Specific attention is given to insulation of the armature of hydraulic system's parts, which are insulated with a $\geq$ 1cm insulation layer.

2.11 Measurement and data acquisition equipment

To attain the aim of study, highly precise measuring equipment was used. This equipment and its placement allow observing the operation of each of the main components of PV-SAC experimental system. All measuring devices are calibrated. It is possible to monitor and save the data obtained during the system's operation in the data acquisition program. In total, the PV-SAC experimental system contains 40 temperature sensors, 6 electricity counters, 8 flow counters, 4 humidity sensors, 1 air pressure sensor, and 1 solar irradiation sensor. Additionally, 8 manual thermometers, 3 manual flow meters and 3 manual pressure sensors are installed for live security monitoring of the system's operation. In conventional PV-SAC systems the number of sensors and their accuracy class should be reduced due to economic reasons and for the sake of simplification.

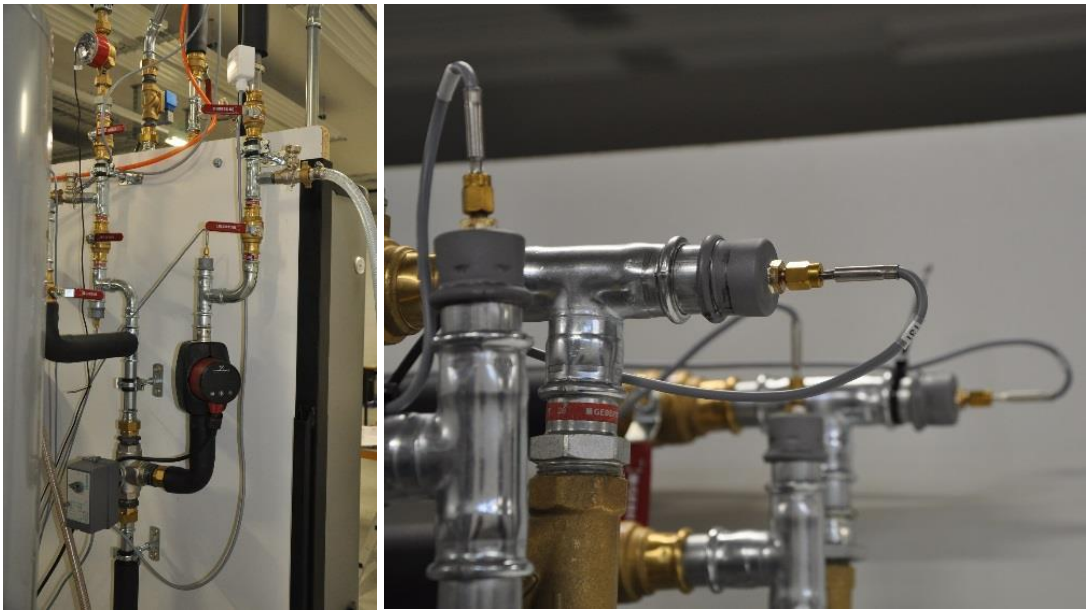

Fig. 2.11. Measuring equipment and active control elements of the system

Measurements of electric energy are done on the DC and AC sides. The PV outcoming current and voltage (cable losses on DC side included) are measured by the meters integrated into PV inverter. The parameters of inverter- produced AC electricity are measured with the AC current, voltage and frequency meters, which are also integrated into the inverter. The accuracy of the voltage measurements is 0.01 V, and of the current measurements it is 0.001 A on both sides. Measurements of incoming DC and outgoing AC powers are done with 1W accuracy, and the accuracy at measuring frequency is 0.01 Hz. In the PV-SAC experimental system three additional electricity meters are installed, which separately measure the electricity

consumptions of HP, OU and other pumps. The accuracy of all electric energy measurements is 1 Wh.

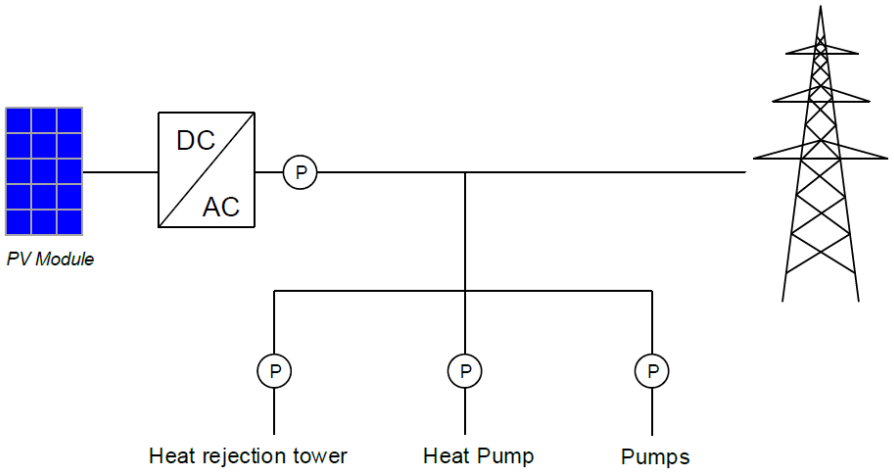

Fig. 2.12. Electricity measuring positions in the PV-SAC experimental system

Flow measurements are done with pull-type flow counters. Six highly precise flow counters are used for flow measurement through the main parts of the experimental system. Flow sensors are shown in fig. 2.13. (marked with symbol “F”).

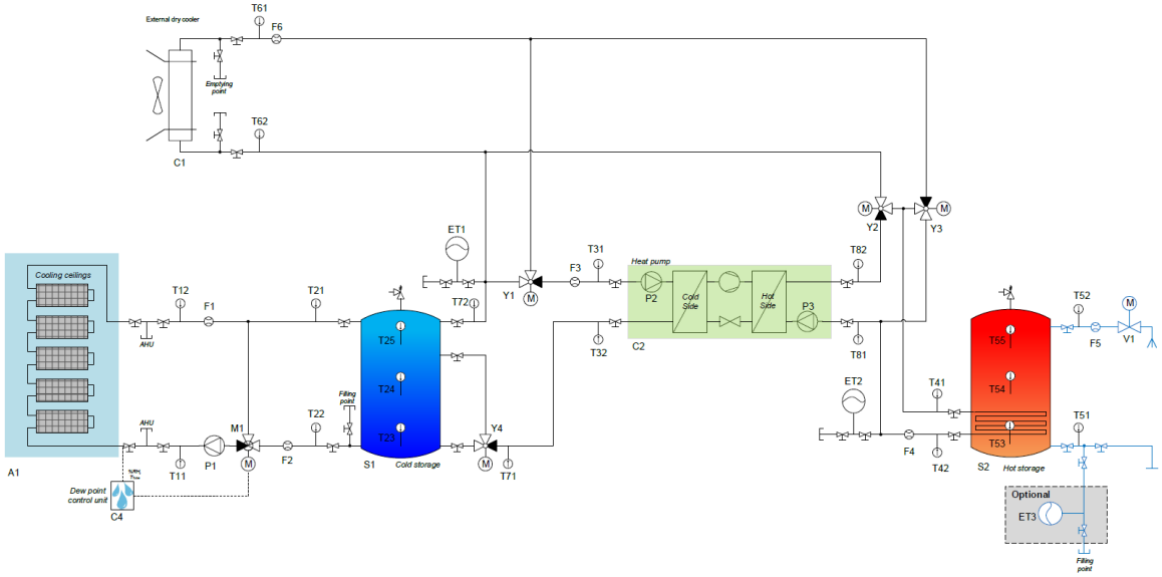

Fig. 2.13. Position of flow counters and temperature sensors
in the PV-SAC experimental system

The temperature sensors measure temperatures of brine, water, and air. Brine and water temperature sensors are mounted in special metal capsules inside pipes and tanks, for which purpose PT100 resistance thermometers (class A, 4 x 0.25 mm^2 wires) are used, with the cable length of 5 m. The temperature range of A class PT100 is from -70 °C to +550 °C, and its

accuracy – from 0.15 °C to 0.27 °C, which is in the PV-SAC operation temperature range. Combination of flow counters and temperature sensors allow accounting the thermal energy.

The heat pump has 11 integrated PT100 B class resistance thermometers, 3 current sensors for each phase, and 2 flow sensors for internal control and energy flow counting. The pump has also high- and low-pressure switches.

The meteorological station makes it possible to determine the key parameter of weather conditions during the PV-SAC operation. It is installed near the PV modules. The station includes sensors for measuring: the outdoor air temperature, air pressure, air relative humidity, and PV module temperature. The range of measurement equipment corresponds to the weather fluctuations at the experimental site (Rapperswil, Switzerland). The outdoor air temperature is measured with the accuracy of 0.2 °C in the temperature range from -20 °C to +50 °C. The resolution of the air relative humidity sensor is 0.1 %, though it measures with the accuracy of 2 % in the whole range from 0 to 100 %. Accuracy at measuring the air pressure is 1.5 hPa in the range from 300 hPa to 1 200 hPa. A 2nd class (highest) thermopile pyranometer is used for measuring the solar irradiance. It is intended for shortwave global solar radiation measurements in the spectral range from 300 to 2800 nm. The thermopile detector measures irradiance up to 2000 W/m² with the response time <18 s and typical sensitivity of 10 μV/W/m² that varies less than 5 % from -10 ºC to +40 ºC [7]. The accuracy of solar irradiation measurement is <1 W/m^2. The module temperature is measured with accuracy 1 °C in the temperature range from -20 °C to +80 °C. The meteo-station collects data with up to 1 min resolution.

An additional air temperature sensor and an air relative humidity sensor are placed near OU. The outdoor air proper parameter is not disturbed by OU operation due to expedient placement of the outdoor air and humidity sensors.

2.12 Conditioning environment

Conditioning environment is an office and a laboratory in one room. It has internal loads from equipment and peoples. The room area is 371.5 m^2 and the floor height is 3.75 m. The room is partly underground. Small windows are on two sides of the walls. Shading does not let direct sun rays penetrate into the cooling room. For heating the room air handling units are employed, which can serve for increasing cooling demand if needed for experiments.

Measurements of room air temperature and relative humidity without PV-SAC operation are done one year in advance.

2.13 Control of the system

To reach a high seasonal energy efficiency ratio (SEER) of PV-SAC self-designed system, a proper control is applied. The control is different in cooling- and non-cooling season.

In a cooling season, the first priority is covering the room cooling demand. The set indoor air temperature is 22 °C, with the maximum comfortable room air temperature being 24 °C. The temperature set for cooling storage is 10 °C. The CS cooling is done in advance, before appearance of cooling demand. Cooling machine – heat pump is used to provide heat transfer from a low temperature environment to a high temperature environment. The HP is power variable and is controlled by its own control box.

The heat rejection to the HR tower or hot storage is controlled by the highest heat rejection potential. To determine this potential regarding HS, the water temperature at the middle level of tank and the internal coil heat transfer coefficient are accounted for. In the HR tower case, the following should be taken into account: outdoor air temperature; OU heat transfer rate; electricity consumption of fan multiplied by primary energy factor.

Free heat rejection of hot storage was observed at the stage of designing PV-SAC technology. Free heat rejection is that from HS to the outdoor air with OU operation and without HP operation. In this process electricity is consumed, with consumers being the OU fan and the hot side pump. Free heat rejection is removed from the system control in compliance with the pre-simulation results (free heating is not used in the PV-SAC).

The non-cooling season control serves for DHW preheating. In this case, some components of PV-SAC operate in the reverse mode, i.e. the OU is a heat source, and its connection is switched to the cold side of HP. The temperature set for hot storage is 50 °C. The aim of this control is to maximally cover the DHW thermal energy demand. The main barrier is here a low outdoor air temperature in non-cooling season. First, this makes freezing dangerous for OU. Second, the low outdoor air temperature increases the temperature difference in cold and hot side of HP. This significantly decreases the heat pump's COP, which might make this mode and the whole system less attractive.

The heat pump is controlled by built-in sensors for flow and return hot side temperatures. Brine return temperatures can, if required, be limited to a minimum.

Control of the heat production can be done in two ways.

In DHW heating regime it is performed based on the “floating condensing” principle – that is, the temperature level needed for heating at a specific outdoor temperature is produced guided by collected values from the outdoor and flow sensors. The room temperature (RT) sensor can also be used to compensate the deviation in RT. [7]

In the second control way, the heat pump delivers heat up to a fixed temperature level. This is known as “fixed condensing”. The automatic heating control system is then replaced by the external unit’s control device [7]

In the PV-SAC experimental system the safety control is installed, which prevents overheating and freezing of system's components. Besides, there is integrated independent control of alarm stop in case of overheating and freezing.

For accrued determination of the system cooling and heating yields as well as of the system's operating parameters, deep investigation should be done.

3 EXPERIMENTAL VERIFICATION OF PV-SAC SYSTEM PERFORMANCE

The pilot PV-SAC system's performance was verified in real weather conditions. The system mostly operated under autonomous regime. Besides, specific experiments have been done with the aim to study thoroughly the heat and mass transfer in the system. Also, the electricity consumption by separate components was evaluated during the tests.

As a result of specific experiments, accurate data of operating parameters have been obtained. First results show that some data of the pilot system's components differ from their technical specification. Therefore, it was important to check and update the data on the parameters and yields of the main system's components: heat transfer coefficients of heat storages; heat transfer coefficient and yield of cooling machine; system's COP and its dependence on the operating parameters.

The following has been verified:

- Cold preparation
    - Heat rejection to the Hot Storage (preheating of tap water)
    - Heat rejection to the ambient through the Outdoor Unit
- Cold distribution
- Free cooling
    - For cold preparation only (charging of the cold storage tank)
    - With cold distribution through the ceilings
- Reverse mode
- HS discharge to DHW (use of DHW)
- HS discharge to the ambient through the Outdoor Unit
- Heat losses of the thermal storages
- Photovoltaic operation
- Autonomous PV-SAC operation

The PV-SAC operation was improved in compliance with experimental results. Therefore some of the tests were performed several times.

3.1 Cold production

Cold production means running the compressor cooling machine in this case. Next, the cooled brine is pumped through the cooling ceilings, which form the cold distribution. There are several options in the cold production operating modes: a) with heat rejection to the hot storage; b) with heat rejection to the outdoor; c) free-cooling. Priority of a specific mode is chosen according to the highest COP value. These values depend on the internal system's parameters (temperatures and flows) and its external parameters (room and weather conditions).

The projected COP is dictated by the system control. This done, the most efficient operating mode is chosen.

Cold production with heat rejection to the hot storage

In this test, heat was rejected only to the hot storage. Starting parameters of the test were similar to those of the system's first start-up. The temperatures were mostly in proximity to the room temperature (+24 °C) in the testing day. The HS temperature was 18 °C due to filling the storage with fresh water from district water supply network. After that HS is heated, its temperature increases and the process of cold production stops.

At the start of test, it is seen in the fig. 3.2 that the temperature distribution is almost equal at all levels of both storages. Results show that the temperature stratification is more evident in the cold storage than in the hot one. The Temperature rise in the middle of hot tank is higher than at the top (for the type and position of the coil heat exchanger used). After operation stops, the temperature becomes higher in top layer due to natural convection.

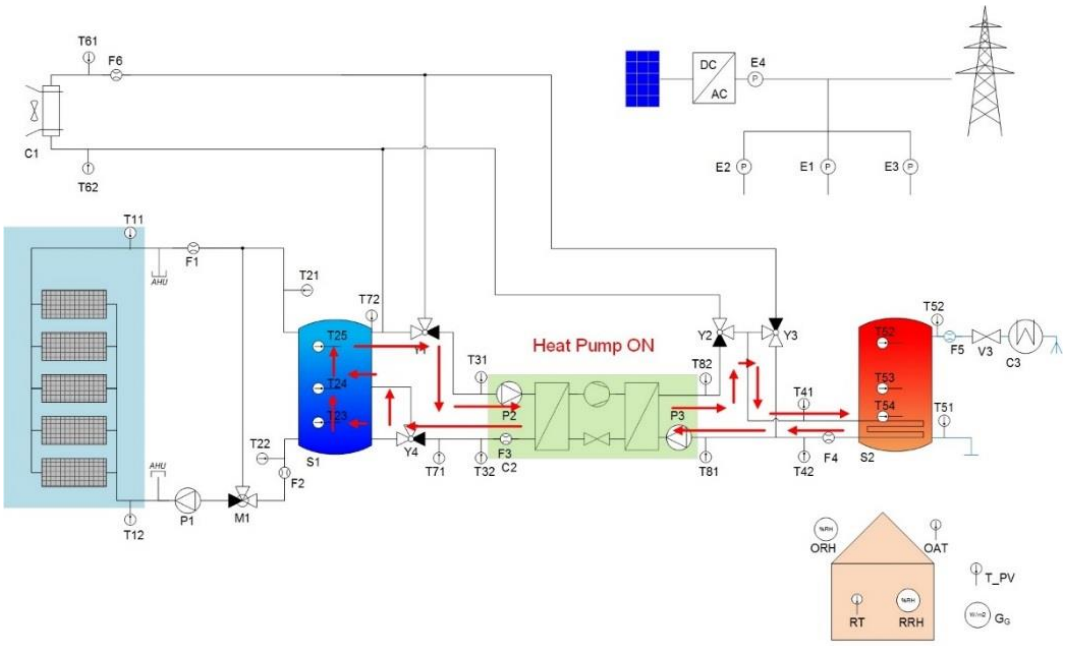

Fig. 3.1. Schematic of cold production with heat rejection to the hot storage

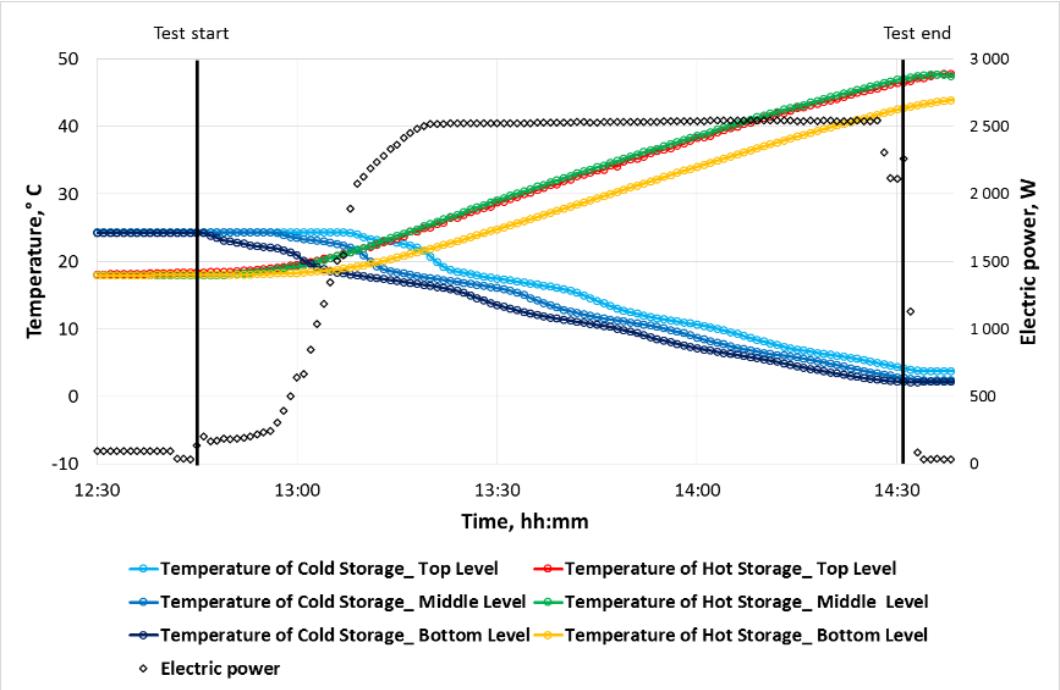

Fig. 3.2. Storage temperatures and electric power of cooling machine during cold production test with heat rejection to the hot storage

The cold storage has no internal heat exchanger. Therefore, cold stratification is here more obvious, with nonlinear temperature changes observed in CS. Such changes receive a plausible explanation at detailed test monitoring. First, cooling machine controls ΔT on cold and hot sides by the speed of circulation pumps. Second, the inlet temperature on the cold side of cooling machine was constant during first 24 min of the test, after which it was blown over freezed for the second time. Also, some small portion of brine with different temperature could be mixed at the bottom level of cold tank (while stratified in several minutes). Thus, these two causes are responsible for the temperature fluctuation at the inlet and, hence, at the outlet of cooling machine on the cold side. Just the temperature fluctuation at this outlet determines the CS temperature.

As seen in figure 3.2., the test duration is 1 h 45 min, which is enough for filling the storages at the start-up parameters. It is a relatively short time needed for system's preparation to the system's filling regime. Since the electricity limitation affects the maximum power of cooling machine as to the PV yield, the time for the system's filling will be extended in autonomous operation mode of the PV-SAC.

Cold production with heat rejection to outdoor air

In this case, heat is rejected only to the outdoor. The starting parameters and conditions of this test are similar to those of previous test, except the temperature of cold storage that can fall to minus degrees at the end of test.

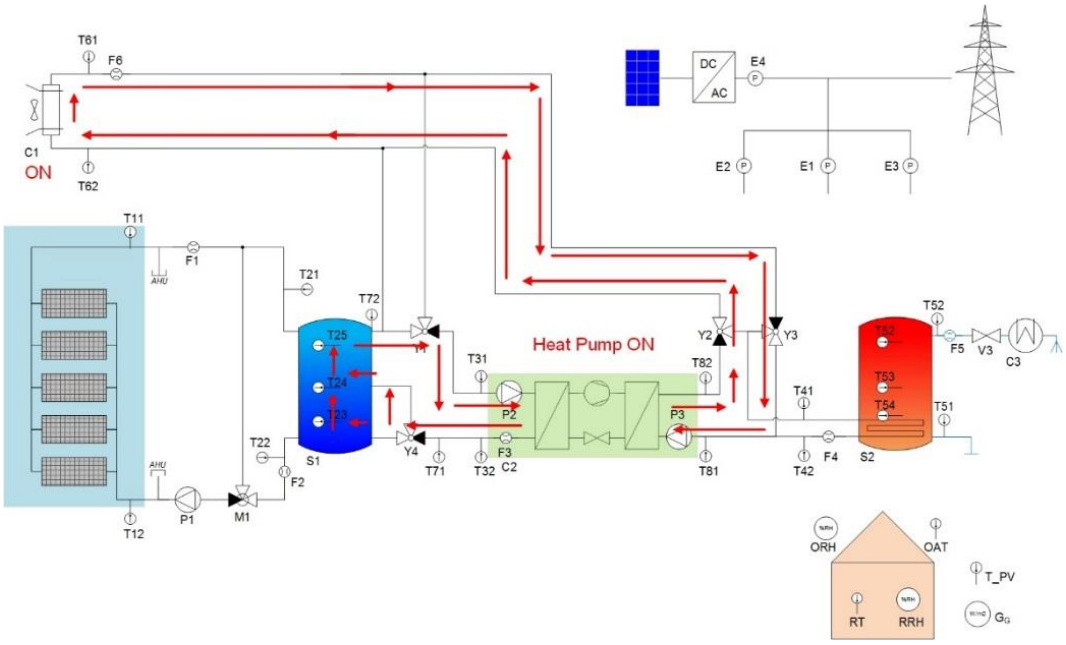

Fig. 3.3. Schematic of cold production with heat rejection to outdoor air

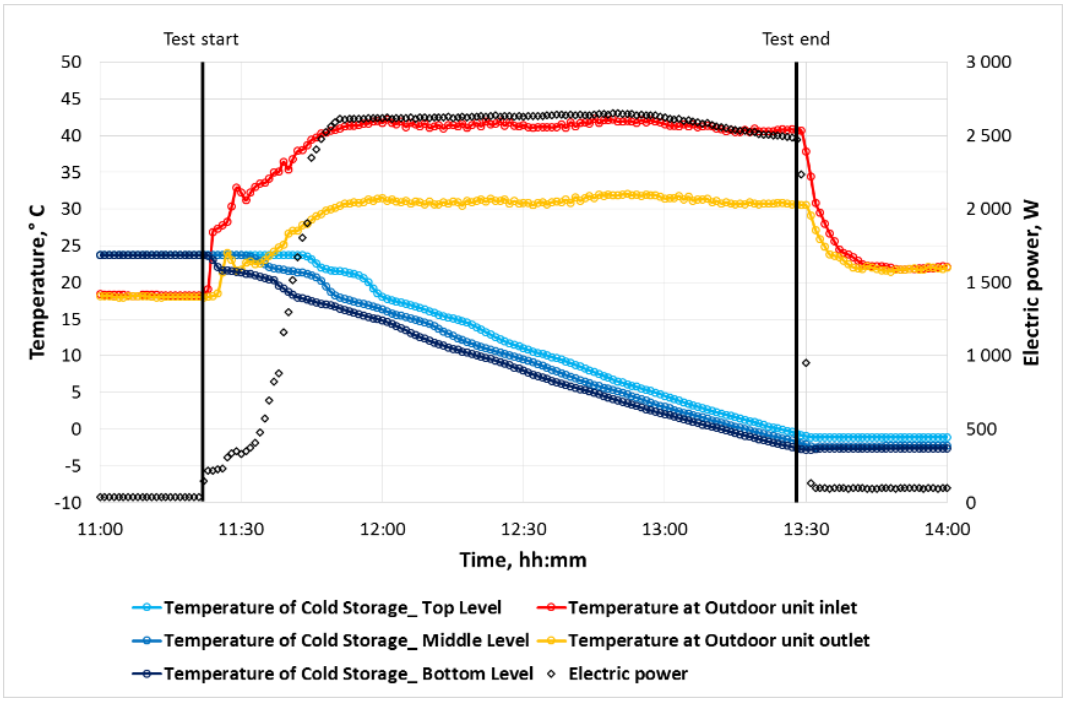

Fig. 3.4. Storage temperatures and electric power of cooling machine during cold production test with heat rejection to the outdoor air

Heat rejection to the outdoor air strongly depends on the outdoor air parameters. The temperature, air humidity, wind speed and direction affect the heat rejection power of outdoor unit. Additional effect could be the direct solar irradiation of outdoor unit. It should be noted that the OU – heat rejection tower has a reflective covering against irradiation in most cases. Moreover, in the pilot PV-SAC the outdoor unit is placed in a shadow.

In the fig. 3.4 the temperature fluctuations could be seen on the cold and hot sides of cooling machine at the beginning of test, while the electricity consumption of cooling machine is affected but minimally.

Since the compressor of cooling machine is speed-variable, the electricity consumption is lower at the beginning of test (see fig. 3.4). The cooling machine is partly operating under load; therefore, compressor is driven at low speed. High temperature fluctuations are absent because of high thermal capacity of heat exchangers on the hot and cold sides of cooling machine.

The electricity consumption starts increasing after the internal part of cooling machine becomes to be warmed-up. It is also shown in figure 3.2 from previous test. The maximum of electric power consumption of cooling machine is in proximity to 2.5 kW_p including running of two circulation pumps. Figure 3.4 shows that the electricity consumption of the system exceeds this value since the OU 200 W speed-variable fan consumes additional electricity. Experiments show that the electricity consumption of fans is from 59W to 62 W in the most of operation time.

As illustrated in figure 3.2 and figure 3.4, electricity consumption is not rising, even at reaching high temperature of the brine. Amount of heat rejected by the OU is increasing with temperature of the inlet brine, since the heat rejection depends on the difference between the brine and the outdoor air temperatures. Therefore, the temperature difference between the inlet and the outlet of outdoor unit remains relatively constant.

Furthermore, all experiments with outdoor unit show that its average thermal power is 502 W per 1K of the temperature difference between the brine temperature and the outdoor air temperature. The average electricity consumption for driving the OU fans is 60.47 W.

3.2 Cold distribution

The cooled brine is delivered to the cold ceiling from the cold storage, which has the minimum operating temperature at the start of test. Before that, one hour CS stabilization is done to exclude additional impacts and prevent distortion of the results. For the stabilization, correct temperature stratification and hence prevention of brine flows is reached. Test duration

(16 h and 10 min.) is determined by full discharge of cold storage, when its inlet and outlet temperatures become almost equal.

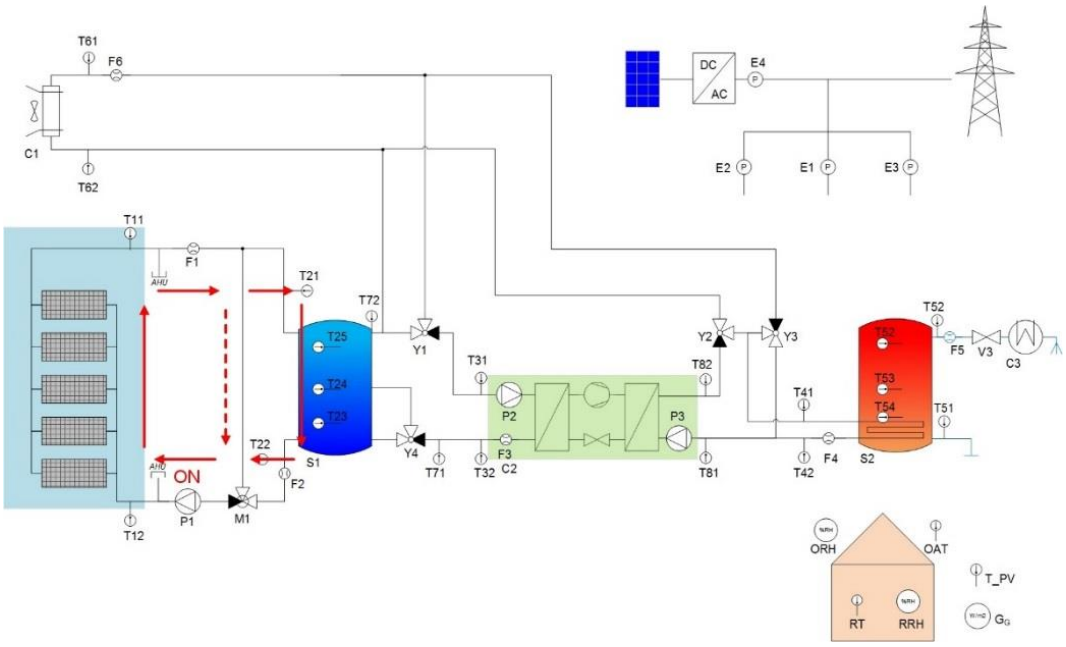

Fig. 3.5. Schematic of cold distribution

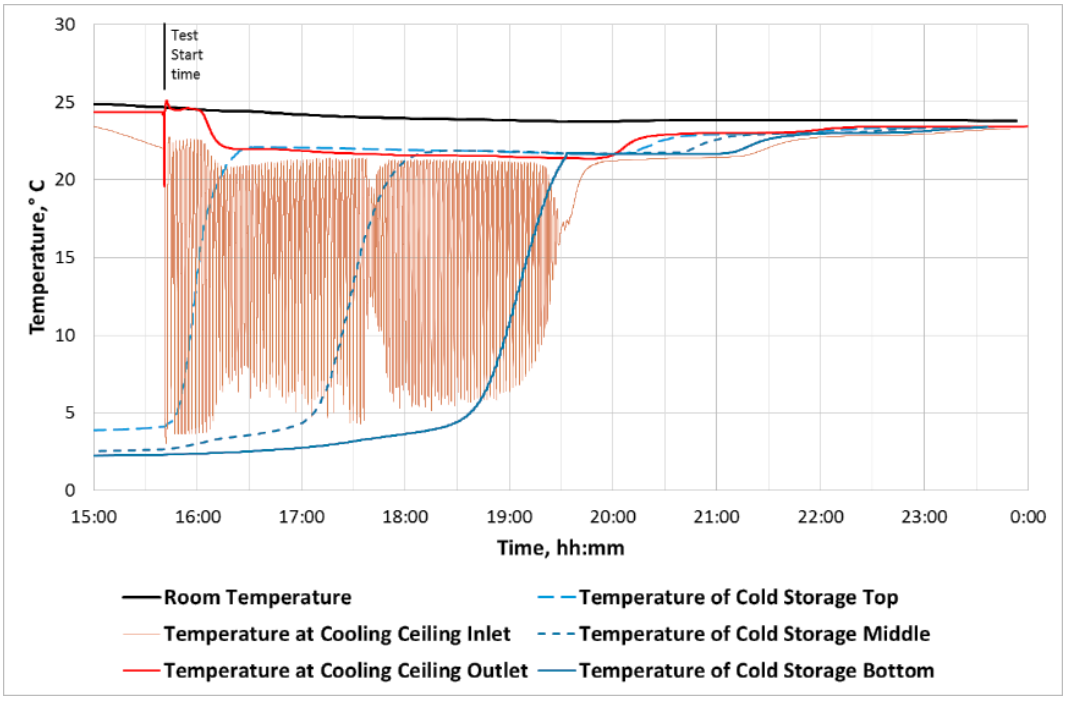

Fig. 3.6. Temperatures during the cold distribution test

The flow speed in cooling ceiling circuit is constant, the amount of cooled brine inlet into which is regulated by a three-way valve. At the temperature of cooling ceiling inlet being less than the dew point of room air, the valve closes the inlet for cooled brine, with only the

recirculation process going. Three-way valve need a time for correct dosing of cooling brine, a definite time is required for valve operation. Considerable fluctuations in the temperature of cooling ceiling are seen in fig. 3.6.

During this test a temperature drop under the dew point is observed (down to 15.1-15.4 °C). The test monitoring shows that the condensate does not deposit on the surface of cooling ceiling, which is explained by high enough thermal capacity of the ceiling. The pipes near the CC inlet and outlet are not insulated, which favours cold distribution. However, some opacity arises on the pipes thus presenting a threat of their corrosion in a long-term use.

The cold storage discharge proceeds in the time interval of approx. four hours, which is seen in the previous figure as a jump on the temperature curve of CS bottom level. It is detected that the cooling power decreases eight-fold in the time less than 15 min. All cooling brine thus circulates via cooling ceiling in one cycle. The 2nd cycle of cold storage discharge is shorter due to coolant temperature becoming higher. The recirculation is not needed any more, since the temperatures are above the dew point.

The experiment was repeated after optimizing the control over the cold distribution.

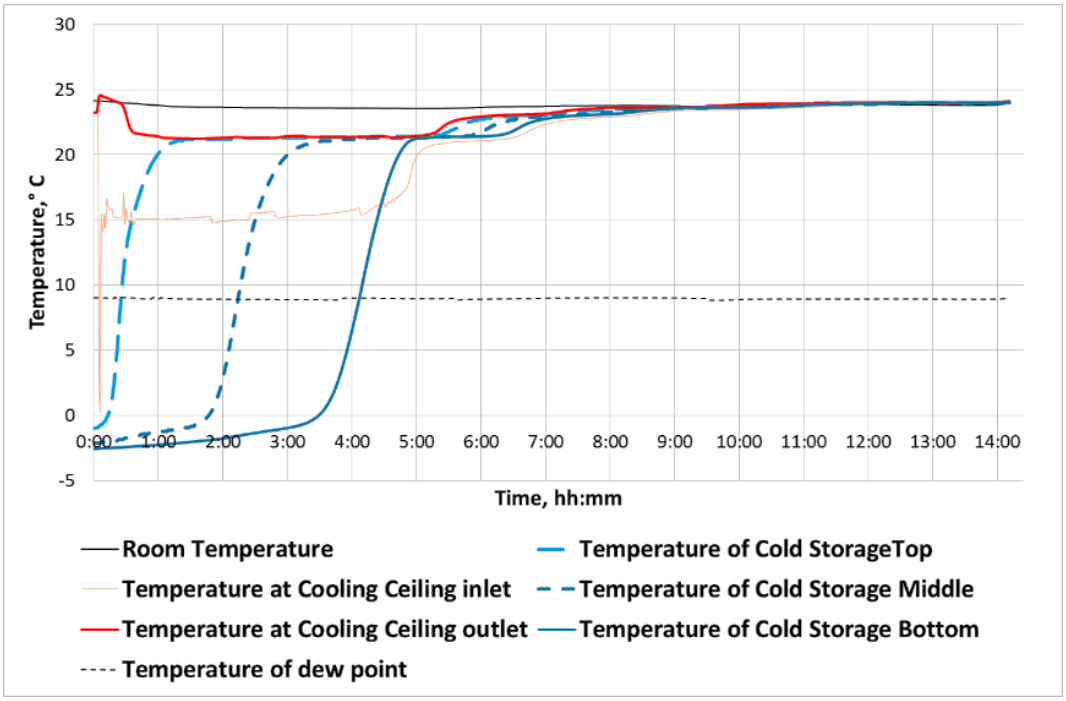

Fig. 3.7. Temperatures during cold distribution second

The three-way valve is operating with delay, which significantly reduces the temperature fluctuations at the cooling ceiling inlet. This also solves the problem of the temperature drop under the dew point. The cooled brine temperature was 4.8 °C less than in the

first cold distribution test, still the inlet temperature was above the dew point. The dew point of the room air was in the lower temperature range as compared with the previous experiment because of reduced humidity of the room air.

The increase in the time of CS discharge is proportional to that in the difference between the cooled brine and room temperatures. As shown in fig. 3.6 and fig. 3.7, the outlet temperature of cooling ceiling is in proximity to the RT in the first 22 minutes of the test. This presents one cycle of the heat carrier's going through the whole cooling ceiling. The test shows that from 88 % to 91 % of the coolant potential energy is absorbed in one cycle.

3.3 Free cooling

Due to efficiency and energy saving reasons, a free-cooling option is realized and applied in the PV-SAC system. The free cooling is a process of cold production without cooling machine operation. Heat is delivered from the cold storage directly to the outdoor unit, then it is rejected to the outdoor air. The only electricity consumers are here the circulation pump and the fan of outdoor unit.

The results of monitoring show that the free cooling is needed but seldom. For its operation the outdoor air temperature must be lower than the CS temperature. In practice this happens at night and early in the morning. Since at night no PV electricity is generated, the free cooling could be performed only early in the morning. The cold production by cooling machine starts at high enough electricity generation by PV array.

Two free-cooling experiments have been run:

- for cold production only,
- with cold distribution.

Free cooling for cold production

The free-cooling test is switched ON early in the morning, when the switch of cold production by using cooling machine was OFF. The results of continuous free-cooling operation is illustrated in fig. 3.9.

Brine temperature follows the air temperature, with a delay owing to high thermal capacity of the brine and its large amount in this circuit. As a result, the brine temperature curve changes smoother than that of air temperature. Free cooling should be stopped before a reverse process starts as illustrated in fig. 3.9 for the time from 7:48 to 16:04.

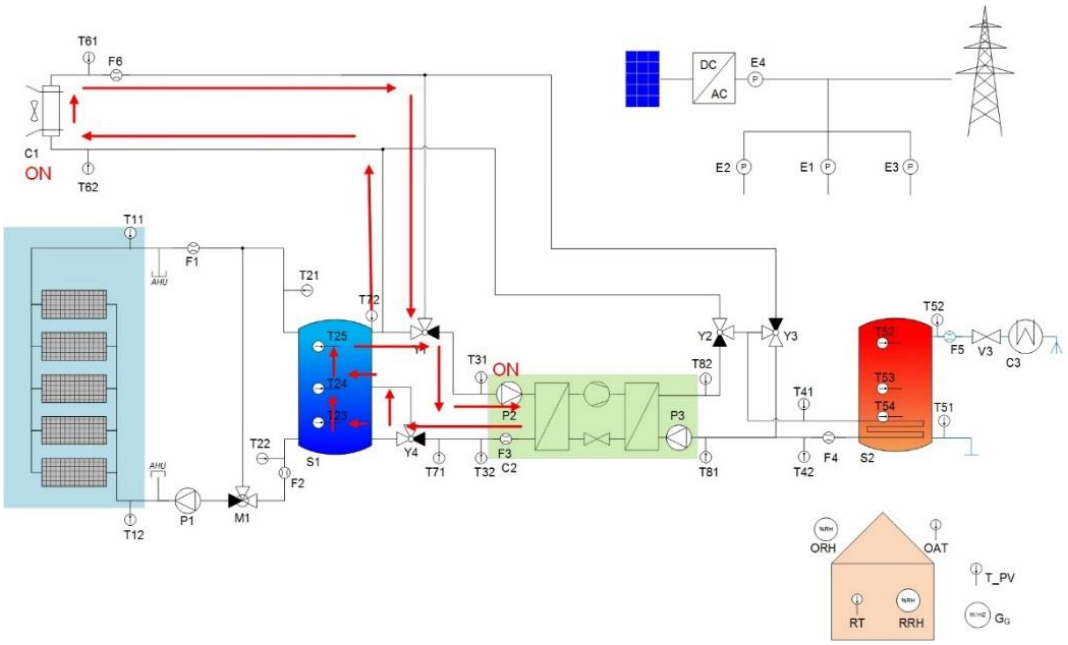

Fig. 3.8. Schematic of free cooling for cold production

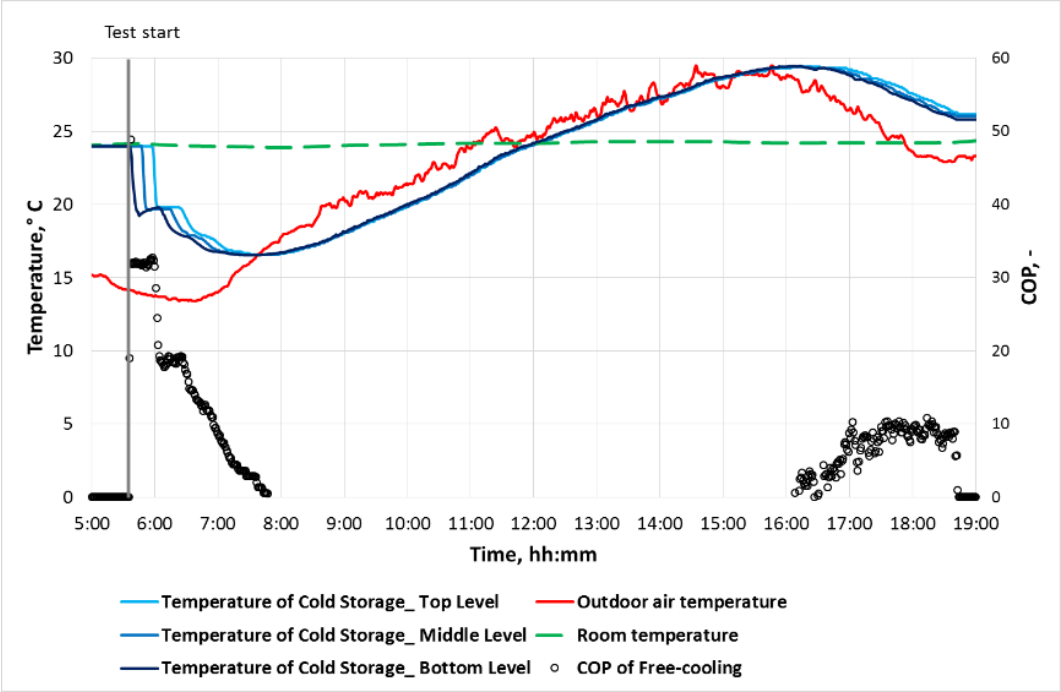

Fig. 3.9. Temperatures and COP during free-cooling operation for cold production

The temperature difference between the brine and the outdoor air is low in this case. The brine temperature approaches the outdoor temperature quite fast. If the brine speed is low, it reaches the outdoor temperature at a halfway of internal pipeline of the outdoor unit. From another point of view, increase in the flow speed leads to a high electricity consumption, which

can reduce the COP of free-cooling operation mode (the speed control of circulation pump has not been studied here and will be considered in the following step).

In this experiment the circulation pump runs at the full speed. The biggest portion of heat is rejected during one cycle of the whole brine running from the cold storage through the outdoor unit. Duration of this cycle is 26 minutes. The full heat rejection could be done in 2-4 steps. The highest efficiency of heat rejection is in the first cycle.

The circulation pump consumes 65 W and the outdoor unit – 60W. Therefore, in total 125W are needed for driving in the free-cooling mode. This is up to 21 time less than that for cold production by cooling machine. The COP decreases to < 3 at a temperature difference below 0.38 °C between the brine and the outdoor air temperatures. It should be stressed that only a relatively small portion of heat could be rejected using the free-cooling method

In the following step, free cooling could be tested without operation of the outdoor unit fan, which reduces almost by half the electricity consumption of free-cooling driving. However, this will reduce the air flow via OU, and, as a result, the heat rejection will also be less (experimental study of this process is beyond the scope of this thesis.

Free cooling with cold distribution

The second free-cooling experiment is on the cold distribution with the cold production at the same time. The cold from cold storage is distributed by the cooling ceiling. This type of free-cooling operation is met much more often than the studied above. Therefore, the relevant analysis would help in understanding the PV-SAC processes.

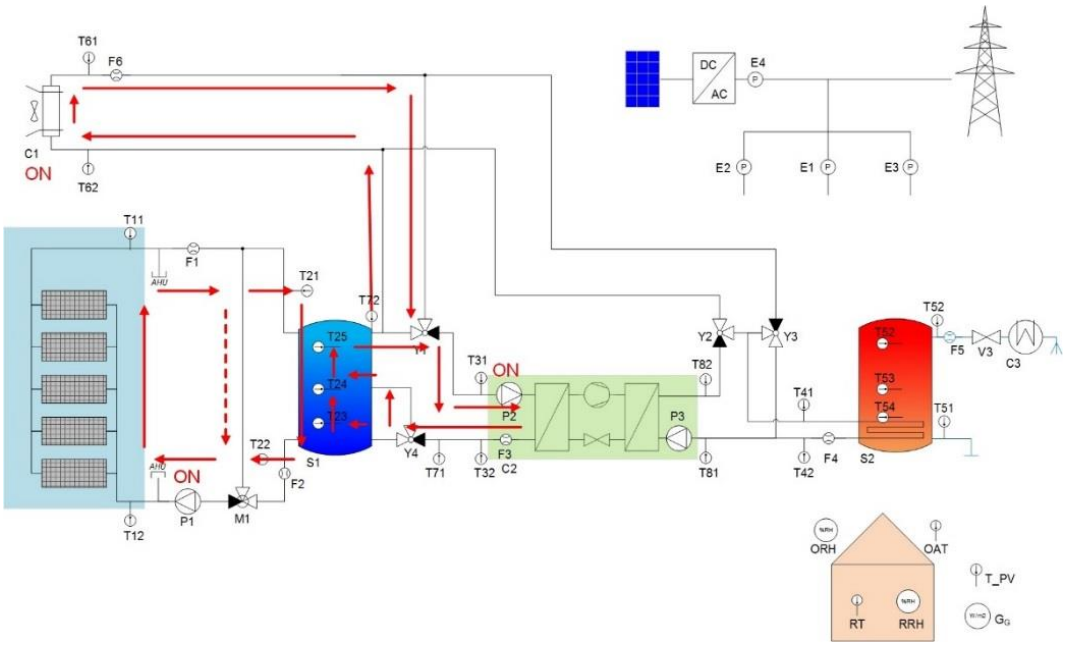

Fig. 3.10. Schematic of free cooling with cold distribution

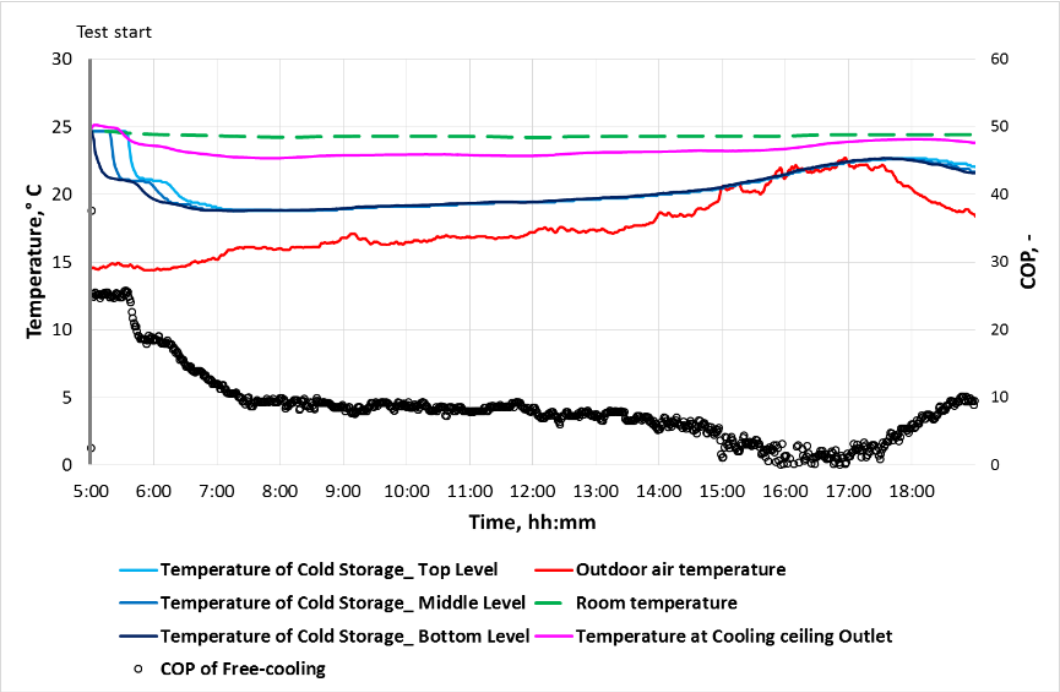

Fig. 3.11. Temperatures and COP during free-cooling operation with cold distribution

The temperature of cooling ceiling inlet – similar to that at the cold tank bottom level – is above the dew point, so no mixing with recirculated brine occurs.

The cooling ceiling inlet temperature is up to 5.6 °C less than room temperature (RT). Figure 3.11 shows that the return temperature differs only by 1.6 °C from RT. The energy meters also show that the greatest part – up to 74 % of the potential heat energy – is absorbed by cooling ceiling. This is less than in the previous experiments with a higher difference between the indoor air and the brine temperatures.

Figure 3.11 shows that efficient use of free cooling may be longer – mainly due to the outdoor temperature being lower than the indoor temperature. A relatively large temperature difference makes the COP higher than 10 at the begging of test (similarly to the previous experiment). Therefore, free-cooling operation is worthwhile and profitable for at least short periods of time.

Free-cooling options of heat rejection to the hot storage were tested at the pre-simulation stage. The results show that this regime lasts less than two hours in a year. Therefore, this type of the system's operation is excluded.

3.4 Reverse mode

A partly reverse mode is used in non-cooling seasons. This could also be called “winter mode”. The reverse mode is used only to generate heat for the DHW; then for this process the main heat source is outdoor air, and the cooling machine operates as a heat pump. Although the Pilot PV-SAC system is not designed for room heating, such possibility is estimated at the system's simulation in the following chapters.

Operation in the reverse mode is possible up to -9 °C of the outlet temperature on the heat pump cold side. The control strategy includes freeze protection as well as defrosting possibility. The maximum heating temperature of heat pump can be up to 62 °C, while the hot storage temperature is lower – from +45 °C to 50 °C. Figure 3.13 illustrates the difference between the two previously mentioned temperatures. The results show that the system could be run until the full charge of hot storage without cool-down stop of the heat pump.

At the beginning of experiment, hot storage temperature was in proximity to RT. The experiment was continued until the HS became fully charged and the temperature rose above 50 °C at all levels of the tank. In the experiment the full charge time was 2 h and 21 min.

Experiment monitoring shows that the temperature at the middle level of hot tank rises faster than at its top level. The top layer temperature becomes higher only after operation due to stratification. Therefore, both temperature sensors – at the middle and at the top levels of hot storage should be used to timely detect the critically high temperatures.

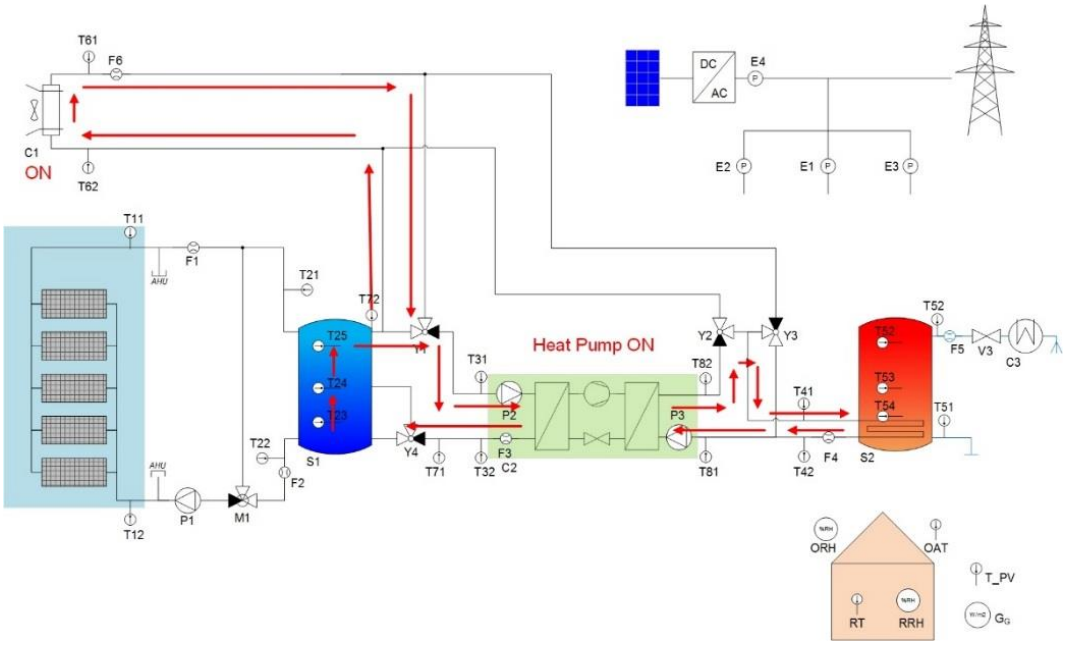

Fig. 3.12. Schematic of reverse mode

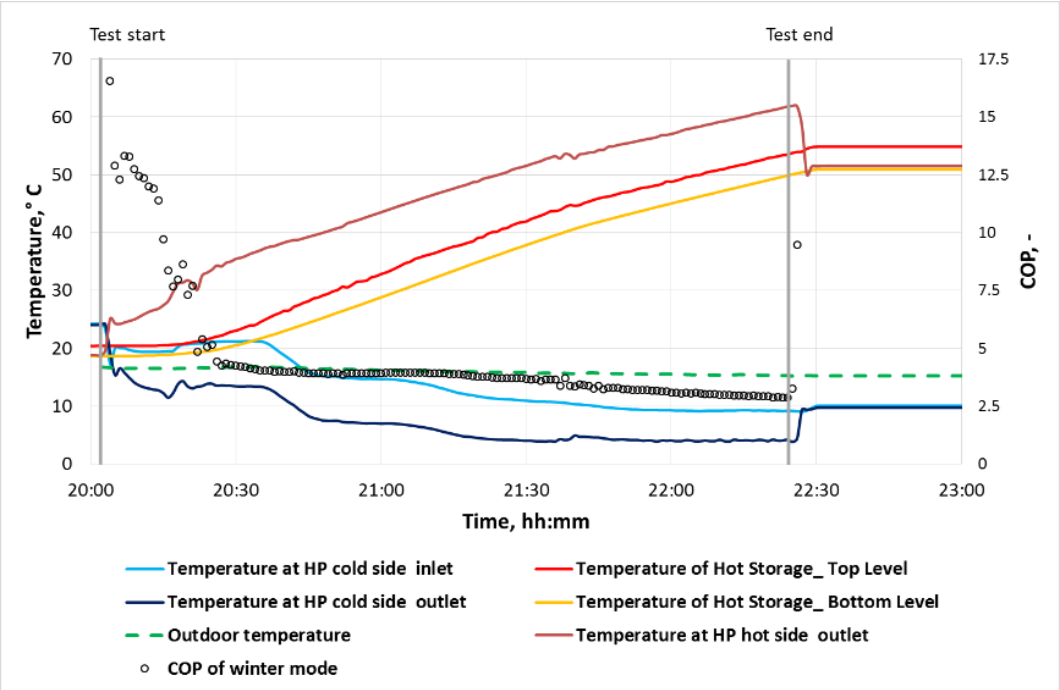

Fig. 3.13. Temperatures and COP during experiment in the reverse (winter) mode

Cold storage also participates in the reverse mode operation, creating a thermal buffer in the heat production circuit (i.e. in such a buffer additional heat stored). A high performance was detected in the first 20 min of experiment, mainly owing to the thermal buffer. The COP decreases and becomes constant after the buffer has been fully used. Figure 3.13 shows that rise in the temperature difference decreases the COP of heat pump.

3.5 Hot storage discharge to domestic hot water

The designed DHW consumption is 45 % from the volume of the tank. Changeable DHW consumption during experiments could distort results. Therefore, DHW was turned off during the previous experiments.

The pilot PV-SAC system was designed for preheating hot water, after which the heating could be done with a primary heat source or an electric flow heater. The relevant monitoring shows that the heat for DHW is mostly produced by the PV-SAC system in a cooling season, while in a non-cooling season the freezing protection restricts the heat production. Hence the PV-SAC covers only partly the heat needed for DHW in most of that time.

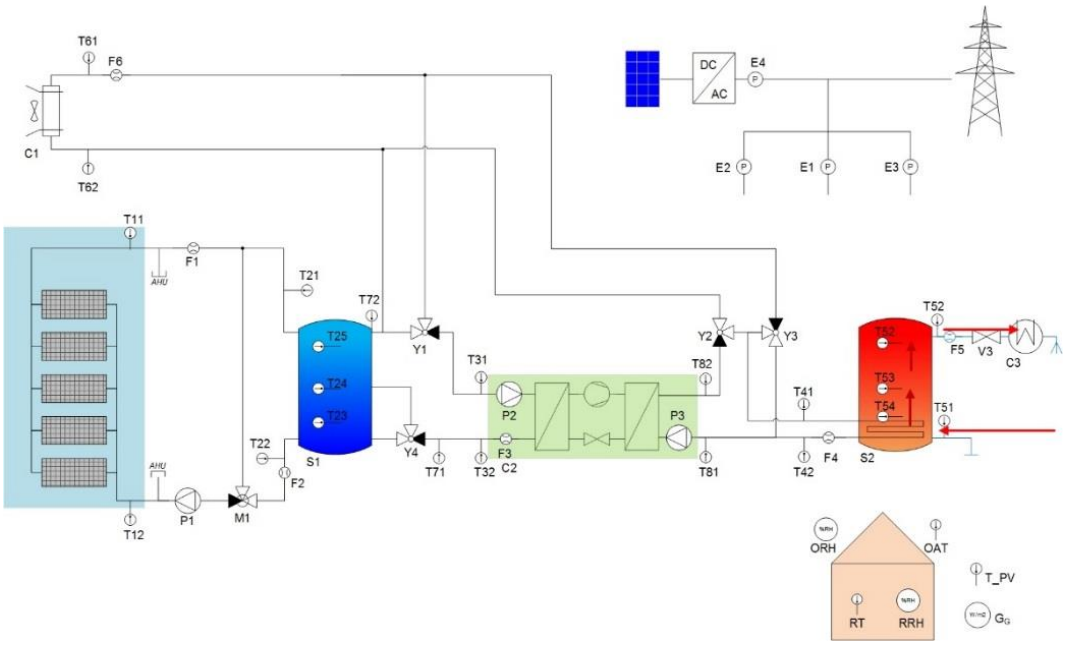

Fig. 3.14. Schematic of hot storage discharge to DHW

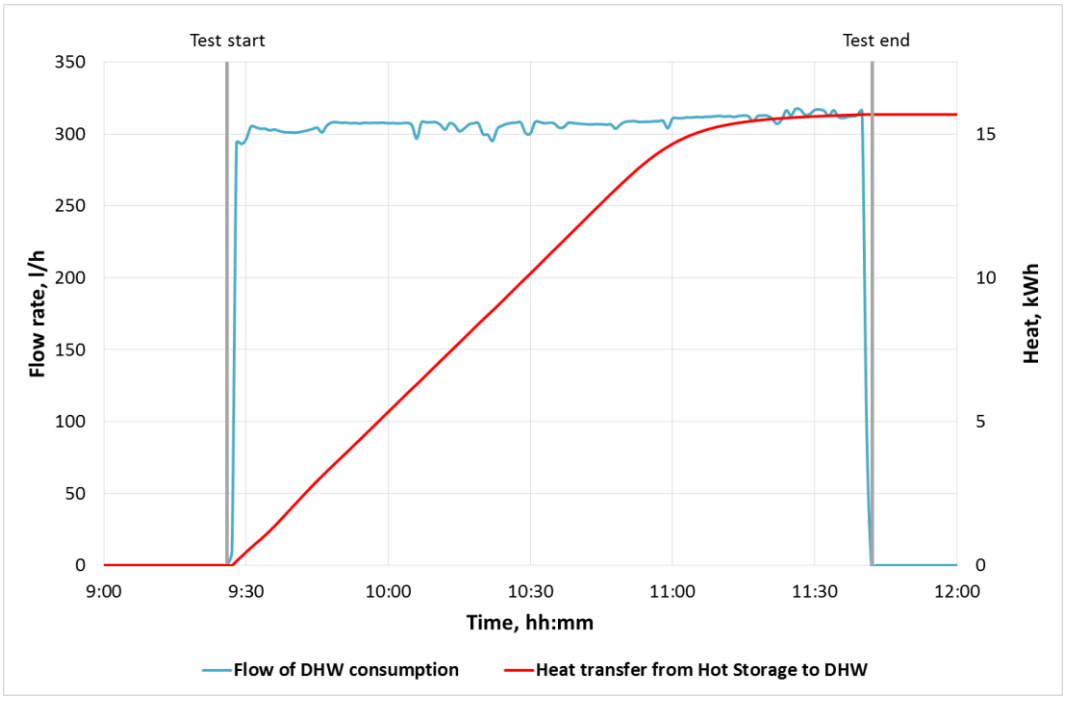

Fig. 3.15. Flow and heat transfer during experiment of hot storage discharge to DHW

Since the tank is filled with water, the DHW consumption is equal to that at the cold water inlet. The average water consumption is 307.6 l/h. Some short-time flow fluctuations of +/-4.8 % can occasionally occur; however, their effect is insignificant.

The HS volume is 445 l. The experimental results show that the total potential of storage is equal to 17.7 kWh. Most of heat is consumed in the time less than 1 h 40 min. Figure 3.16

shows that the temperature at the cold water inlet is in proximity to 19 °C. Higher temperature of domestic cold water was observed at the begging of test, since water is warmed up indoors in the pipes. Moreover, the experiment was done in a relatively warm time (in the middle of September). After 11 min of the experiment, the water temperature at the cold inlet becomes equal to that of district water. The temperature of cold water from district water supply decreases down to 5 °C in the winter time, so higher amount of heat should then be added to the storage. It should be noted that in conventional use the HS heat capacity is up to 24 kWh.

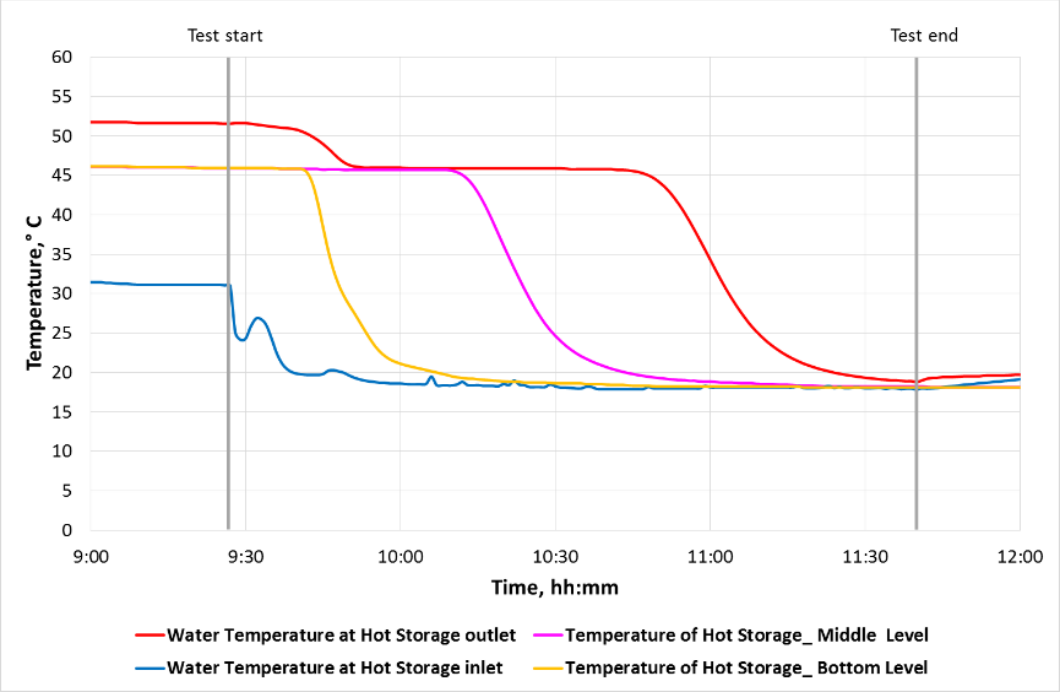

Fig. 3.16. Temperatures during experiment of hot storage discharge to DHW

Before the start of experiment a 10 h stabilization was done. Therefore, the required stratification was reached at the beginning of experiment. The results show that the temperature at HS outlet is described by a smooth curve. This means that DHW consumption as well as cold water inlet do not destroy stratification in the hot storage tank.

In the experiment, the storage tank was fully charged. The temperature was up to 45 °C at the bottom level of the tank, for which warming of the top layers was needed. It should be emphasized that this temperature was still within acceptable levels (i.e. below the level of limescale formation).

3.6 Hot storage discharge to the outdoor unit

Heat exchange between the HS and OU units without cooling machine operation can be used in two ways. First of them is a free heating, while the second is defrosting the OU unit. To drive these processes the circulation pump of cooling machine on the hot side is used.

If the outdoor air temperature is higher than that of hot storage, the free-heating mode can be employed. Warm outdoor air is available only in a cooling season. However, the HS is fully charged in the cold production mode in that time. Pre-simulation results show that the use of free-heating mode is impractical.

The OU defrosting could be done with electrical heater or using the heat transfer from hot storage. This option gives a higher efficiency. On one side, here the heat prepared for DHW is consumed, but on the other the defrosting removes ice from the outdoor unit and let it use again. The heat for defrosting is significantly less as compared with defrosting gain. As the frosting-defrosting cycles are repeated, the quantity of retain water gradually increases, which leads to a 11 % decrease in the heating capacity and a corresponding 10 % decrease in the energy efficiency [26]. Rising of air humidity enhances the ice appearance on the water-air heat exchanger. Respectively, heat losses by the OU defrosting rise in the regions with high humidity.

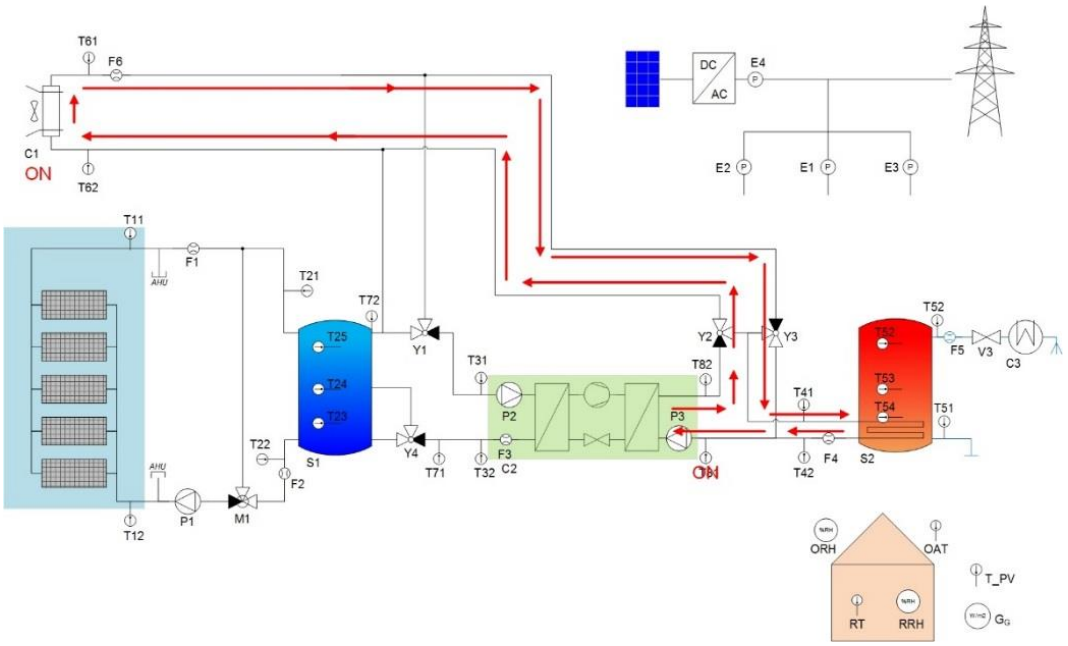

Fig. 3.17. Schematic of hot storage discharge to the outdoor unit

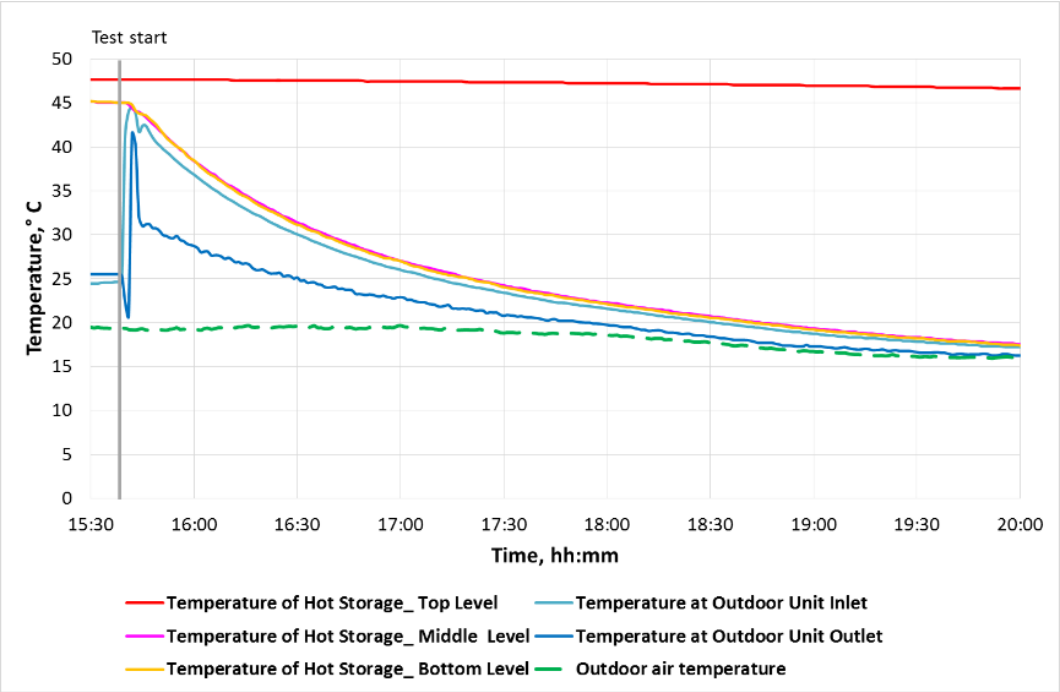

Fig. 3.18. Temperatures of hot storage and outdoor unit
in the experiment with HS discharge to OU

In turn, a full HS discharge to the outdoor unit is needed for cooling down the system cool down before expected service maintenance. It has been shown that the top level of HS keeps its temperature. The top of coil heat exchanger is at the level of 76 % from the tank height. The adequate temperature of stratification does not allow rejecting heat from the top of hot storage. Hence, in this case the heat rejection to DHW or the full water discharge is necessary.

The 7 m long HS-OU pipeline causes temperature fluctuation at the of outdoor unit inlet. As much as 95 % of hot storage heat is rejected from its bottom and middle layers in the time less than 3 h. Increasing the temperature difference between the outdoor air and the hot storage will extend this period of time. Electricity consumption at this regime is almost 100 W per h. In this operation, the OU fan and the brine circulation pump are the main electricity consumers.

3.7 Heat losses of thermal storages

In this experiment, two accumulation tanks (for cold and hot storages) were tested. The relevant heat losses coefficients were experimentally obtained and compared with the technical specification data. Cold and hot storages were tested simultaneously. The test was conducted in three steps: check on heat losses, determination of the energy amount left in tanks and the full energy load.

Heat losses of accumulation tank (Q_{hl}) are calculated by the following equation:

$$Q_{hl} = Q_{load} - Q_{left} \quad (3.1)$$

where

Q_{load} - is the energy at full load, kWh;

Q_{left} - is the energy left after the check on heat losses in a storage, kWh.

The high difference between the fluid temperature in the storage and RT reduces the influence exerted by error of measuring instruments and makes the test results more precise. Therefore, at the beginning of experiment the cold and hot storages temperatures are in proximity to those for critical operation – i.e. the storages reach full load. The CS brine temperature is then -7.08 °C to -5.44 °C depending on tank level. The HS water temperatures +50.63 °C to +54.89 °C.

At the check on heat losses done at the first step of experiment the whole system was switched off for 64 hours. Fluid CS and HS temperatures were measured on three levels: bottom, middle and top. During this step more than 30 000 measurements were automatically collected. Results of measuring the CS and HS temperatures are shown in fig. 3.19.

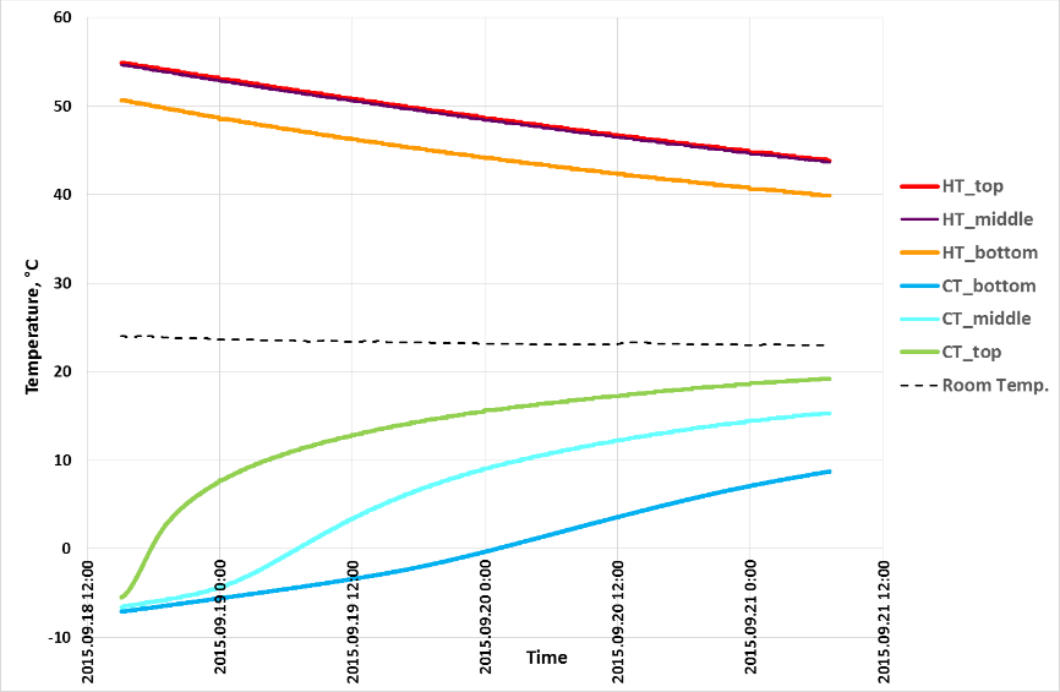

Fig. 3.19. Temperatures of cold and hot storages during the check on heat losses

Placement of CS and HS results one diagram makes the changeable heat losses more visual. As a rule, the rate of storage temperature changes is a result of heat losses during the test.

In this figure, stratification of water temperature in hot storage is clearly seen. It is also seen that the HS temperature fall depends on its deviation from the RT. In turn, the cold storage has higher temperature changes with time. The greatest heat losses are observed at very low temperatures.

Fig. 3.20. Condensate on the pipe connection to the cold storage

The pipe insulation was partly unmounted at the pipe connections, where intensive condensation was observed, see figure 3.20. The condensate arose at the places with temperature below the dew point. In the experiment, the dew point was in the range 9.1-10.6 °C, and in proximity to this point a change in the temperature curve angle is observed. This proves that such condensate significantly increases the heat losses of cold storage.

Fig. 3.21. Ice on the pipe connection to the cold storage

Moreover, ice arising was observed on the pipe conn in proximity to the cold storage starting from the brine temperature below -2 °C (fig. 3.21). The ice covering was observed at a distance of up to 14 from CS. Ice propagation is however inhibited due to heat losses.

It should be stressed out that appearance of water and especially of ice leads to fast degradation of some system's components. While water causes corrosion of metal parts, the ice growth can lead to construction damage. Therefore, thermal insulation is needed to reduce heat losses and prevent fast degradation of the system.

A negative influence of thermal bridges and thermal points on the heat losses was also revealed at comparing their experimental and calculated values. The experimentally found HS losses are 3.989 W per 1K of ΔT and CS losses – 11.683 W per 1K of ΔT.

The calculation of heat losses ($\dot{Q}_{St}$) is done for three components (bottom, top and side) of both thermal storages:

$$\dot{Q}_{St} = \dot{Q}_{B.St} + \dot{Q}_{T.St} + \dot{Q}_{S.St}\,, \tag{3.2}$$

$\dot{Q}_{B.St}$ - heat flow through the thermal storage bottom;

$\dot{Q}_{T.St}$ - heat flow through the thermal storage top;

$\dot{Q}_{S.St}$ - heat flow through the thermal storage sides.

The top and bottom surfaces of storage tank are almost flat. Hence, the relevant heat flow is calculated as that for flat insulation:

$$\dot{Q}_{B.St} = \dot{Q}_{T.St} = A \times \frac{t_1 - t_2}{R_0}\,, \tag{3.3}$$

where

$$R_0 = \frac{1}{\alpha_1} + \sum \frac{\delta}{\lambda} + \frac{1}{\alpha_2}\,, \tag{3.4}$$

A - area of flat insulation, m^2;

t_1 - fluid temperature, K;

t_2 - air temperature, K;

R_0 - thermal resistance of all layers, $(m^2 \cdot K)/W$;

α_1 - coefficient of heat transfer from fluid to the first layer, $W/(m^2 \cdot K)$;

α_2 - coefficient of heat transfer from the last layer to air, $W/(m^2 \cdot K)$;

δ - thickness of layer, m;

λ - thermal conductivity of layer, $W/(m \cdot K)$,

$\sum$ - Summation.

The thermal storage sides are of cylindrical form. Therefore, the heat flow is calculated as for cylindrical layers:

$$\dot{Q}_{S.St.} = \frac{t_1 - t_2}{\frac{1}{\pi \cdot d_1 \cdot \alpha_1} + \sum \frac{1}{2 \cdot \pi \cdot \lambda_i} \cdot \ln \frac{d_{i+1}}{d_i} + \frac{1}{\pi \cdot d_2 \cdot \alpha_2}}\,, \tag{3.5}$$

d_1 - inner/internal diameter, m;

i - layer number;

d_i - corresponding layer's diameter, m;

d_2 - outer/external diameter, m;

λ_i - thermal conductivity coefficient of corresponding layer, W/(m·K),

$\sum$ - Summation.

The main difference between hot and cold storages is that the HS has no bottom insulation, so the heat losses are there higher. In practice, the influence of bottom insulation absence is reduced due to fluid stratification in hot storage. The calculations give the following heat loss values: 3.686 W per 1K of ΔT for hot storage and 2.312 W per 1K of ΔT for the cold storage. The experimental HS heat losses are 7.6 % higher than the calculated. For CS, the difference is much higher, since the condensate and ice increase its heat losses 5 times. As seen in figure 3.19, after crossing the dew point the heat losses significantly decrease.

3.8 Photovoltaic operation

The photovoltaic array was installed on the canopy (roof slope), with the tilt angle of PV field being 15°. Such a value was chosen from considerations of maximal PV production in a cooling season. Almost horizontal PV mounting increases the electricity generation in a cooling season while decreases it in a non-cooling season when the Sun is in proximity to zenith. The PV field is south- oriented, with a 8.5° westward deviation.

The cooling machine as well as other electricity consumers of PV-SAC system receive AC electricity (P_{AC}) generated by the PV component of system. More than 83 % of solar energy cannot be converted into AC electricity using modern technologies. In some experiments [16], the losses were reduced down to 75 %. However, so far this technology has been unprofitable.

The losses under consideration could be of three types: pre-photovoltaic losses, module losses, and system losses. Pre-photovoltaic losses (η_P) are due to reflection of solar irradiation before it hits the photovoltaic material. Its first portion decreases due to pollutions such as dirt and snow, while the second is shading plus reflection. The module losses consist of reflection from glass cover and the losses arising in photo voltaic process. The PV cells lose energy because of: photon recombination, too low and too high photons not caught, depletion zone losses, and thermal losses. Module losses (η_{PV}) are specified by PV manufacturers. The third type losses – the system ones – mainly consist of DC line losses (P_{L_DC}), inverter losses

($\eta AC/DC$), and AC line losses (P_{L_AC}). A consistent pattern between the losses and the yield of PV generation is explained in the following equation:

$$P_{AC} = (G \times \eta_P \times \eta_{PV} - P_{L\_DC}) \times \eta_{AC/DC} - P_{L\_AC}\,, \tag{3.6}$$

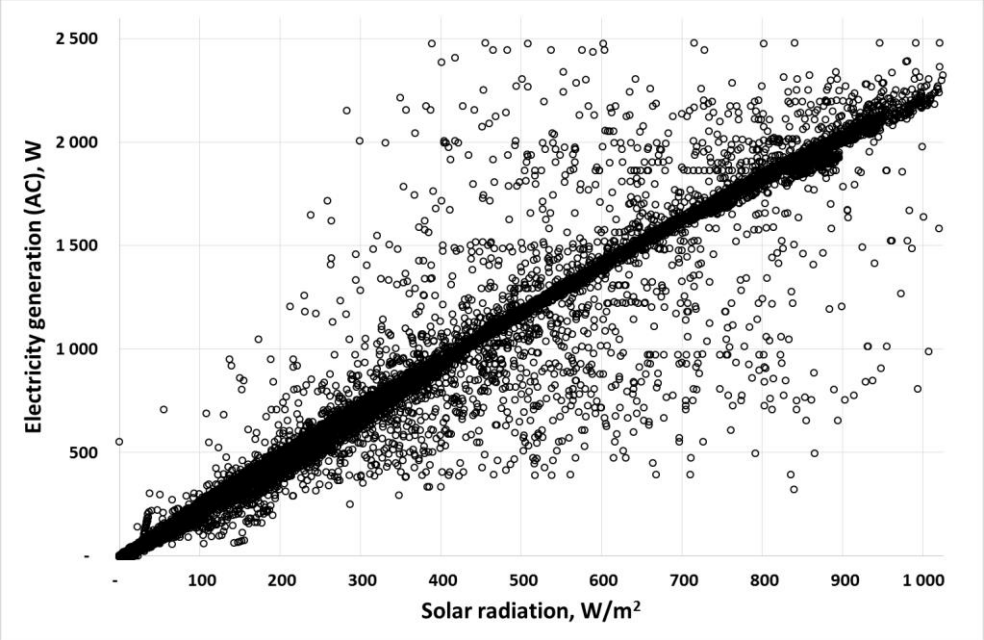

Fig. 3.22. Correlation of global solar irradiation and AC electricity generation

Measurement results show that the correlation between solar irradiation and PV generation is stable, with deviations due to two reasons. First, a deviation in the range +4 to -11 % arises under the influence of PV module temperature. The PV design let the air flow under PV modules. Experiments show that PV modules warms up more than the roof. The second reason is active fluctuation of solar irradiation. Monitoring results show that it happens in a cloudy weather. As shown in fig. 3.22, the range of this type deviation is rather wide.

The building in which our laboratory is accommodated makes insignificant shades on the East side, see fig. 3.24. The shading effect from 6:00 to 7:05 in summer is seen in fig. 3.23. The pre-simulation results show that this shading reduces the PV electricity output by 0.3 %. The main effect of this shadow is exerted on the free-cooling operation when 125W of electric power is consumed. According the our calculations, free cooling operates no longer than 8 min. Temperatures of outdoor air and cold storage are not suitable for every-day free-cooling operation, therefore, loss of the type is insignificant as compared with other losses.

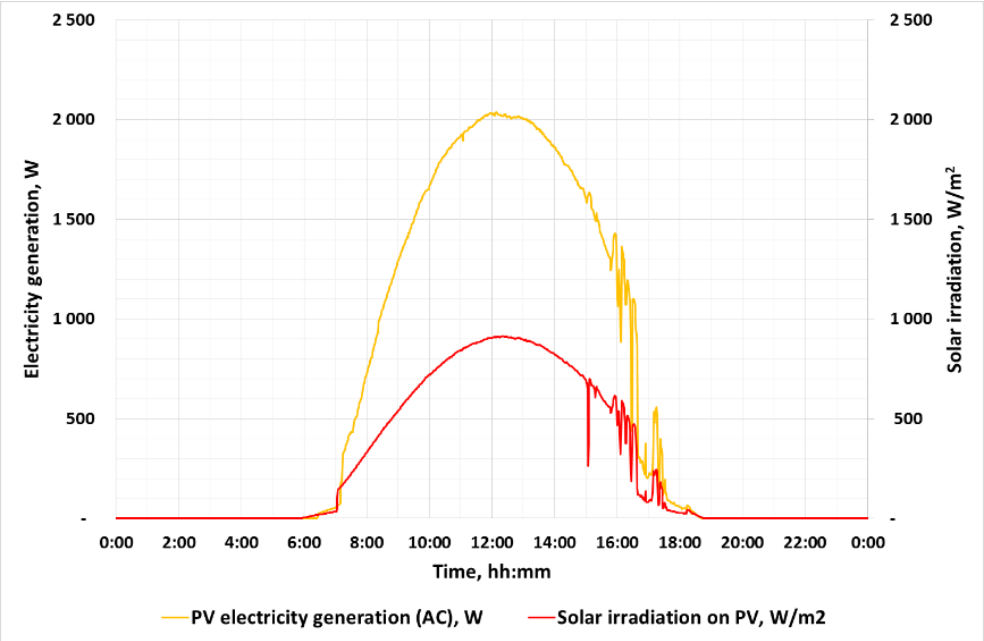

Fig. 3.23. One-day example (9.09.2015) of solar irradiation on 15° roof slope and PV electricity generation with AC/DC conversion losses included

The maximum PV-generated power is up to 2.65 kW_p, with the highest values observed from April till July. Low air temperatures affect positively the PV generation in the spring time.

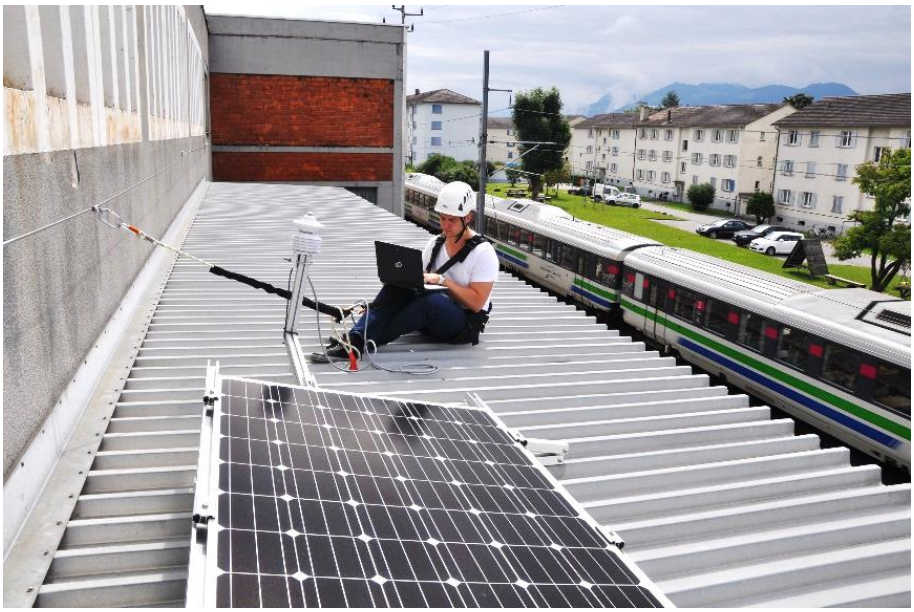

Fig. 3.24. Metrological measurement equipment near PV array

In experiments, the highest accuracy class measuring equipment was installed near PV field. Measuring the global solar radiation was done at the same tilt angle with that of PV array

(i.e. 15°, see fig. 3.24.). The PV module temperatures, the air temperature and the air humidity were measured near the PV filed.

The AC/DC inverter is placed indoors. The cables have shielding, and all the system components are well grounded. Hence, the influence of neighbouring electric lines is excluded.

3.9 Autonomous PV-SAC system operation

Autonomous operation of PV-SAC proceeds in compliance with standards without external intervention. This operation is based on priorities set according to the cooling and heat demand (including efficiency of such auxiliary operations and sub-operations) as well as on safety regulations.

Search among the market offers has shown that there are no control systems for cooling machine operation that is needed for PV operation; therefore, for the pilot PV-SAC technology a self-made autonomous control system was used.

The above mentioned pre-experimental results describe in detail the main process in the PV-SAC technology and also the electricity consumption and efficiency of auxiliary operations. This makes it possible to set the operation of cooling machine according to the PV generation.

The experiment with autonomous system control operation was conducted in the middle of September, 2015 (shown in fig. 3.25 on the example of one-day operation). The outdoor air temperature was +14 °C to +19 °C (i.e. a relatively low temperature for a cooling season), therefore, room air cooling was needed due to high heat inflow from indoor heat producers and sun irradiation through windows.

The cold production starts according to the cooling demand and accumulated electricity. The free cooling needs less electricity, so it could start faster. The consumed electric power can be higher than the PV electrically generated power depending on accumulated reserves.

The experiments with autonomous operation show the existence of high temperature fluctuation in the time of switching between the heat rejection modes. The temperature change of hot brine circuit is up to 30 K while that of cold brine circuit – up to 7 K within less than one minute.

Figure 3.25 illustrates the changes in electricity consumption during non-stop operation (time 9:42). This is a result of fast response of cooling machine control to sharp temperature changes. At this time, the autonomous control of compressor and of both circulation pumps smoothes the temperature changes in the secondary circuit.

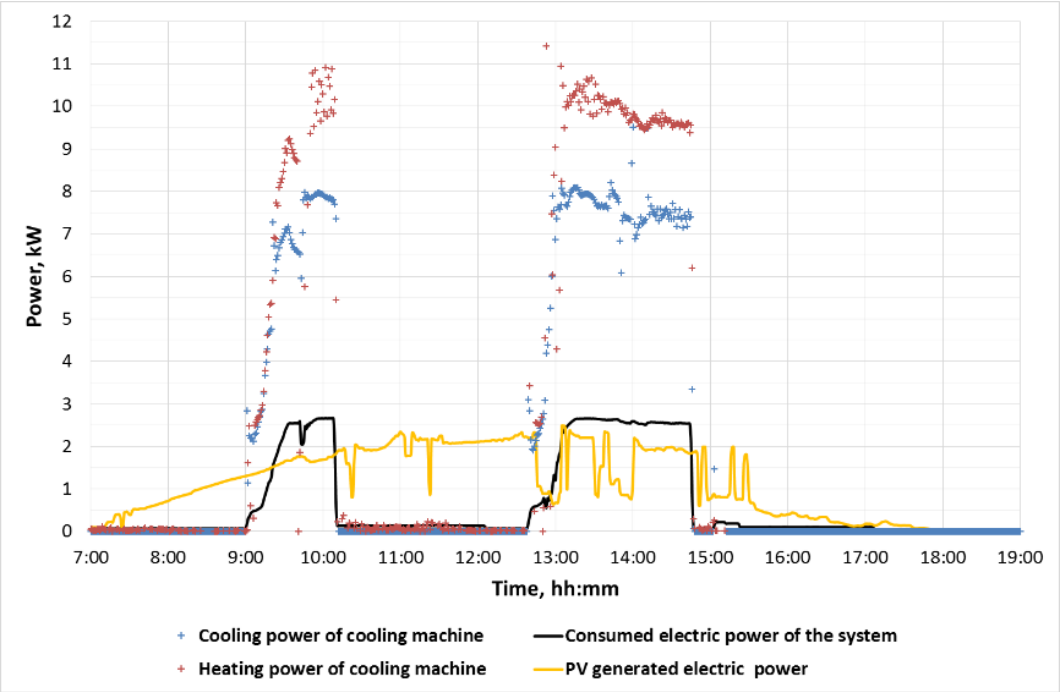

Fig. 3.25. Power values of cooling machine and PV generation

The monitoring shows that such temperature jumps disturb the temperature stratification in the cold storage. This disturbance is self-restored, not affecting negatively the control of cold distribution.

To ensure heat flowing through all parts of cooling machine a definite time is needed. Therefore, a time shift exists between the temperature jumps on one side of cooling machine and the aftereffect on its second side. Experiments show that the time shift is 17-26 s. Duration of time shift depends mainly on the compressor load and, second, on the load of circulation pumps. This is taken into account in the following energy and efficiency calculations.

Early in the day, the RT was in proximity to the set conditioning temperature. This means small-portion cold distribution and at relatively long intervals. While the CS tank becomes partly loaded, a considerable amount of brine has a lower temperature than that of outdoor air in the bottom layers of the tank. Therefore, free-cooling regime lasts only a quarter of an hour at the beginning of the day, so only the upper level of cold storage is then cooled down. This prevents the partly cooled brine entering into the bottom layers already containing fully cooled brine. Besides, this makes temperature stratification safe.

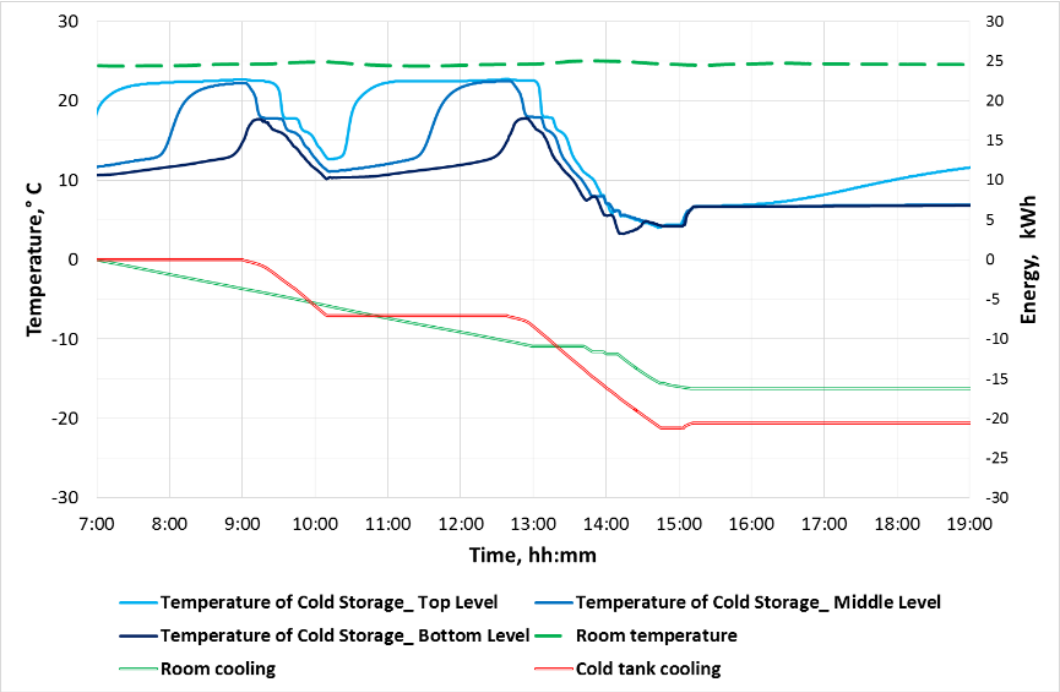

Fig. 3.26. Temperatures and energy flows in cold storage

The inlet-outlet temperature difference of the cooling ceiling is up to 12 K, while the cooling machine provides the temperature difference of 5 K. As shown in fig. 3.26, there are different flows and different operation times for cold distribution and cold production. Hence, to keep the required stratification a CS stratifier is needed. An additional cold water input at the middle level of cold storage makes possible its full charge, simultaneously operating as stratifier.

The internal stratifier is additional option to provide CS stratification. In this case, the three-way valve can be removed thus making the system simpler. At the same time, internal stratifiers are often made of plastics, which means that the water-ethanol brine can react with the stratifier at critically high temperatures during specific tests. Therefore, for the pilot system a double-inlet stratification method has been selected.

Figure 2.27 shows that the rejected heat is mainly directed to the outdoor air. Redirection of rejected heat to the hot storage makes up heat reserves for DHW preparation, which occurs several times in a day. For obvious reasons, this is impossible in the night time.

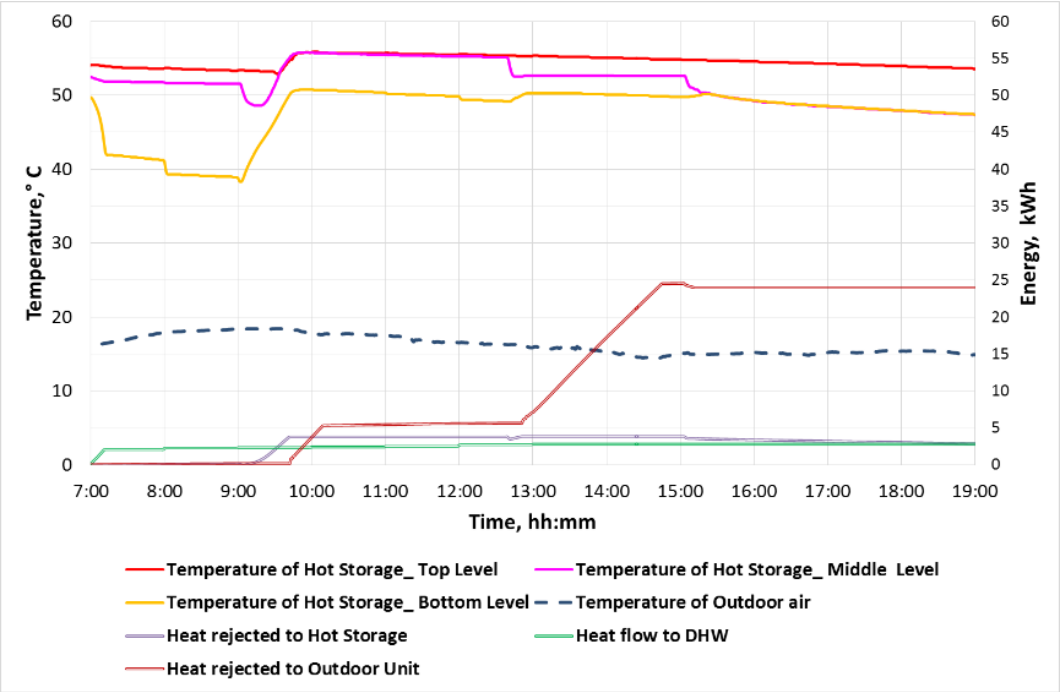

Fig. 3.27. Temperatures of the hot storage and flows of rejected heat

In fig. 3.27. the stratification in hot storage is clearly seen. This allows production of hot water according to the necessary temperature until almost full HS discharge. It is worth noting that the volume of hot storage ensures DHW consumption for more than two days. Taking into account both previously mentioned factors, hot storage reserves and recharges should cover everyday necessities, exceeding DHW demands.

A long lasting heat rejection only to the outdoor unit increases the temperature on the hot side of cooling machine, which affects negatively its performance. This rejection time is possible to split, so that OU cooling down can be done during the stops of heat rejection. Therefore, starting up a new cycle can be done in better conditions. Nevertheless, extended heat rejection increases the heat losses. Besides, more frequent on-off switches of the compressor will reduce the lifetime of cooling machine.

All the previously described tests give accurate values of heat and mass flows in the system, with illustration of specific effects – such as ice and condensate appearance in the pipeline. This proves the validity of the system's model which will be used in the following step of PV-SAC technology investigation.

4 SIMULATION OF PHOTOVOLTAIC SOLAR AIR CONDITIONING MODEL

4.1 Model design and simulation methods

In the study, assessment of a solar air conditioning system has been done. In particular, a design study was carried out using Polysun® (Version 8) simulation program. A simplified schematic of the analyzed system is shown in fig. 4.1. The visualization of system's full schematic not shown because of high complexity and large size.

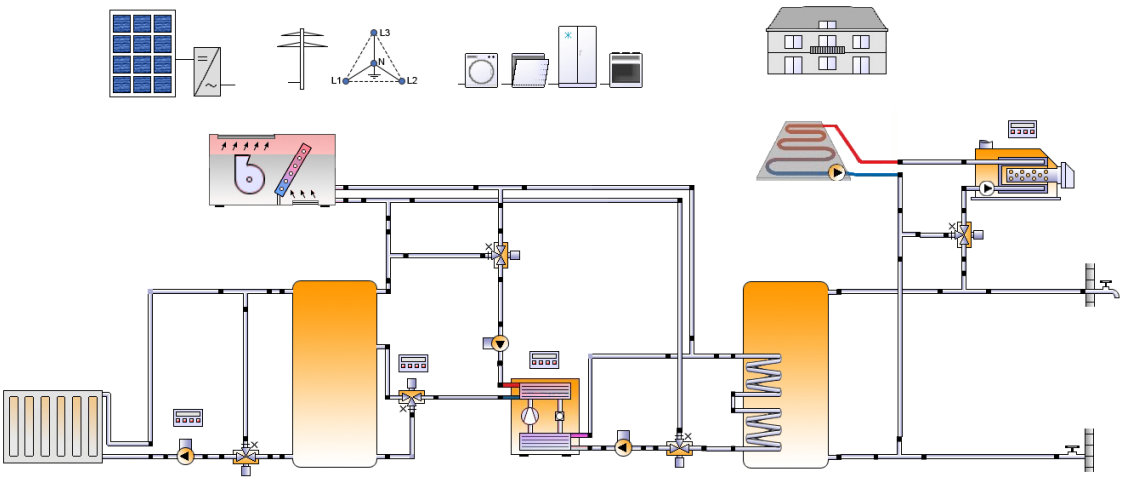

Fig. 4.1. Simplified schematic and illustrative elements of the PV SAC system

In simulations, the reference building was used. In our case this was a single-family house with a heated/air-conditioned living area A=100 m^2 and a room height H=2.5 m. The overall heat loss coefficient (*U-value*) of the building is 0.5 W/K·m^2 and the heat capacity is 500kJ/K/m^2, which corresponds to an average insulated light construction building. The ratio of window glazing to the building wall area is 25 %, and is constant for all building sides. The solar irradiation transmittance of the windows is η_{sol}=0.82. The natural ventilation produces an exchange rate of 0.3 h-1 and infiltration is 0.2 h-1. The internal heat gains are $\dot{Q}_{int}$=0.44 kW$_n$. The ON of the cooling machine is at T_{room}>22 °C, and shading becomes active at T_{room}>25 °C.

4.1.1 Reference system

The reference system is located in Rapperswil (Switzerland). The global solar irradiation on a horizontal surface is G_h=1,103 MWh/m^2/a. The irradiation on the PV module plane with southern orientation and a tilted angle of 15° is G=1,205 MWh/m^2/a.

The specific annual DC yield of PV modules is almost 0.914 MWh/kW$_n$/a, and the overall AC energy production of the PV array is 2,344 MWh/a. The 57.4 % proportion of the

PV electricity is produced in a cooling season. The overall inverter efficiency during the year is 94.9 %. The DC electric energy losses of the DC lines are in the range of 36 kWh/a.

The cooling season (RT requirements) is in the time from middle May until the beginning of October.

The specific cooling energy demand is Q_{cool}=49 kWh/m^2/a. In the cooling season, the building heat gain is approx. 13.9 MWh, where the solar gain through the windows is 74.9 %, with 2 % stemming from the heat flow through the building envelope, 1 % – from natural ventilation and infiltration, and the rest 22 % is the internal heat gain obtained building. In turn, when the outdoor temperature is lower than that of indoors, a high proportion of 9.02 MWh is rejected via the building envelope, natural ventilation and infiltration. The cooling system rejects 35.1 % of the building heat gain, 35.9 % is rejected by the building envelope, and 29 % is rejected by natural ventilation and infiltration. The building indoor average temperature during a cooling season is slightly lower than 22 °C most of the time, varying in the range of T_{room}=17.5 °C to T_{room}=24.3 °C.

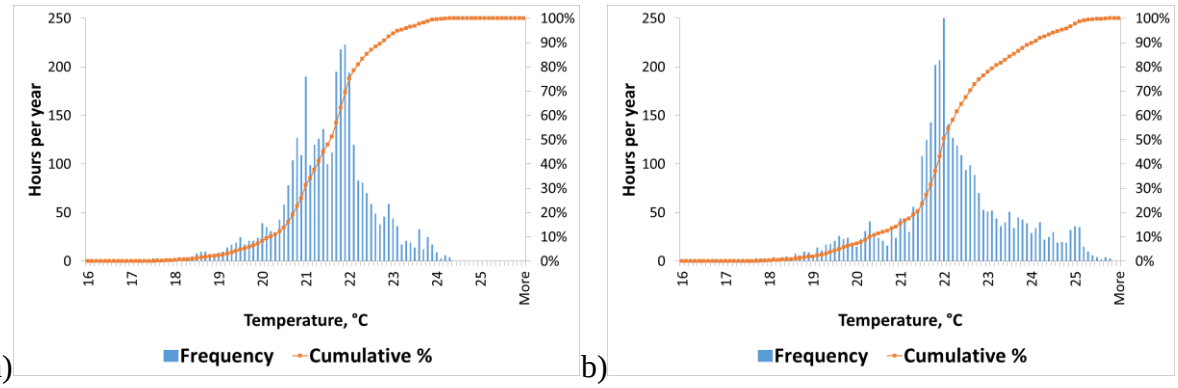

Fig. 4.2. Histogram of indoor air temperature in cooling season:
a) with PV-SAC operation; b) without PV-SAC operation

This figure illustrates the effect of PV-SAC on the room temperature. The room air remains in the comfort temperature range at PV-SAC operation. The excess of air temperature over the conditioning set temperature (+22 °C) is reduced at the system operation. The PV-SAC system covers 2 350 K·h/a of the cooling demand.

Electricity is consumed to drive the heat pump, the heat rejection unit, and the fluid pumps. The total electricity consumption in the cooling season is 1 040 MWh, where 95.6 % is used to run the heat pump, 2 % – for the heat rejection unit and 2.4 % – for the pumps. The electricity consumption of system control is almost insignificant.

An average of 42 % of the PV produced electricity is used by the HP for cold production. The PV-SAC system produces 1 35 MWh/a with the PV array, and 1.04 MWh/a are consumed by all system's electricity consumers in the cooling season. In this case, the PV-SAC system is able to fully provides itself with electricity. Moreover, 30 % of generated electricity could be stored in reserves. This means that a high potential of optimization is hidden in the availability of the PV array electricity as well as in the low electric energy consumption for cold production.

A proportion of the waste energy from the heat pump is redirected to the hot storage for DHW preheating (although it is not the first priority for the PV-SAC in the cooling season). The use of this energy improves the system's overall performance. For DHW needs, it suffices 1.29 MWh/a of redirected heat, which is 99.6 % of the heat demand plus heat losses. On average, the DHW temperature increases by ΔT=34.6 °C, and in the case of good conditions the water can even be preheated up to T=39 °C. Figure 4.3 shows the yearly HP operation temperatures of the cold (chilling) and of the hot (heat rejection) sides.

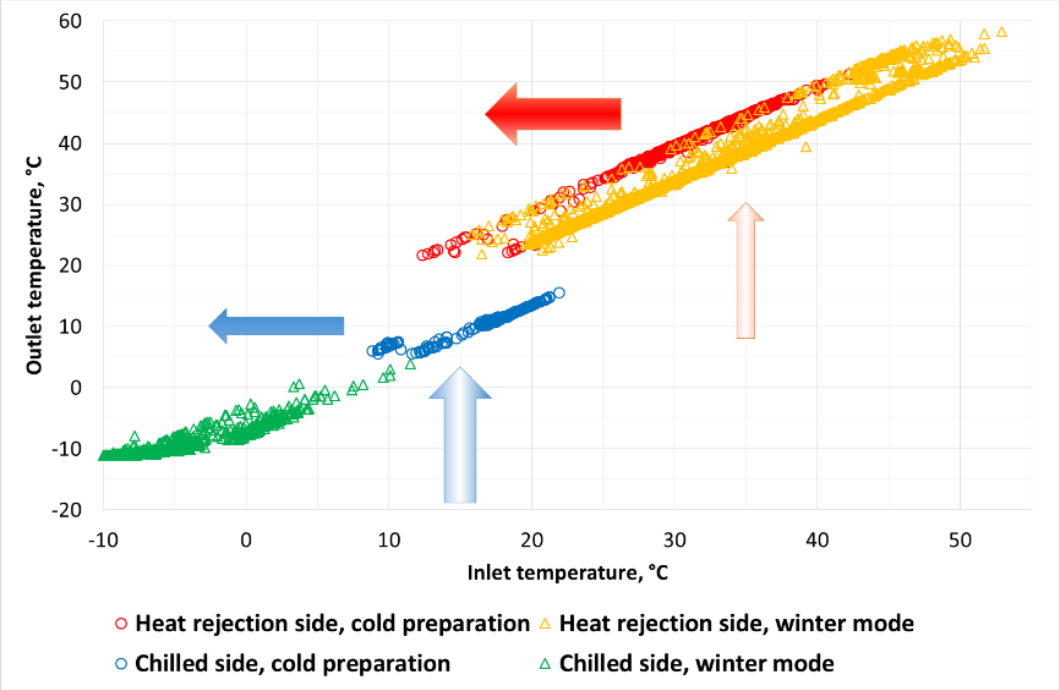

Fig. 4.3. Working temperatures of heat pump fluid

*For fluid inlet temperature on the horizontal axis and fluid outlet temperature on the left vertical axis; the cold (blue and green) and the hot (red and orange) HP side.

The operation time of cooling machine is 590 h in a cooling season and 150 h in a non-cooling one. The inlet and outlet temperatures of cooling machine are shown in fig. 4.3 by circles (cooling season) and triangles (non-cooling season).

The efficiency of the whole system significantly decreases at a rising temperature of the heat rejection loop temperature. The rate of fluid flow in the cold loop is lower than a half of that in the heat rejection loop. Consequently, ΔT of cold loop fluid temperature is higher than the ΔT of heat rejection loop. This difference increases rather fast up to ΔT=15.4°.

The brine flow rate increases to maximum at the temperatures in proximity to the critically low on the cooled side. This allows for enhanced operation of the cooling machine. The bend of inlet-outlet temperature curve is shown in fig. 4.3 at temperature -10 °C to -5 °C.

The coefficient of performance strongly depends on the brine temperatures on the cold and the hot sides of cooling machine. The low temperature difference favours the effective use of cooling machine in all seasons. It should be emphasized that for the cold distribution 1.4 % of additional electricity are consumed. In turn, 26 % of rejected heat is used for DHW heating.

The electricity consumption is constant at free cooling, while the heat rejection mostly depends on the difference between the cold storage and outdoor air temperatures. This process significantly improves performance of PV-SAC technology. The seasonal energy efficiency ratio (SEER) of free cooling is 23.51.

The SEER calculated by the folowing formula:

$$SEER_{el} = \frac{\int(\dot{Q}_H+\dot{Q}_C+\dot{Q}_{DHW}+\dot{Q}_{aux}+\dot{Q}_{hl})dt}{\int\sum(P_{el,PV-SAC})dt} \quad (4.1)$$

where, gain of the system include heat flow rates of heating ($\dot{Q}_H$), cooling ($\dot{Q}_C$),domestic hot water ($\dot{Q}_{DHW}$), auxiliary heat source ($\dot{Q}_{aux}$) and heat loses ($\dot{Q}_{hl}$). The electricity consumption of the PV-SAC ($P_{el,PV\text{-}SAC}$) consist from electrical power of heat pump ($P_{el,HP}$),outdoor unit ($P_{el,OU}$),hot side circulation pump ($P_{el,Hcp}$),cold side circulation pump ($P_{el,Ccp}$),cold distribution circulation pump ($P_{el,CCcp}$),system control box($P_{el,A}$) and of each electrically driven valve ($P_{el,ev,}$):

$$\sum\left(P_{el,PV-SAC}\right) = P_{el,HP} + P_{el,OU} + P_{el,Hcp} + P_{el,Ccp} + P_{el,CCcp} + \\ + P_{el,A} + \sum_{i=1}^{n}(P_{el,ev,i}) \quad (4.2)$$

The annual production of cooling machine together with free cooling is 4.954 MWh of cold. Less than 1 % of generated cold is scattered in the technical room. The overall electrical SEER in the cooling season is 6.02. When the SEER of PV-SAC takes into account the cold production, the heat is redirected to DHW and free cooling. In this time, the total electricity

consumption by the cooling machine and other electric-driven equipment is covered by the PV electricity.

In percent, 42.6 % of the PV electricity is produced in a non-cooling season and could be used for heating, e.g. employing the cooling machine as a heat pump or feeding into the public grid. In this case the outdoor unit is used as the heat source. The HP can not cover totally the room heating and DHW heating loads. Therefore, an auxiliary heat source is necessary. In these cases the HP is used for preheating where the room heating has the first while the DHW preheating the second priority. Higher DHW temperatures make this process less efficient. The gap between the heat production and the DHW consumption was reduced by the system's heat storage. In figure 4.4 the monthly energy flows are shown in detail.

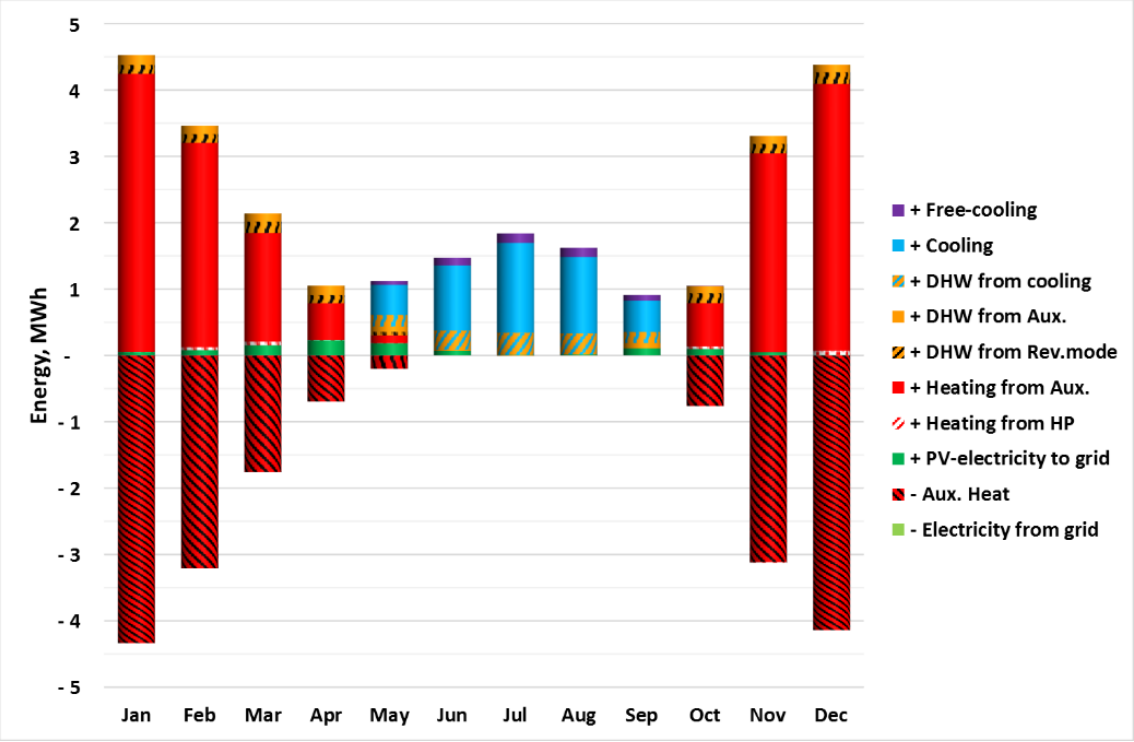

Fig. 4.4. Monthly energy flows in different operation of PV-SAC

*location: Rapperswil

The electricity consumption from the grid was higher in the non-cooling season than in the cooling season, since in the former case high PV electricity production was not required. As a result, 1.2 % of room heating demand and 57.7 % of DHW heating demand was covered by the PV-SAC system. The rest of heat should have been produced with a primary heat source.

High performance of reverse mode is achieved due to production of heat for the low-temperature heating. Reduced averaged temperature difference between the hot and the cold

sides of HP significantly affects its coefficient of performance. The effectiveness of heat production for domestic hot water is almost two times less than for low-temperature heating. Therefore, the production of heat for domestic hot water needs is of a second priority. The heat pump operates on the absorbed heat and consumed electricity after deduction of heat losses.

In a non-cooling season the SEER of HP is 4.8, which is lower than in a cooling season. Considering the above mentioned, the annual electrical SEER of PV-SAC is 5.76.

The equipment, except the heat rejection unit, is installed in a technical room, and the relevant heat losses should not affect the cooling or heating demands of the cooled/heated rooms. It could be possible to equalize the energy balance by adding the heat rejection/heat absorption energy flows via the outdoor unit and by excluding the PV effect.

The amount of rejected heat exceeds the DHW demands in a cooling season. As seen in figure 4.4, only 26.1 % of rejected heat is redirected to the DHW heating. Consequently, most of the rejected heat is rejected the ambient.

The temperature range of the hot side fluid loop is from +15 °C to +59 °C. This heat could be used for heating swimming pools, which will reduce the temperature of the high temperature fluid loop thus enhancing the technology efficiency. The results of calculations and simulations of swimming pool water heating using PV-SAC technology are not included in this thesis because of low market demand.

The use of outdoor air heat is limited due to the freezing protection in the outdoor low temperature and high humidity conditions. Therefore, heating and DHW preheating are reduced in the time from November to March. This is the main disadvantage of the PV-SAC technology.

Low usage of free cooling at the beginning and at the end of cooling season is due to low cooling consumption. Discharge of cold storage is slower than its recharging by the cooling machine. This is especially noticeable in the time of high PV generation. Consequently, there is no need for free-cooling in the time of low solar irradiation, and the PV generated electricity feeds into the grid in that time.

The ratio of the consumed electricity and the gains of the use PV-SAC system's use is shown in figure 4.5, where the electric energy flow is divided into three parts: the PV el. to the system is the PV electricity gain used for its cooling; the PV el. to grid is a surplus PV electricity that is fed into the public grid; and el. from grid – additional electricity demand covered by the grid. The data shown in this figure indicate that one of the technology targets is achieved: PV-SAC reduces the peak of electricity consumption from the grid for cold production.

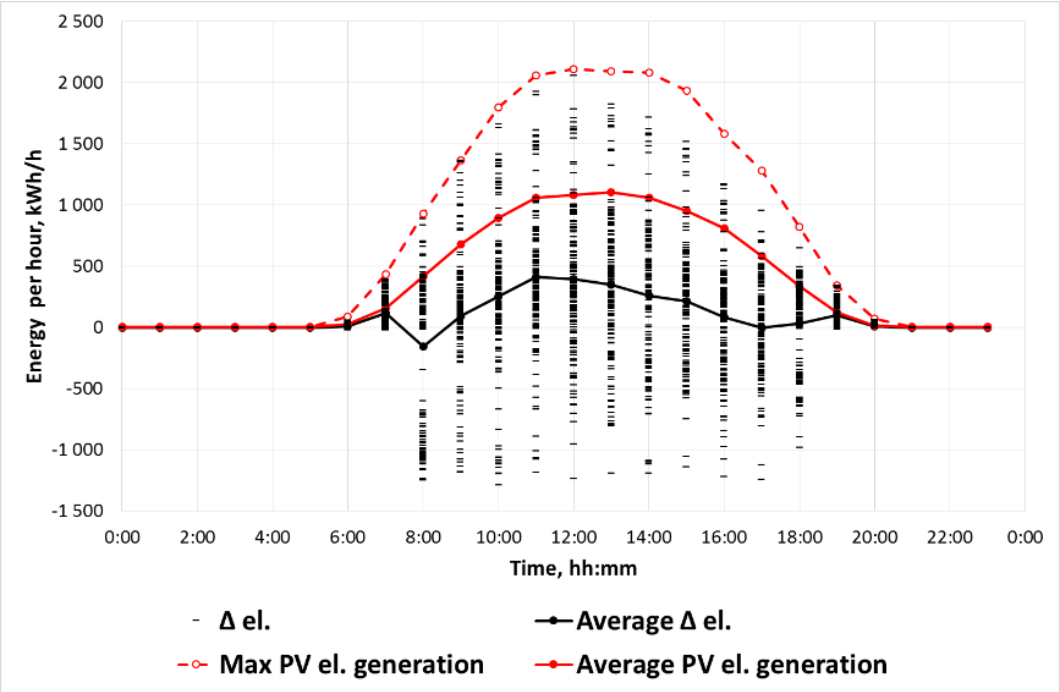

Fig. 4.5. PV electricity generation and consumption (-)/feeding (+) into the grid in the cooling season

*Δ electricity – the balance between the PV generated electricity, and the grid electricity consumption

The monitoring results show that considerable cooling consumption occurs at nights. Hence, the cold storage needs a recharging at the beginning of the day. Therefore, the electricity consumed by the cooling machine exceeds the PV generated electricity in the morning time.

Conventional air conditioning systems have daily peaks of electricity consumption in the afternoon, when the PV-SAC technology produces an electricity surplus. This means that this technology has a high application potential for cooling in the future.

The annual electricity balance has an excess of almost 1 040 kWh/a. Most of the electricity overproduction occurs during transitional periods of cooling-to-heating seasons, see fig. 4.4. In these periods heating and air conditioning energy i.e. power needs are low. But, a favourable outdoor weather conditions decrease the temperature difference between the heat rejection sub-systems and therefor is beneficial for the efficiency of cooling machine in the DHW preheating mode.

Overproduction of electricity is especially noticeable in spring time. And it can be seen that the PV electricity generation is higher in spring than in autumn. This is due to a lower outside air temperature in spring time, which thus increases the efficiency of PV modules.

4.2 Impact of system's enhancement

In the framework of the thesis, the system's extension by adding sub-system components were investigated as to their effect on the overall system performance. In all cases the requirement was that the cooling demand has to be covered in all type systems. The base cooling system schematic consists of a cooling machine, cold ceilings and a heat rejection unit. Additional relevant components are added one by one until the reference system is reached.

The BS without extension has a smaller number of components, which significantly and obviously reduces the installation costs and simplifies the technology. The cooling machine produces cold according to the cold demand that is difficult to forecast. Therefore, exceeding the cold generation and hence electricity consumption can take place. It should be noted that the cooling capacity of the system is in this case insufficient, and the temperature set for building is not reached. Consequently, the power of cooling machine should be increased in the case of base system. Table 4.1 presents the simulation results for all system versions.

Table 4.1

Results of varying the system type – base system + extension

System & extension	CS	HT + DHW	Free-cooling	Reverse mode	Δ electricity (MWh/a)	Cold generation (MWh/a)	Heat + DHW (MWh/a)	Annual electrical SEER
Base system (BS)	-	-	-	-	0.895	5.763	0	**3.98**
+ Cold Storage (CS)	X	-	-	-	1.393	4.545	0	**4.78**
+ Hot Storage (HS) and DHW	X	X	-	-	1.294	4.580	1.327	**5.63**
+ Free-cooling	X	X	X	-	1.306	4.956	1.291	**6.02**
+ Reverse mode (building with normal insulation)	X	X	X	X	1.040	4.945	2.580	**5.76**
Building with poor insulation	X	X	X	X	1.232	3.904	2.391	**5.66**
Building with highly efficient insulation	X	X	X	X	0.773	6.266	2.344	**5.90**

One of the main targets of the cold storage implementation is reducing the peak electricity demand. Therefore, if the system is upgraded with a cold storage, the RT fluctuations could be considerably reduced by shifting the peak load. In the PV-SAC system the cold storage serves to bridge the gap between the solar energy gain and the cooling demand. With the insertion of a cold storage tank the cooling machine operation is closer to the optimum driving temperature range, which slightly increases the HP seasonal efficiency. As a result, the annual electricity consumption decreases, and the cold demand can be covered up to 92 %. Moreover,

with the current cooling load, due to this extension the operation time for cooling production could be reduced.

The implementation of heat rejection via domestic hot water preheating reuses more than a quarter of the rejected heat. Correspondingly, the cooling machine performance improves, and thus the electrical SEER is higher.

To cover the cooling demand in periods of low solar radiation the free-cooling method can be applied if the outdoor temperatures are in an appropriate range. This system's extension allows an efficient covering of the cooling demand. The monitoring results show that the free-cooling operation time is in the morning and in the evening. The low temperature of heat rejection makes impossible redirection of the heat to DHW preheating. Besides, the heat demand of DHW is fully covered with compressor operation in a cooling season.

In the non-cooling season the heat rejection unit of the cooling machine is used as heat source for DHW preheating, for which a total of 270 kWh/a is spent. Because the SEER is 4.80 in a non-cooling season, the annual SEER of conditioning/DHW preheating in the system decreases from 6.02 (in cooling season) down to 5.76.

In general the cooling demand of a building is affected by its envelope insulation, by the ratio of window-to-wall area as well as by the amount of natural ventilation and infiltration and the internal load. The effect of the cooling demand on the air conditioning system is exemplified by the system located in Rapperswil, where the buildings with a low U-value of 0.8 W/K/m^2 are mostly single-family detached houses built in the years 1982-1995 or earlier and the buildings with U-value of 0.2 W/K/m^2 are mostly passive heating type multi-family detached houses.

Table 4.1 summarizes the results of building envelope insulation effect on the PV-SAC operation. The use of materials with lower thermal conductivity means higher investment costs and can lead to higher cooling power needs in the cooling season.

Improvement of the building insulation increases the annual cooling demand. High thermal capacity reduces the short peaks of cooling needs. Simulation data indicate that PV-SAC technology can cover the cooling demand in the reference building by better thermal insulation. In this case, the electricity consumption exceeds the PV generation in the months from July until August.

The influence on the annual SEER depending on the driving proportion in the cooling and the non-cooling seasons can be seen in Table 4.1.

4.3 PV-SAC operation in different climatic conditions

With the reference PV-SAC system's template, simulations for other climatic zones have been performed. Most of the SAC systems are installed in European regions [33]. Therefore, our simulations were restricted to the regions under consideration. The system simulation and the energy analysis have been done for three climatic zones with the reference cities:

- Cold Temperate, seaside – Riga (Latvia), 57° Northern latitude;
- Hot Temperate, continental – Rapperswil (Switzerland), 47° Northern latitude;
- Mediterranean, seaside – Almeria (Spain), 37° Northern latitude

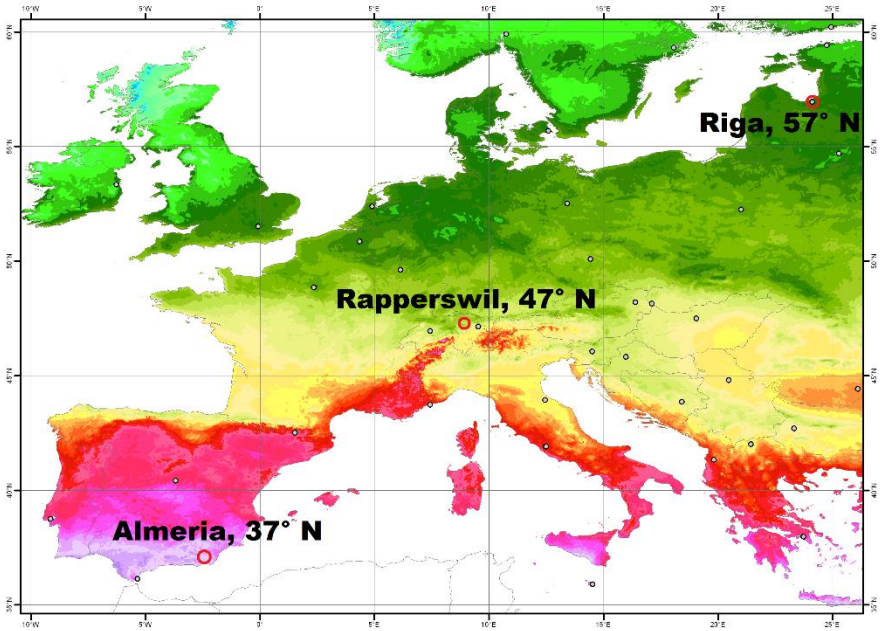

Fig. 4.6. Location of the reference cities on the solar irradiation map of Europe

*The annual data on solar irradiation were collected in the time span 1986-2005. [31]

In Riga, the northernmost solar air conditioning system is installed. For this area strong cold winds are typical. The climate in the territory in proximity to the Baltic See is highly humid.

In turn, for Almeria (Spain) typical is a hot and wet weather, which is not suitable for cold production. The simulations were done using meteodata from Meteonorm (version 7 – the latest meteorological database).

In fig. 4.7 b, the building temperatures without heating and cooling are shown. The curves indicate that the heating and cooling systems are needed to maintain the room comfort conditions in all the three climatic zones. Obviously enough, the cooling demand in the Mediterranean climate is much higher than in the cold and hot temperate climates.

a) 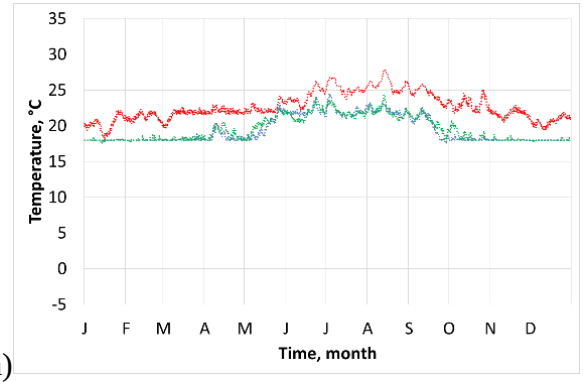

b) 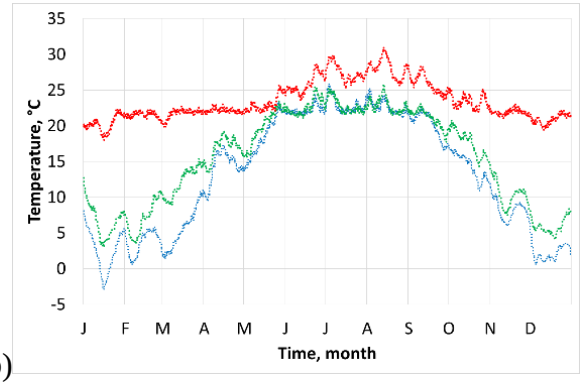

Fig. 4.7. Cooling and heating system effect on RT in the same building but in different conditions: a) with PV-SAC and a primary heat source; b) without heating and cooling systems

*Colours: blue – Riga; green – Rapperswil; red – Almeria.

The system's reverse operation mode is almost not used in Almeria. Figure 4.7 b shows that air conditioning is needed there in all moths of the year, otherwise the temperature in the living rooms of the building will no longer be comfortable. As mentioned previously, driving the system in a non-cooling season is a process of lower efficiency because of unfavourable temperature levels. Testing the system in the Mediterranean climate shows that its nominal power per m^2 is at the limit. In the case of higher internal loads and external heat gains (solar, high outdoor temperatures) this rather small system will let the RT rise out of the comfort range. This will even aggravate the situation in a wet climate, when the system's power of at least 2.7 times higher is necessary.

In Almeria (subtropical zone) the proportion of the total energy demand covered by PV-SAC system is higher than in other locations. This is due to several reasons. The first is a higher electricity production from the same size PV array due to a higher solar irradiance. The second is that the PV electricity production better matches the annual electricity demand. Finally, the third is a lower OFF time in the system because of freezing limitations. However, a prolonged and incessant cold generation leads to overheating the heat rejection tower. Moreover, a high outdoor temperature raises the heat rejection temperature. As a result, the cooling machine performance becomes worse. In Almeria, the electrical SEER of PV-SAC is 5.32.

In the cold-temperate (Riga) and the hot-temperate (Rapperswil) zones a small cooling energy deficit is observed (see fig. 4.8) and the room temperature exceeds 22 °C only a few days. An increase in the system power will reduce the RT peaks, while leading to irrationally low system SEER because the system operation time at nominal load occurs but seldom.

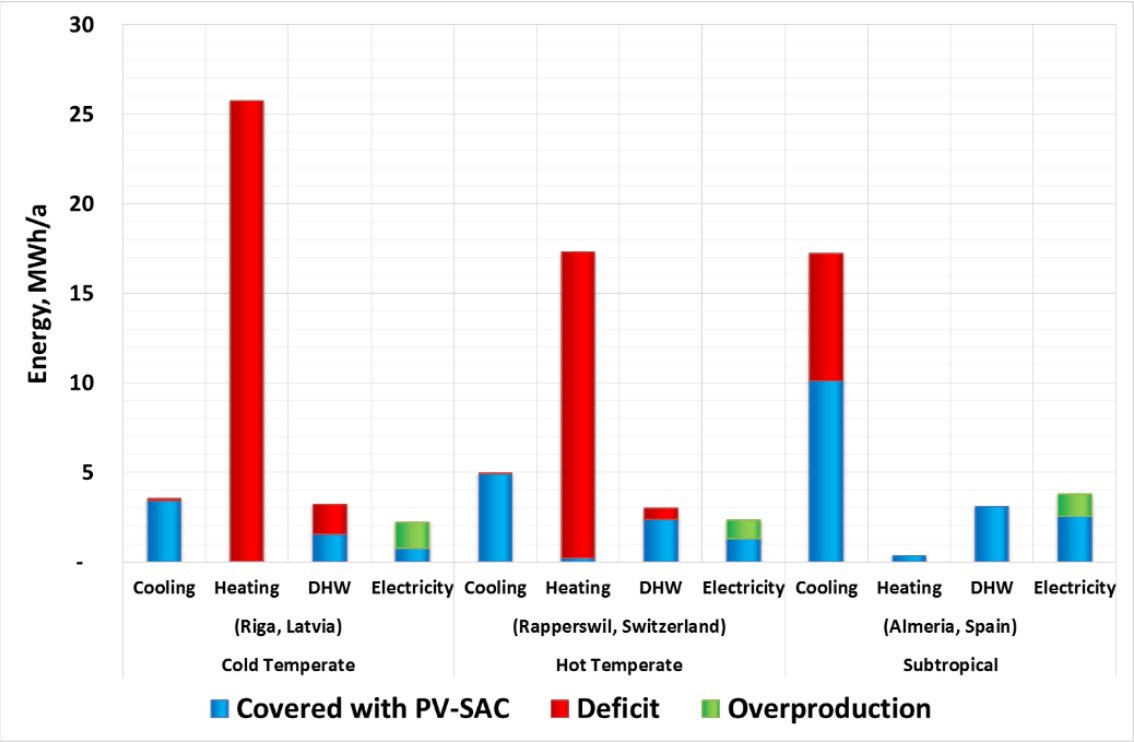

Fig. 4.8. PV-SAC annual demand for heating, cooling and DHW in different climatic zones

The difference in duration of cooling seasons in Riga and Rapperswil is almost one week. It should be pointed out that the outdoor air temperature under critically freezing temperature can be longlasting in the winter time. This prevents using the reverse mode by the PV-SAC technology. Therefore, DHW and heat production in Riga is less than in a hot climatic zone. In these cases the technology components such as cooling machine and heat carriers should be replaced.

New components are to operate at lower temperatures (below -20 °C). In a non-cooling season, this will make more rational the use of available PV electricity at PV-SAC operation in Riga weather conditions. Additionally, in the cold-temperate climatic zones a 1.3-1.6 times higher heating power is required.

The low outdoor air temperature and low use of reverse mode improves the technology performance. In Riga, the electrical SEER of PV-SAC is 6.57.

4.4 Comparison of PV-SAC with thermal SAC technologies

The reference PV-SAC technology was compared with the ABsorption and ADsorption solar air conditioning technologies. The operation in autonomous mode followed by experimental testing has been investigated in order to determine the yields and operation parameters of thermal sorption type SAC systems. Both the mentioned systems were tested in

real weather conditions. In particular, the absorption cooling machine was tested at the Institute for Solar Technology, University of Applied Sciences Rapperswil, while the adsorption cooling machine – at the Institute of Physical Energetics in Riga. The data on yields and performance were integrated in the simulation model, in which the reference weather conditions of Rapperswil were used to compare all the three SAC technologies.

4.4.1 ADsorption solar air conditioning

In the summer (May-September), the average outdoor air temperature in Riga is ~ +15 °C, with the maximum daily temperature in the range +15 °C - +23 °C (maximum average + 32.2 °C) and the average solar irradiation of 1100 kWh/year [42]; the driving circuit of experimental equipment operates in the temperature range of 55-95 °C. Therefore, the potential for use, the advantages and disadvantages of each system were to be properly evaluated taking into account reduced fossil fuel consumption for cooling.

Thermally driven chillers start cold production at a specified temperature of heat source, for which purpose a solar collector's heat output at temperatures above 70 °C was determined to estimate the potential of its use in combination with thermally-driven chillers. The results show that the solar collector yields above a definite temperature meet the needs of thermally driven chillers.

The time proportion for the cooling machine operation and according to the solar collectors' production at temperatures above 55 °C in a cooling season is 91 % of the total operational time, and above 65 °C it is 85 %. Detailed analyses shows that additional heat source is required in warm but cloudy weather conditions.

The rated power of the developed adsorption chiller is 8 kW_n with the maximum cooling capacity of 11kW_p. The tested technology is based on the water-silica gel adsorption principle, with the water being the refrigerant, and silica gel being the sorbent due to its high heat of water evaporation. It is important that the water - silica gel mixture is non-toxic.

The performance of adsorption cooling machine varied according to the temperature of heating side, chilling side, and heat rejection sides. The cooling machine starts operation at the heat source temperature of 55 °C. The load of cooling machine increases with the heating source temperature. The COP of cooling machine increases at temperature rising from 55 °C to 68 °C. Further temperature rise exponentially decreases the COP of cooling machine.

The cooling temperature is +6 °C. Decreasing the cooling temperature decreases the COP of cooling machine. The heat rejection temperature should be strictly controlled. Decreasing this temperature below +22 °C could rise crystallisation in the cooling machine,

while its rising over +45 °C could stop the cooling process. This is due adsorption of water by silica gel at a temperature of ~ 45°, which is restored by desorption at temperatures over 50 °C. The heat source temperature increasing over 110 °C leads to a permanent damage of the sorption material. The fraction of heat transferred to cold using adsorption cooling machine varies from 0.25 to 0.57.

Fig. 4.9. ADsorption SAC system in the solar energy park (Riga, Latvia)

*Components: vacuum tube solar collectors, hybrid heat rejection tower, adsorption cooling machine, and hot storages.

The obtained heat (mainly derived from the solar thermal system) was used for thermally-driven cooling. The solar thermal system used has a thermal power of 15 kW_p at ΔT=70K and contains a 1 m^3 accumulation tank with an 8 kW_p electric heater.

A cold water buffer was used for peak alignment, and a 21 kW_p hybrid cooling tower – for heat rejection. Excessive heat from the solar thermal system is redirected for hot water preparation.

In the work, a combined solar cooling and hot water production system has been designed, with proposals for its further optimization defined. As the first priority, the thermal energy from solar collector is partly used for cooling the thermal-driven chiller during a cooling season.

The mentioned system enables covering up to 75 % of the maximum cooling capacity. Its main features are the following:

- the system is used for air conditioning and hot water production. Therefore, it is necessary to choose solar collectors with a lower heat loss coefficient (<1.5 W/m^2/K). This mostly increases the solar collector's yield in a non-cooling season. Also, solar collectors with higher optical efficiency (η>0.74) have to be chosen for increasing the total solar thermal yield;

- based on the previous studies and the data of Latvian Environment, Geology and Meteorology Centre on weather conditions, the ratio of solar collector power at ΔT=70K to the adsorption chiller power for the low-power and medium-power solar air conditioning systems is found to be in the range 1.65 - 1.85;

- the annual cold production of solar air conditioning system is up to 396 kWh per kW$_p$ of adsorption chiller nominal power. For this, 840 kWh of thermal energy are used (mostly produced by solar collector). In this process, the re-cooler consumes 19 kWh of electricity for rejection of heat spent in the thermally-driven cooling process and of waste heat from indoors.

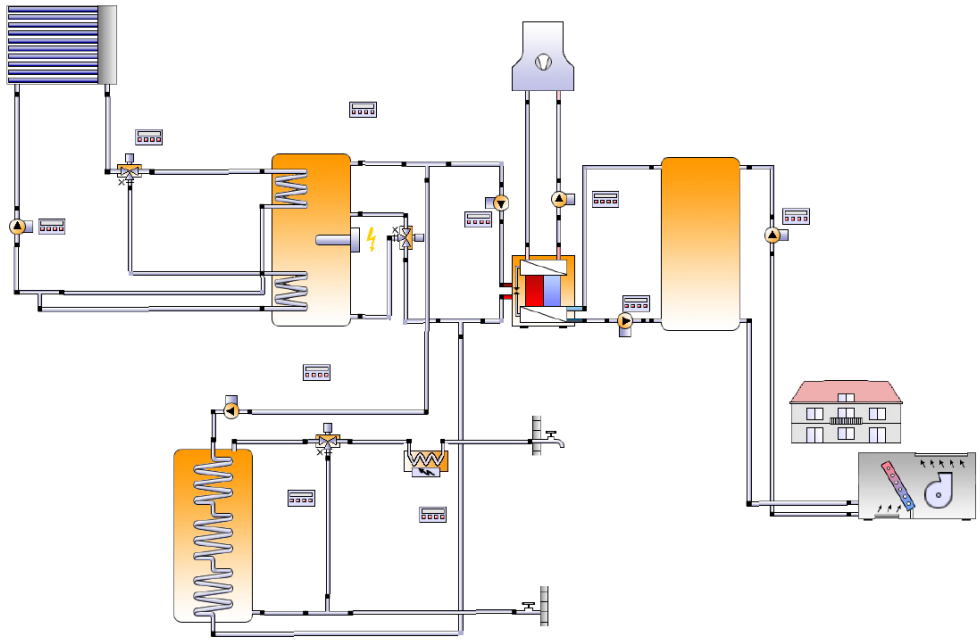

Fig. 4.10. Schematic diagram of ADsorption solar air conditioning and hot water preparation

Simulation results show that the yield of cold by the given solar air conditioning system is 2.4 MWh/a in the Riga weather conditions. The operation time of thermal-driven chiller is 766 h/a. In the given study, this yield includes the rejected heat from indoors. The heat rejection demand in a cooling season has been adapted to the space heating under definite climatic

conditions. The study is aimed at household and office space cooling (the cooling demand for technical processes not included).

The above-mentioned cold production by thermal-driven chiller mainly consumes heat. The heat supplied by generator is 6.7 MWh/a. Re-cooling heat from the hybrid re-cooling tower is 8.9 MWh/a. Both water and electricity are used during the hybrid re-cooling tower operation. Electricity is mainly consumed for the fan's operation, and 0.15 MWh/a is used for the given heat rejection. The SEER of the hybrid cooling tower is 59.4.

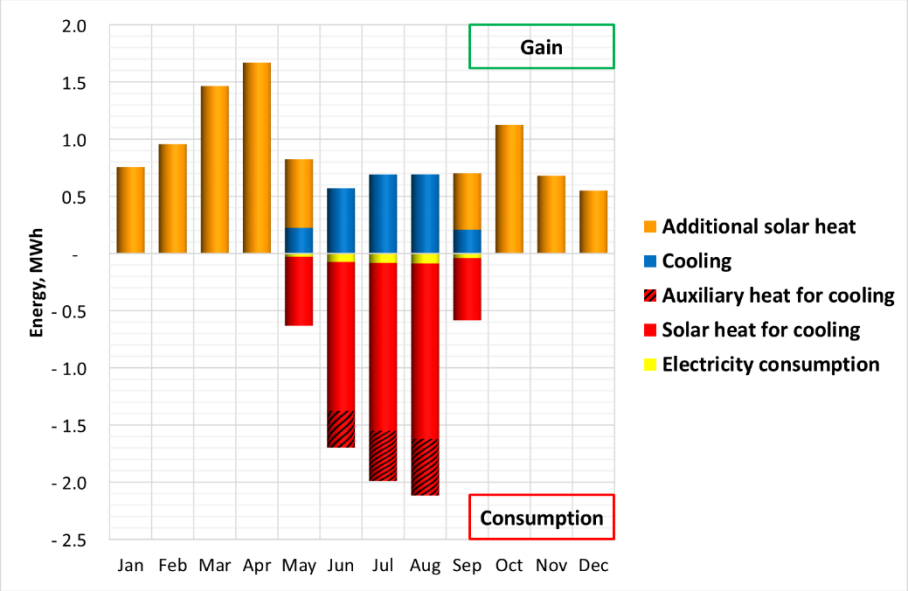

Fig. 4.11. Monthly energy balance of adsorption solar air conditioning and hot water preparation systems

As seen from fig. 4.11, the highest heat energy proportion is obtained from the Sun. For proper reflection in the cold generation process, in a cooling season the auxiliary heat source for hot water production is switched off.

The auxiliary heating is not necessary from the second half of April and in May, since the heat demand is fully covered by solar energy. The cooling demand exists only during the summer months; therefore the solar air conditioning is powered only in a cooling season.

At the beginning of a cooling season begins, heat carriers are supplied to the thermal-driven hot storage with the maximum temperature; as a result, the adsorption chiller operates at full capacity. Within two days, the cold storage is fully chilled, while the auxiliary heat source is not run at that time. The heat carriers are chilled from the indoor temperature until the minimum cooling temperature (~ 8 °C). Generally, the auxiliary heat demand for the adsorption chiller requires only 10.2 % in a cooling season. The rest is provided by solar collectors.

Most of electricity is consumed by the pumps: 50.1 % of the total electricity consumption in the cooling season. The leader of electricity consumption is the circulation pump in the re-cooling loop. This loop has the highest energy flow (the observed ΔT in the flow return is < 9 K). Some pumps can be switched off, and the system can operate on the thermo-siphon effect with electrically-driven valves, thus reducing the electricity consumption. However, operation of the solar air conditioning system becomes much more difficult, and the cooling yield rapidly decreases in this case.

Spending an average of 0.96 from the heat energy and 0.04 from electricity it is possible to generate a 0.34 fraction of cold. It should be highlighted that 90 % of heat is provided by the vacuum tube solar collectors, and the rest 10 % – by the auxiliary heater. Detailed investigation shows that auxiliary thermal energy is needed only several weeks in a year. If only solar energy is used, the RT rises above 25 °C in three days.

The heat rejection tower operates in the low temperature regime, mostly without water consumption. Hence, the water consumption for hybrid cooling towers is not included in the calculations. The electrical SEER of ADsorption solar air conditioning is in proximity to 7.7. The heat overproduction by the solar thermal system is 7.8 MWh. This energy can be used for DHW preheating or other heating needs.

4.4.2 ABsorption solar air conditioning

Absorption cooling machines with liquid sorbent are most widespread in SAC systems, where single-stage and double-stage technologies are used. The latter give a higher performance, though needing high temperatures (above 120 °C) for starting-up the cold generation process. In a double-stage absorption SAC system the concentrating solar collectors should be used. This type solar collectors are difficult to apply in households.

Therefore, comparison is made between the single-stage absorption SAC technology and the PV-SAC technology. The tested absorption cooling machine is based on the water/lithium bromide (H_2O/LiBr) vapour absorption refrigeration where H_2O is used as the refrigerant/ while LiBr - as the absorbent.

The nominal heat supply for cooling machine is from 75 °C to 85 °C. Practically, the cooling process starts at the heat source temperature of 70 °C, and can go up to 110 °C. Increasing heat source temperature increases the load of cooling machine. The highest efficiency is reached at temperature of 73 °C. The temperature of heat source affects the COP of cooling machine up to 7 %, which is several times less as compared with the adsorption cooling machine.

Fig. 4.12. ABsorption solar air conditioning system
in the Institute for Solar Technology (Rapperswil, Switzerland)
Components: flat-plate solar collectors, absorption cooling machine,
cooling ceilings, open wet heat rejection tower.

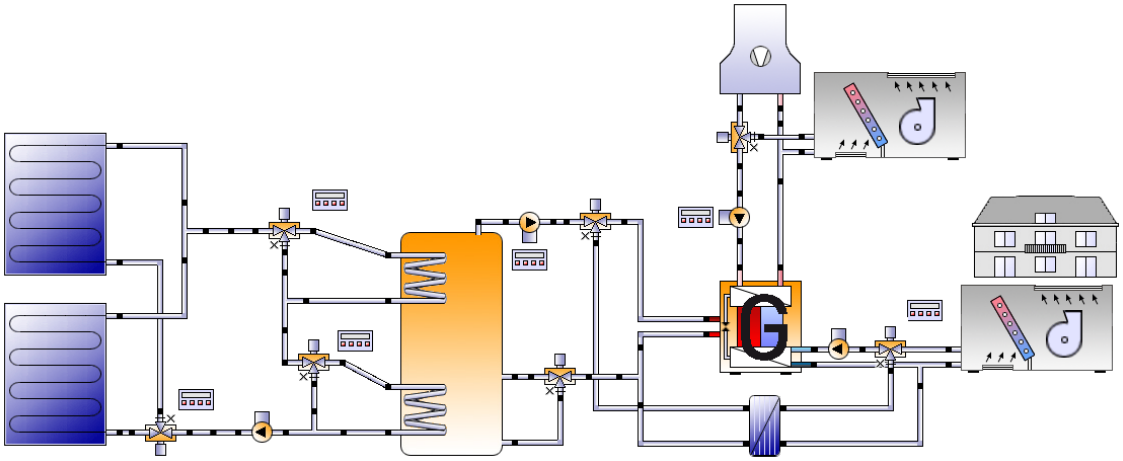

Fig. 4.13. Simulation model of ABsorption solar air conditioning and heating

The absorption machine can chill the brine temperature down to +6 °C. The chilling side temperature causes up to 10 % decrease in the COP of cooling machine. The heat rejection

temperature has the highest effect on the performance of absorption cooling machine, reducing by up to 38 % the cooling COP.

The pilot absorption system consist of: thermal cooling machine, flat-plate solar collectors, heat storage, cooling ceilings, and heat rejection tower. The nominal power of absorption cooling machine is 10 kW_n. It should be noted that the power of thermal cooling machines strictly depends on the temperatures on heating side, on chilling side, and on heat rejection side. The tests show that this power varies in the range 7 - 11.5 kW.

In the pilot system also heating is provided through the heat storage and the heat distribution unit connection bypassing the cooling machine. To split the heating and cooling circuits a heat exchanger is required. Switching between heating and cooling is done by automatic three-way valve.

The concept outlined above does not include the DHW preheating. All the heat generated by solar collectors is spent on driving the cooling machine or on room heating. Unutilized heat is accumulated till its next use. Since in the system is no auxiliary heater, all the heat is generated by solar collectors only.

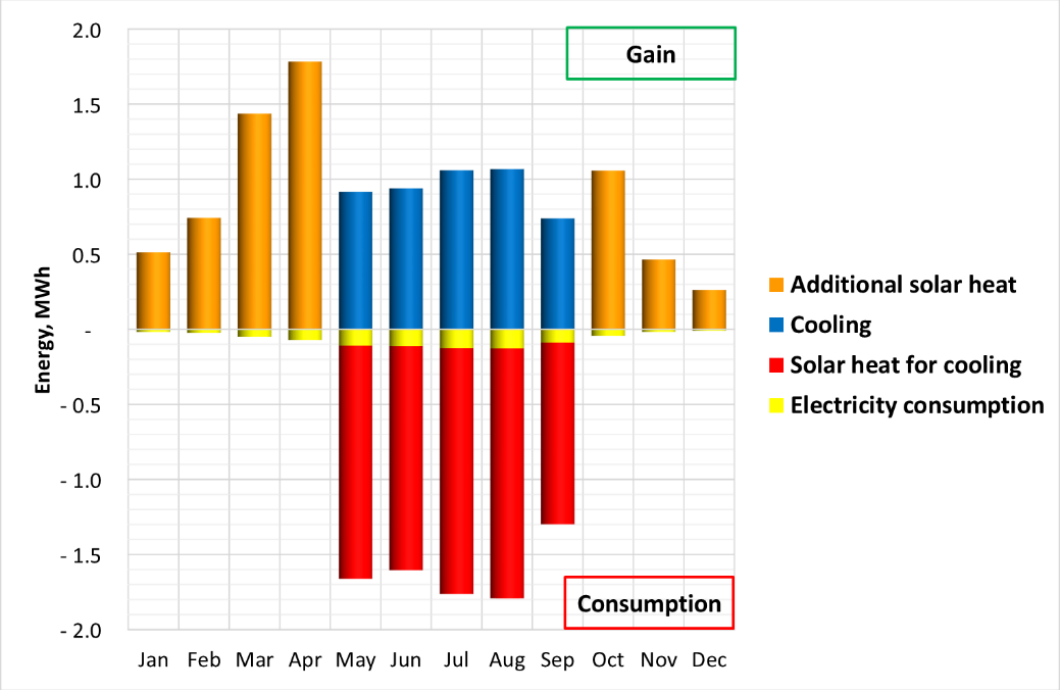

Fig. 4.14. Monthly energy balance of absorption solar air conditioning and heating system

It should be noted that the cooling power of absorption system is higher than that of adsorption one. Almost the same surface of solar collectors – 32 m^2 – is used in both thermal SAC systems. Flat-plate collectors are chosen for the absorption system instead of vacuum tube

collectors that are components of adsorption system. These latter have higher thermal resistance, increase in which decreases the heat losses of solar collectors. Therefore, the heat gain of absorption system is less than in the case of adsorption system in the months from October to April.

The seasonal ratio of heat to cold transfer is 0.67 for the absorption cooling machine. The electrical SEER of cooling machine is 17.5. In the thermal solar air conditioning technology there are additional electricity consumers such as pumps and heat rejection tower. Taking it into account, the electrical SEER of absorption solar air conditioning is 8.4. In other words, spending an average of 0.93 parts of heat energy and 0.07 parts of electricity it is possible to generate 0.62 parts of cold.

Comparison of electricity consumption by ab- and adsorption cooling machines shows almost a tenfold greater its value for the former. Indeed, the absorption cooling machine has several pumps, which are the main electricity consumers.

In practice, the cold generation lags behind the cooling demand. The gap between them is greater than one hour. With integration of cold storage the generated cold can be accumulated until the beginning of the next operation, thus reducing the gap between the cooling demand and consumption. While the integrated cold storage makes necessary the cold generation when cooling is demanded, respectively at the next cooling demand this generation could be decreased due to availability of accumulated reserves.

4.4.3 Summary of comparison

Detailed investigation of the PV-driven, the ADsorption and the ABsorption solar air conditioning technologies has been described previously. Advantages and disadvantages of all the three technologies were considered in view of the system’s installation and operational experience, its operation monitoring, the results of experiments under the critical operation conditions, results of long-term autonomous operation, and simulation results.

Absorption and adsorption technologies are thermal-driven, while the PV-SAC is driven electrically. Hence, the primary energy factor (PEF) is used to compare the yields of these technologies. The mentioned factor indicates the total primary energy required to produce one unit of consumed specific final energy, including also the extraction of energy, its transportation, storage, distribution, delivery, and the losses associated with these processes. [49] Consequently, the PEFs reflect the reality of a complete energy system's operation – from generation to the final consumption:

$$PEF_{technology} = PEF_{heat,EUmix} \cdot \int (\dot{Q}_H + \dot{Q}_C + \dot{Q}_{DHW} + \dot{Q}_{aux} + \dot{Q}_{hl})dt + \\ + PEF_{el,EUmix} \cdot \int \sum_{i=1}^{n} (P_{el,i})\, dt \quad (4.3)$$

where,

$PEF_{heat,EUmix}$ - primary energy factor of heat, the Europe average in 2013;

$PEF_{el,EUmix}$ - primary energy factor of electricity, the Europe mix in 2013;

$P_{el,i}$ - electrical power of each electrically driven part of the system, W;

$\sum$ - Summation.

For heat, the primary energy factor (PEF_{heat_EUmix}) is equal to 1.35, and for electricity this factor is PEF_{el_EUmix} – 2.47 (the Europe mix in 2013) [14]. The PEF values differ widely (up to several times) in particular countries,. With the electricity PEF varying the most – e.g. from 1.7 in Denmark to 3.4 in France [12]. The PEF is especially affected by the available energy sources and the related energy generation technologies.

In the thesis, the PV-SAC technology is compared with the most widespread solar air conditioning technologies, such as previously mentioned small-scale ABsorption (AB) and ADsorption (AD) solar air conditioning technologies. Parameters of the building under consideration – cooling, heating and DHW loads – are the same as in the PV-SAC system. The system simulation has been done for the reference location – Rapperswil, Switzerland. For simulation, industrial available thermal-driven chillers were taken.

Comparison of the primary energy consumptions (conventional heating and cooling system included) is shown in fig. 4.15. It is seen there that all SAC systems save primary energy, with the PV-SAC leading.

The thermal-driven systems generate only 75-95 % of the total cooling demand. Therefore, the cooling deficit was covered using the conventional air conditioning technology to equalize all the three technologies. As well, the same flat-plate solar collectors were used in the model for simulation the adsorption and absorption SAC systems. For equalizing such different systems the same field (14.8 m^2) of solar collectors was taken. This area is equal to that of PV modules of the reference PV-SAC system. The auxiliary components are respectively scaled.

The thermal-driven chillers have a lower COP in comparison with the vapour-compressor chiller. On the other hand, solar collectors have higher COP as compared with the photo voltaic modules. Both factors bring the systems' final yields into the same level. Observing the thermal- and electric-driven cooling combinations it is seen that PV-SAC has several important advantages, which are as follows.

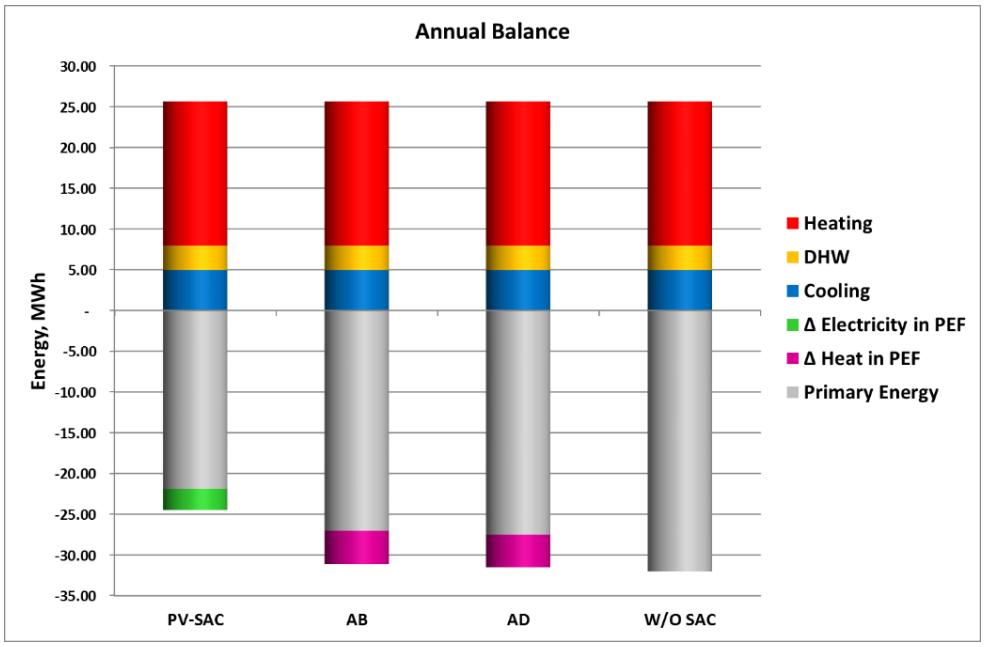

Fig. 4.15. Yield comparison of solar air conditioning technologies according to the primary energy factor

Δ Electricity in PEF indicates the electricity overproduction,
and Δ Heat in PEF – the heat overproduction regarding the primary energy factor

The PV-SAC needs less solar irradiation for rejecting the same amount of heat from indoors. Less roof field for the solar absorption equipment is required by PV-SAC with the cooling power being equal. Moreover, PV-SAC components are more compact. Also, the thermal-driven cooling technologies need electricity for driving the outdoor unit, pumps, chiller and controlling equipment. This electricity amount is less as compared with that needed for the compressor evaporator based cooling technology; however, it is not covered by PV modules in a conventional set of thermal-driven cooling system. Besides, additional heat is required for thermal-driven chillers in the cases of insufficient heat from solar collectors. Increasing the solar collector field allows covering this gap. At the same time, this solution poses the overheating problems.

Thermal-driven SAC technology produces additional heat in a non-cooling season. This energy could be used for DHW preheating or even for covering partly the heating demand. Nevertheless, the existing data indicate that in the PV-SAC technology some electricity overproduction takes place. This extra electricity could also be used for household electricity needs.

5 PV-SAC PERFORMANCE EVALUATION

The experimental results confirm the operability of PV-SAC technology. Additionally, the parameters of operation under critical conditions have been obtained. The experiments have shown appropriate functionality of the system at temperature and power fluctuations. Even in critical situations no failures of the system's inside and outside components took place. Stable and predictable operation of the system was also observed in the autonomous regime.

The simulation results show that the full cooling demand can be covered using PV-SAC technology in a standard single-family house. It was found that PV power is sufficient for the maximum electricity consumption of the system. The results show that for effective use of PV-generated power the electricity accumulation is needed.

a) 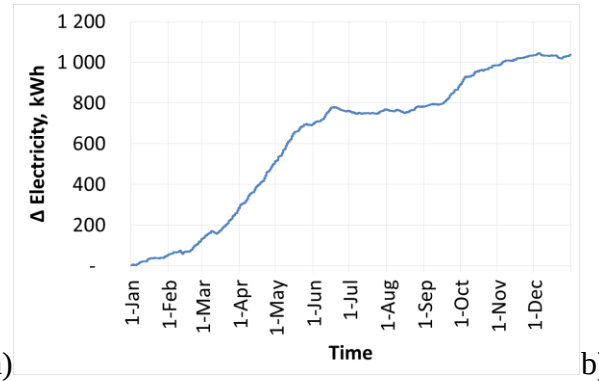

b) 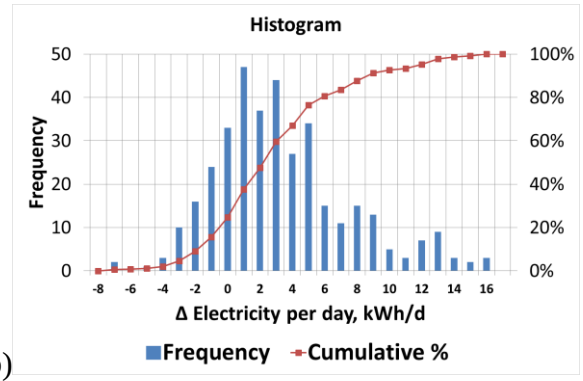

Fig. 5.1. Imbalance of electricity generation and electricity consumption of the system (Δ Electricity): a) cumulative annual result, b) daily results of one year operation

Figures 5.1 a show imbalance between the electricity generation by the PV array and the electricity consumption by the cold production and distribution component of the system. It is seen that such imbalance is more stable in a cooling season in compliance with the design of PV and SAC components. For DHW preheating in a non-cooling season the reverse mode is used. Higher electricity overproduction is observed in the inter-seasonal periods, which is due to combination of high PV electricity generation and freezing protection. Enhancement of defrosting the outdoor air-water heat exchanger leads to a significant decrease in the electricity overproduction. The daily electricity imbalance seen in fig. 5.1 b is from -3 kWh/day to +9 kWh/day in 90 % of the days. The installation of an electrical accumulator with the capacity of at least 6 kWh covers periodical electricity overconsumption in a cooling season. Decreasing the accumulator's capacity exponentially increases the cooling deficit up to 41 %.

Electricity unavailability might lead to immediate shutdown of the system. Such being the case, first of all the heat from the hot side of cooling machine should be rejected, while its

cold side should be protected from freezing. For this purpose, two circulation pumps continue operation after the compressor stops. Second, the prepared cold should be distributed, for which electricity is also consumed. Respectively, PV-SAC operation without electricity accumulators will extremely reduce the lifetime of the system as well as its efficiency. Moreover, this may cause unrecoverable destruction of the system components.

The thermal energy storages allow smoothing the peaks of cold production and heat rejection, thus reducing the load of cooling machine and improving its performance. As well, the heat production and redirection is possible owing to hot storage implementation. The our results show that 26 % of rejected heat is redirected to the DHW heating, with the heat needs for DHW fully satisfied by PV-SAC in a cooling season.

High cold preparation performance is achieved by free cooling. Unfortunately, free-cooling regime could be limited by weather conditions.

5.1 Financial profitability assessment

In the financial profitability assessment the results for PV-SAC yield are used. In the reference building and under reference conditions the PV-SAC technology meets a cold demand of 5 MWh/a and a heat demand of 2.6 MWh/a. Additionally, 1 MWh/a of electricity is generated.

The costs of PV-SAC components are shown in Table 5.1. Additional costs of the high precision measuring equipment are excluded as not required in conventional PV-SAC applications.

Thermal insulation is included. Thermal storages are pre-insulated. The cooling machine contains two circulation pumps. The CM-integrated control unit is able to control the operation of compressor, the cold side and the cold side circulation pumps, and the outdoor unit. To control the operation of cold distribution pump, mixing valve, three-way valves as well as the free-cooling mode an additional control unit is required.

The installation costs are highly variable due to several reasons. First, these costs depend on the particular location and building type. Second, they depend on the salary level in the engineering sectors in the particular region. Third, the costs of equipment to be installed are determined by its class. Future widespread applications of PV-SAC technologies would improve the workmanship, thus reducing the installation costs. In the financial profitability assessment the estimated average costs of PV-SAC installation in European regions are applied.

Table 5.1

Capital investment in PV-SAC (value-added tax not included)

Description	Price [Euro]
PV Module	2 455
PV installation frame	270
Inverter	1 040
W/W cooling machine (CM)	5 840
Cooling ceilings	2 210
Heat rejection tower	720
Cold storage	490
Hot storage	990
Pump, hot side	included in CM
Pump, cold side	included in CM
Pump, cold distribution	140
Pipes, fitting and valves.	1 815
Brine	215
Automatics	310
Plumbing	700
El. installations	150
Automatic installation	360
Total	**17 705**

Maintenance costs include periodical system's check and adjustment. Brine should be replaced every 7 years of system operation. The lifetime of the main system part is 20 years. Three circulation pumps have a shorter lifetime: they should be replaced after 10 years. Respectively, the average maintenance costs are 87 Euro per year.

The financial profitability of PV-SAC is assessed in comparison with the conventional air conditioning (CAC). The cost of a split-type CAC system with the COP rate of 3.0 is 1200 Euro including installation, and its average lifetime is 5 years.

The average price of electricity for household consumers in the EUmix (the prices for 28 European Union member states are weighed according to their consumption by the household sector) was 0.208 Euro per kWh in the second half of 2014. [43] The price of heat energy includes the natural gas price and takes into account the efficiency of boiler. In the second half of 2014, the price of natural gas for a medium-sized household within the EUmix was 0.072 Euro per kWh [43], with the average efficiency of a residential boiler being in proximity to 90 % of the annualized fuel utilization efficiency. [47]

In the above assessment the installation cost of auxiliary heating is not included, since PV-SAC generates heat only periodically. The PV overproduced electricity of up to 2.5 kWh/d could be used for household needs; therefore it is calculated as electricity saving.

Increase in the comfort level is achieved by using cooling ceilings. The lifetime of these elements exceeds 20 years. Therefore, the relevant costs could be added to the investments in conventional air conditioning.

In the system's financial profitability assessment the following parameters are used:

a) payback time;

b) accounting rate of return (ARR);

c) Net Present Value (NPV);

d) Internal Rate of Return (IRR).

The ARR is the ratio of the estimated accounting profit of a project to the average investment in the project.

$$ARR = \frac{Accounting\ Profit}{Investment}, \tag{5.1}$$

The initial investment in PV-SAC is 17 705 Euro. Maintenance costs are 1 695 Euro in 20 years of PV-SAC operation. The expected gain of electricity overproduction is 4326 Euro in the same time period.

For comparison, the initial investment in CAC is 1200 Euro, and in cooling ceiling it is 2 560 Euro including installation. The total investment in CAC (maintenance included) is 19 400 Euro in 20 years. Therefore, the profit of 3 767 Euro using the PV-SAC technology could be obtained by its substitution for the conventional air conditioning and heating technology (CAC&H). The ARR is here

$$ARR_{20} = \frac{21\,472}{17\,705} = 121.3\ \%, \tag{5.2}$$

Figure 5.2 shows that investment and maintenance costs of conventional technology will exceed the costs of PV-SAC technology after 15 years. The jumps of the curves show periodical replacement of system parts. The estimated payback time seen in the figure is 15 years.

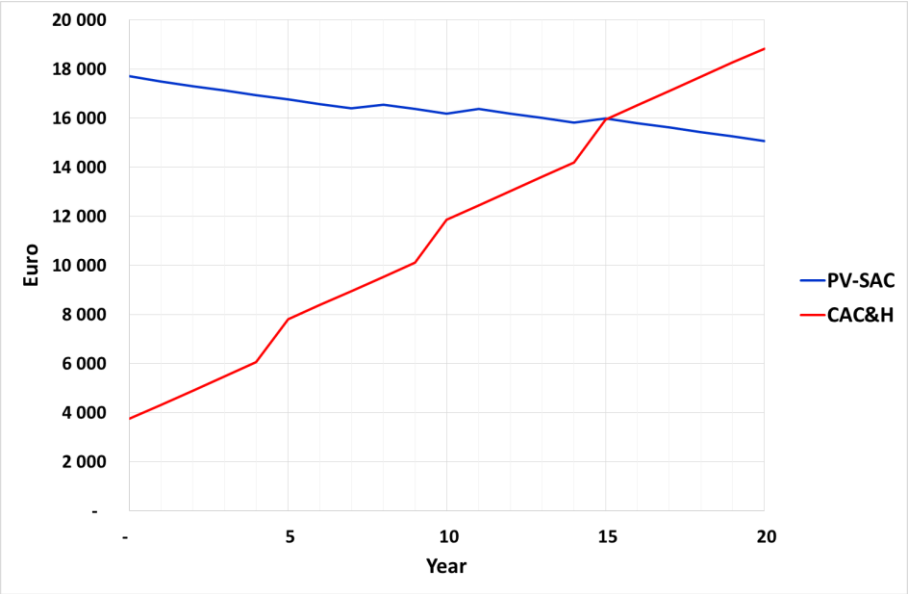

Fig. 5.2. Initial investment and maintenance costs of PV-SAC and CAC&H technologies

The NPV is the value of stream of future cash flows presented in today's currency. This value (see Table 5.2) includes the discount rate and is used for determination whether an investment in expensive PV-SAC systems is worth doing. A positive NPV value indicates that the investment earnings generated by PV-SAC exceed the expected costs in present currency. The NPV value is calculated as:

$$NPV = \sum_{tp=1}^{nT} \frac{C_t}{(1+r)^t} - C_0 \,, \tag{5.3}$$

where

C_t - is the net currency inflow during time period (tp),

C_0 - are the total initial investment costs,

nT - is the number of time periods,

r - is the discount rate.

The discount rate is a variable value depending on several factors:

$$r = f(r_1, \dots, r_n) \,, \tag{5.4}$$

where

r_1 - is the cost of alternative investments,

r_2 - is the assessed inflation, etc.

The costs of electricity, heat, and equipment replacement are exposed to inflation. Hence, the inflation would increase the revenue of PV-SAC in the future. Possibility of alternative investments decreases the value of future revenue, in which case bank deposit

interests could be of help. The deposit interest rate is from 1 % up to 5 %, and the annual inflation is usually up to 4 %. Respectively, the discount rate could be from -3 % to +5 % in a long-term projected future.

Table 5.2

Net present value (NPV) determination during the PV-SAC system's lifetime

		Discount rate					
		5 %	**3 %**	**1 %**	**0 %**	**-1 %**	**-3 %**
Initial costs		13 945	13 945	13 945	13 945	13 945	13 945
The discount savings, EUR	1st year	730	744	758	766	774	790
	2nd year	690	717	746	761	776	809
	3rd year	657	696	739	761	784	834
	4th year	626	676	731	761	792	860
	5th year	1 513	1 666	1 837	1 931	2 031	2 249
	6 th year	568	637	717	761	808	914
	7 th year	541	619	710	761	816	942
	8 th year	288	336	393	426	462	544
	9 th year	491	583	696	761	833	1 001
	10 th year	1 185	1 437	1 748	1 931	2 135	2 619
	11 th year	234	290	359	401	448	561
	12 th year	424	534	675	761	859	1 097
	13 th year	404	518	669	761	867	1 131
	14 th year	384	503	662	761	876	1 166
	15 th year	768	1 024	1 375	1 596	1 856	2 520
	16 th year	349	474	649	761	894	1 239
	17 th year	332	460	643	761	903	1 277
	18 th year	316	447	636	761	912	1 317
	19 th year	301	434	630	761	921	1 357
	20 th year	239	351	520	634	775	1 166
NPV, Euro (€)		-2 905	-797	1 948	3 633	5 577	10 444

The PV-SAC revenue seen in Table 5.2 shows comparative savings of maintenance costs for PV-SAC and CAC&H systems. Initial costs include savings obtained by PV-SAC installation instead of CAC&H. The cost of cooling ceiling installation is not included in the initial cost due to the previously mentioned reason.

The internal rate of return (IRR) is the discount rate at which the net present value of an investment becomes zero. The IRR of PV-SAC is 2.36 %. In other words, the results of work indicate that investment in PV-SAC technology is worth doing at the discount rate up to 2.36 %. Besides, the payback time is extended by increasing the discount rate.

The PV-SAC provides electricity for its own needs, e.g. for cold generation at the peak cooling consumption. Hence, additional benefit of PV-SAC technology is the utilization of electricity reserves. The price of long-term electricity reserves is 30 Euro/MWh [15] up to 80 Euro/MWh [25]. The long-term simulation shows that the peak cooling demand is lasting for several weeks a year. Respectively, extra 672 Euro per reference system is saved by utilization of electricity reserves.

5.2 Environmental impact

Energy generation and conversion always include environmental impacts. The use of PV-SAC technology promotes environment-friendly energy generation. Solar energy is renewable, clean, and predictable energy source, so its help to protect environment. Solar energy does not release carbon dioxide (CO_2), nitrogen oxides, sulfur dioxide, mercury, etc. into the atmosphere as is done using many of conventional heat and electricity sources. Not polluting the air, solar energy does not contribute to global warming, acid rains or smog.

The CO_2 content of atmosphere is one of the parameters for revealing the environmental impact of technology use. The potential of CO_2 reduction takes into account the CO_2 emission factor of the energy used. Therefore, substitution of solar energy for CO_2 producing (e.g. fossil) electricity sources reduces its emission into the air thus reducing global warming.

The world total emission is 35.67 Gton per year [45] in CO_2 equivalent. Trends of global emission show that nowadays CO_2 emission is 23 % higher than 10 years ago, and 55 % higher than 20 years ago. Electricity and heat production emits 25 % [5] of global greenhouse gas (GHG) emission. Therefore, the reduction of such emissions is one of the main targets of the leading projects of environmental protection.

The estimates of carbon dioxide emissions from the energy sector are based on the methodology worked out by Intergovernmental Panel on Climate Change (IPCC). The European emission factor for the consumed electricity (EF_{el}) is 460 kg/MWh [8].

The CO_2 calculation assumes that for heat generation the natural gas with density (ρ_{NG}) of 0.717 kg/m^3 is used. The molecular weight of carbon dioxide (MW_{CO2}) is 44.0098, g/mcl, and of carbon (MW_C) – 12.011 g/mcl. The carbon content of the fuel (i.e. natural gas) is assumed to be 74.2 %. The lower calorific value of natural gas (LCV_{NG}) is 13.09 kWh/kg. Consequently, the emission factor of stationary combustion heat is 208.86 kg of CO_2/MWh. This factor decreases to EF_{NG} = 207.82 kg of CO_2/MWh by taking into account the CO_2 oxidation factor.

The PV array generation is 2.344 MWh/a, with an amount of electricity consumed for cold and heat generation and the rest fed into the grid. Overproduction of electricity is 1.04 MWh/a. Conventional air conditioning consumes 1.652 MWh/a of electricity for the same amount of cold generation. The auxiliary heat source in the CAC&H system consumes 219 kg/a of natural gas for heat generation equivalent to the evaluated technology. Respectively, the reduction in global GHG emission is 1 835 kg of CO_2 per year.

Solar energy – as a renewable energy source – is available at the same time as room cooling is needed, and in this case a SAC system is a reasonable alternative to the systems using fossil fuel. As previously mentioned, the PV-SAC technology decreases CO_2 emission, at the same time increasing the comfort level in living rooms.

CONCLUSIONS

1. Based on the technical analysis presented, it is possible to integrate PV-SAC technology in the common HVAC engineering field. Currently, the PV electricity driven solar air conditioning systems are unavailable on the market, so no experience exists as to running such type of systems, despite the commercial availability of all PV-SAC components.

2. The pilot PV-SAC system has been developed and optimized in compliance with the pre-simulation results for a solar PV electric-driven compression chiller system. The conceptual definition of the PV-SAC and the analysis of working parameters have been presented.

3. The annual seasonal energy efficiency ratio (SEER) of transformation from the PV generated electricity into the useful cold and heat energy is found to be 5.76. A PV array generates more electricity than is consumed by the cold- and heat-production components of PV-SAC system in a long term. The PV-SAC technology fully covers the cooling demand of building under consideration.

4. In analysis of the system, its extensions by different components have been investigated as to their effect on the overall system's performance. In particular, the PV-SAC system contains a cold storage (CS) to bridge the gap between the solar energy gain and the cooling demand. Besides, such CS reduces temperature fluctuations in the room. The implementation of heat rejection via domestic hot water preheating makes it possible to reuse 29 % of the rejected heat. The heat needed for DHW is completely covered by the compressor operation in a cooling season. With the insertion of CS and HS the cooling machine operation becomes closer to the optimum driving temperature range, which also improves the performance of cooling machine and, therefore, increases SEER of PV-SAC technology. The cooling demand is covered by 11 % through the use of free cooling in the time of low solar irradiation. In a non-cooling season, the cooling machine with the heat rejection unit is used as the heat source for DHW preheating. The results obtained indicate that for this purpose 7 % of heat demand is covered by the PV-SAC.

5. Comparison of PV-SAC technology with small-scale absorption and adsorption solar air conditioning technologies has shown that the PV-SAC needs less solar energy irradiation for rejecting the same amount of heat energy. Also, a smaller field of solar absorption equipment is required for a PV-SAC system, with the cooling power being the same. Moreover, indoor components of this system are more compact.

6. The results show that the system should be adapted to a particular location; also, the appropriate controller design is needed for high performance. The pilot PV-SAC system is able to completely meet the cooling demand in cold-temperate and hot-temperate climatic zones. At the same time, the results of PV-SAC experiments in Mediterranean climate zone evidence that a significant increase in the cooling power is necessary.

7. The investments and maintenance costs of conventional SAC technologies are expected to exceed those of PV-SAC technology after 15 years. Investment in the PV-SAC technology is worth doing at a discount rate up to 2.36 %.

The PV-SAC application promotes environment-friendly energy generation. PV-SAC technology reduces CO_2 emission without reducing the comfort level. Reduction of global greenhouse gas emissions is 1 835 kg of CO_2 per reference system per year. This improves the air quality and promotes implementation of environment protection directives.

8. Considering all the previously mentioned information, the concept of enhanced technology of photovoltaic electrically driven compressor of cooling machine has a high potential for widespread application in the future.

REFERENCES

1. Achrichtenmagazin über Photovoltaik, Solarenergie und Erneuerbare Energien / Internet. – www.photovoltaik-guide.de
2. AC/DC inverter manufactory - SMA Solar Technology / Internet. – www.sma.de
3. Aguilara F. J., Quilesa P. V., Aledob S. Operation and energy efficiency of a hybrid air conditioner simultaneously connected to the grid and to photovoltaic panels// Energy Procedia. - 2012. - Volume 48. - 768-777 pp.
4. Ban-Weiss G. Electricity production and cooling energy savings from installation of a building-integrated photovoltaic roof on an office building// Energy and Buildings. – 2013. - Vol. 56. - 210–220 pp.
5. Climate Change 2014. Mitigation of Climate Change/ Edenhofer O. Pichs-Madruga R. Sokona Y. et al. Cambridge, UK: Cambridge University Press, 2014. 16 p.
6. Cooling ceiling manufactory - Zehnder Group AG / Internet. – www.zehnder-systems.com
7. Cooling machine manufactory - Nibe Industrier AB / Internet. – www.nibe.com
8. Covenant of Mayors, The Emission Factors, Technical Document. – Geneva, Switzerland: The Intergovernmental Panel on Climate Change, 2015. – 4 p.
9. Cullhed P. The Almedalen Library – an energy low-cost solution// 71th IFLA General Conference and Council, Libraries - A voyage of discovery. – Oslo, Norway: World Library and Information Congress, 2005. - 14–18 p.
10. Directive 2009/28/EC of the European Parliament and of the Council of 23 April 2009 on the promotion of the use of energy from renewable sources and amending and subsequently repealing Directives 2001/77/EC and 2003/30/EC.
11. Directive 2010/31/EU of the European Parliament and of the Council of 19 May 2010 on the energy performance of buildings.
12. Energy balances of OECD countries, edition 2015. Paris, France: International Energy Agency, 2015. – 8 p.
13. Fontaine B. Record - year for photovoltaic markets in 2013, Asia taking over the leading role. / Internet. – www.epia.org/fileadmin/user_upload/Press_Releases/MW_PR_2014_01.pdf
14. Fritsche U. R., Gress H. W. IINAS ReEport, Development of the Primary Energy Factor of Electricity Generation in the EU-28 from 2010-2013 prepared for the European Heat Pump Association. - Darmstadt, Germany: EHPA, 2015. - 13 p.
15. Fundamental drivers of the cost and price of operating reserves/ Hummon M., Denholm P., Jorgenson J., et al. – Denver, USA: National Renewable Energy Laboratory, 2013. - 57 p.

16. Green M. A. The Path to 25 % Silicon Solar Cell Efficiency: History of Silicon Cell Evolution// Progress in Photovoltaics. – 2009. – Volume 17. 183–189 pp.
17. Ha Q. P. Modelling and optimal control of an energy-efficient hybrid solar air conditioning system// Procedia Engineering, - 2012. - Vol. 49. - 116–123 pp.
18. Handbook-Heating and Ventilating, and Air-Conditioning Systems and Equipment, IP Edition / Atlanta, USA: American Society of Heating, Refrigerating and Air-Conditioning Engineers, Inc, 2008. – 880 p.
19. Haynes W. M., Lide D. R. CRC Handbook of Chemistry 44th ed. -Florida, USA: Boca Raton, 1962. – 2391 p.
20. Hening H. M., Mota M., Mugnier D. Solar Cooling Handbook. – Vienna, Austria: Ambra, 3rd Revised & enlarged edition, 2013. – 368 p.
21. International Conference on Solar Air-Conditioning / Internet. - www.solaircon.com
22. International Energy Agency, Solar Heating & Cooling Programme. Task 53: New Generation Solar Cooling & Heating Systems / Internet. – www.task53.iea-shc.org
23. Jakob U. Status and perspective of solar cooling in Europe// Australian Solar Cooling 2013 Conference. – Sydney, Australia: CSIRO Riverside Life Sciences Centre, 2013. – 30 p.
24. Jakob U., Saulich S. Development and Investigation of Solar Cooling Systems Based on Small-Scale Sorption Heat Pumps// 1st International congress on heating, cooling and buildings. Lisbon, Portugal: Eurosun, 2008. – 7 p.
25. Just S, Weber C. Pricing of reserves: valuing system reserve capacity against spot prices in electricity markets// Energy Economics. – 2008. – 30Volume. – 3198–221 pp.
26. Kim M. H., Kim H., Kim D. R., et al. A novel louvered fin design to enhance thermal and drainage performances during periodic frosting/defrosting conditions// Energy Conversion and Management. – 2016. - Volume 110. - 494–500 pp.
27. Kohlenbach P., Jakob U. Solar Cooling: The Earthscan Expert Guide to Solar Cooling Systems. – Abingdon, UK: Routledge, 2014. - 224 p.
28. Kühn A. Thermally driven heat pumps for heating and cooling. – Berlin, Germany: Universitätsverlag der TU, 2013. – 244 p.
29. Lange N. A., Dean J. A. Lange's Handbook of Chemistry 10th edition. - Columbus, USA: McGraw-Hill, 1973. - 1525–1528 pp.
30. Manufactory of measurement instrument of solar radiation / Internet. – www.kippzonen.com
31. Map database / Internet. – www.mapsontheweb.zoom-maps.com

32. Masson G., Orlandi S., Rekinger M. Global Market Outlook for Photovoltaics 2014-2018. – Brussels, Belgium: European Photovoltaic Industry Association, 2014. – 60 p.
33. Mauthner F., Weiss W. Solar Heat Worldwide Markets and Contribution to the Energy Supply. – Gleisdorf, Austria: IEA Solar Heating & Cooling Programme, 2014. – 61 p.
34. Mouchot A. Die Sonnenwärme und ihre industriellen Anwendungen. – Oberbözberg, Switzerland: Olynthus-Verlag, 1987. – 224 p.
35. Mouchot A. La Chaleur solaire et ses applications industrielles. – Paris, France: Gauthier-Villars, 1869. – 260 p.
36. Mugnier D. New generation solar cooling & heating systems. Task description and Work plan. - IEA Solar Heating & Cooling Programm, 2013. – 30 p.
37. Photovoltaik Zentrum / Internet. – www.photovoltaikumfrage.de
38. Renewable Energy and Jobs/ Ferroukhi R, Khalid A., Lopez-Peña et al. - Abu Dhabi, UAE: The International Renewable Energy Agency , 2015, – 16 p.
39. Renewable Energy News & Information / Internet. - www.renewableenergyworld.com
40. Sanner B. et al. Common Vision for the Renewable Heating & Cooling sector in Europe. – Brussels, Belgium: Renewable Heating & Cooling, 2011. - 48p.
41. Shahsavar A. Energy saving in buildings by using the exhaust and ventilation air for cooling of photovoltaic panels// Energy and Buildings. - 2011. - Vol. - 2219–2226 pp.
42. State Ltd - Latvian Environment, Geology and Meteorology Centre / Internet. – www.meteo.lv
43. Statistical information centre - Eurostat. / Internet. – www.ec.europa.eu/ eurostat
44. Tagliabue L. C., Maistrello M., Del, P. C. Solar heating and air-conditioning by GSHP coupled to PV system for a cost effective high energy performance building// Energy Procedia. - 2012. - Vol. 30. - 683–692 pp.
45. The Emissions Database for Global Atmospheric Research / Internet. – www.edgar.jrc.ec.europa.eu
46. Treberspurg M., Smutny R. New technical solutions for energy efficient buildings. State of the Art Report, Solar heating & cooling// Sci-Network. – 2011. – July. – 16 p.
47. Truong N. L., Gustavsson L. Cost and primary energy efficiency of small-scale district heating systems// Applied Energy. – 2014. - Volume 130. - 419–427 pp.
48. Vougiouklakis Y., Theofilidi M., Korma E. Report on market situation & trends about small scale chillers. WP2: Market Analysis. - Pikermi Attiki, Greece: Centre for renewable energy sources, 2008. - 29 p.

49. Wilby M. R., Rodríguez Gonzalez A. B., Vinagre Díaz J.J. Empirical and dynamic primary energy factors// Energy. – 2014. - Volume 73. -771–779 pp.
50. World Renewable Energy Congress / Internet. - www.wrenuk.co.uk
51. Дорошевский А. Г. Физико-химические свойства водно-спиртовых растворов. - Москва, Российская империя: Изд-во МГУ, 1911. – 224–233 стр.